Master Thesis, Department of Geosciences

Late Smithian (Early Triassic) ammonoids from the uppermost Lusitaniadalen Member (Vikinghøgda Formation), Svalbard

Veronica Piazza

UiO : Naturhistorisk museum

UNIVERSITY OF OSLO
FACULTY OF MATHEMATICS AND NATURAL SCIENCES

Late Smithian (Early Triassic) ammonoids from the uppermost Lusitaniadalen Member (Vikinghøgda Formation), Svalbard

Veronica Piazza

Master Thesis in Geosciences

Discipline: Palaeontology

Department of Geosciences

Faculty of Mathematics and Natural Sciences

University of Oslo

29.05.2015

Table of contents

Acknowledgments

While writing these words I find it still unbelievable to have come this far. It‘s been more than a year since I approached the topic treated in these pages and finally, after a hard and exciting path, I‘m ready to see this thesis printed in my hands. I will recall this time as full of surprises and discoveries. I have been feeling very lucky to get the chance to study one of my favourite fossil groups, and that gave me motivation to continue when frustrations paid their visit.

So first and foremost I dedicate my warmest thanks to my great supervisors Øyvind Hammer and Hans Arne Nakrem, who provided me with this exciting project and were always supportive, patient and understanding. Your advice and support were helpful and encouraging!
I would also like to thank the colleagues with whom I shared enjoyable and unforgettable moments at the NHM in Tøyen. My stay without you would have not been the same. A particular mention goes to Krzysztof Hryniewicz, who kindly spent some of his time helping me with the mechanical preparation of the specimens and shared some of his experience.
Moreover I want to kindly thank the people at the museum of the University of Zürich: I was so glad to meet you! It has been a wonderful experience to meet others working in the same field: I feel I learned so much during those few days I spent with you. Thank you for sharing your knowledge with me and for being so friendly. These words are dedicated in particular to Dr. Hugo Bucher and his PhD student Romain Jattiot, who showed interest in the project and found time to take care of me and my fellow ammonoids. We are all very grateful!
And last but not least I cannot forget thanking the ones who supported me from behind the curtains: my families and friends in Iceland and Italy. We have been apart a very long time since I moved to Norway to make another step towards my dream, but you always gave me warmth and support every time I came home, or whenever I thought I couldn‘t manage.

Achieving this goal would not have been possible without all of you wonderful people I met on my path.
Thank you everyone!

Abstract

Late Smithian (Early Triassic) ammonoids from a single carbonate concretion in the uppermost Lusitaniadalen Member ("Fish Niveau", Vikinghøgda Formation) at Stensiöfjellet, Spitsbergen, are studied and compared with similar assemblages from other areas.

Late Smithian ammonoid assemblages are characterised worldwide by low diversity and predominance of the family of the prionitids. The species identified here are: *Wasatchites tridentinus, Wasatchites* cf. *distractus, Anasibirites kingianus, Arctoprionites nodosus, Arctoprionites resseri* and *Xenoceltites subevolutus*. The group named *Wasatchites* spp. indet. includes juveniles of the genus *Wasatchites* which were hard to identify at species level. Two new taxa are proposed: *Arctoceras* sp. nov and Gen. et sp. nov. (prionitid).
Difficulties in taxonomic identification have arisen due to the high intraspecific variation and the immature stage of most of the specimens.

The assemblage is discussed in a broader context to infer information about the ecological, biostratigraphic and palaeogeographic implications. The good preservation and lack of evidence of transportation suggest deposition in a low energy environment, in accordance with sedimentological observations. The lack of true juveniles and adult individuals may indicate separation of the groups until maturity and high juvenile mortality. From a biostratigraphic point of view, the Spitsbergen fauna is in good agreement with other assemblages within and outside the Boreal Realm. Most similarities, as already pointed out in previous literature, are with the Boreal Canadian Province, though the studied fauna seems to present some peculiarities. The presence of newly recorded taxa such as *Wasatchites* cf. *distractus* and *Arctoprionites resseri* that are more typical for lower latitudes may suggest more marked connections with warmer water than expected (in a similar fashion as in Canada). The finding of arctoceratids at this level confirms their range up to the *tardus* Zone.

1. Introduction

This thesis is an investigation of the ammonoid fauna collected by Dr. Wolfgang Weitschat (Hamburg University) in 1987 from a single carbonate concretion in the uppermost Lusitaniadalen Member ("Fish Niveau", Vikinghøgda Formation) at Stensiöfjellet, Spitsbergen. The age is Late Smithian (Early Triassic), which corresponds to the ammonoid biostratigraphic level of the *tardus* Zone. The collection includes also bivalves and nautiloids, but they have not been considered in favour of more detailed observations on ammonoids. No field work was conducted, and the collection locality not personally visited. The material was originally stored in Hamburg, but was moved in recent years to the Natural History Museum (NHM) in Oslo and proposed as study material for a MSc project by Weitschat.
Weitschat suggested that the material consisted of a new species of the ammonoid genus *Anasibirites* but further observations have rejected this idea, as presented in the thesis. The study collection was discussed also with Dr. Hugo Bucher and PhD student Romain Jattiot from the ammonoid research team at the University of Zürich, Switzerland, during a one-week visit in December 2014. Discussions and comparisons with other material have led us to suggest the erection of two new ammonoid taxa, among the others described.

The presented project was conducted with multiple goals in mind. First of all, a deeper insight on the morphological variability (intraspecific variation), very common in Boreal Triassic ammonoids and extensively studied by Weitschat himself, is achieved. The ammonoid assemblage is studied through systematic descriptions and morphometrics, which regards the measurements of the shape and size and their statistical analyses. The results obtained are viewed in a wider context to infer information about palaeoecology and taphonomy. Moreover, the implications regarding biostratigraphic correlations and taxonomy are considered. Ammonoids, for this purpose, are of great value. The findings in the studied assemblage of undescribed ammonoid genera and of species that have not been recorded from Svalbard before may be helpful to strengthen and improve the existing correlations within and outside the Boreal Realm, to which Svalbard belonged.
Through the results presented in this thesis it is hoped to reach a greater understanding of the Late Smithian in Svalbard, as well as of the Boreal Realm.

2. Geological background

The archipelago of Svalbard is an uplifted part of the NW Barents Sea Shelf. Its geological record spans almost completely the last one billion years (Precambrian to Palaeogene) of the Norwegian arctic shelf and only a few major breaks are recognised (Worsley et al. 1986; Worsley 2008).

In particular, Early Mesozoic sediments from Svalbard are very similar to the sequences in Greenland, Sverdrup Basin and Siberia: all these localities were at that time located on the northern margin of the supercontinent Pangaea, facing the Panthalassa Ocean (Vigran et al. 2014) (see Chapter 3). The importance of this tectonic setting for correlations will be further discussed in the next chapter.

The sedimentary environment was mainly influenced by the relationship between tectonics and climate. Svalbard shifted northwards from the equator during Devonian/Carboniferous times to high northern temperate latitudes by the Palaeogene (Mørk et al. 1982; Worsley 2008) (in particular Svalbard moved in the Triassic from 40°to 50°/60°N). A consequence of this shift towards a more humid climate was the increasing predominance of clastic sedimentation. As for the tectonic factor, NNW-SSE major lineaments have been active since the early history of Svalbard, though variably through time and in the different areas of the archipelago. The Triassic record shows for example no sign of major tectonic activity, though tectonics still influenced the accommodation space development through e.g. the extensional movements in the North Atlantic and the Uralian orogeny (Worsley et al. 1986; Glørstad-Clark et al. 2010, 2011).

An overview of the geological setting of the archipelago is presented in the geological map in Fig. 1.

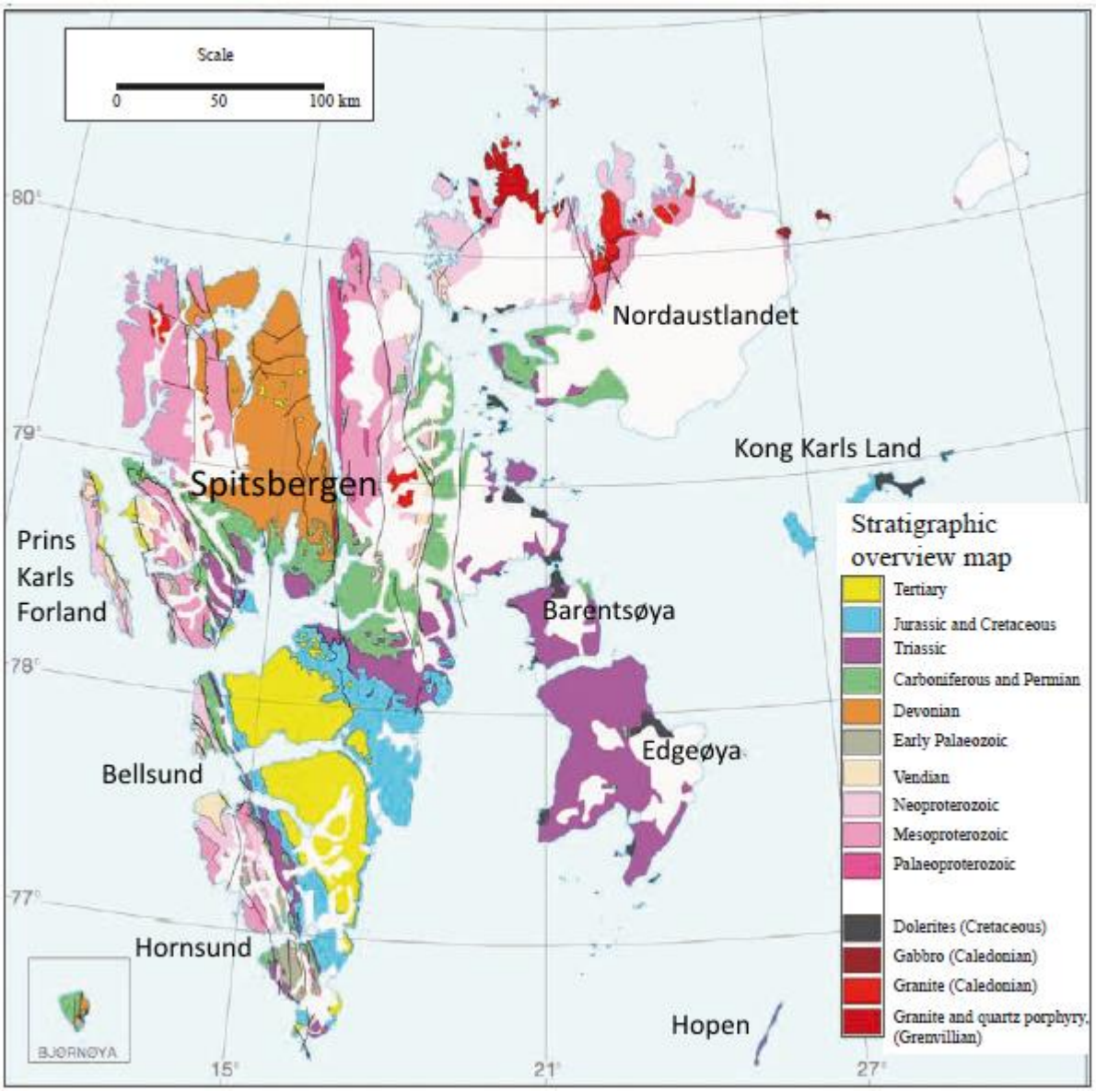

Fig. 1 Geological map of the Svalbard archipelago showing also the fault lineaments (modified from Dallmann et al. 2002 in Osmundsen et al. 2014, fig. 2).

2.1 Sedimentation and tectonics in the Early Mesozoic

The Permian and Triassic beds are separated by a sharp transition from carbonate/chert to clastic sedimentation (Vigran et al. 2014), which indicates a shift towards more humid temperate conditions that were prominent throughout the Mesozoic. The deposition occurred in an arid to humid climate with periodically restricted circulation – these variable conditions are expressed in the variability in lithologies (Glørstad-Clark et al. 2010). From the syn-sedimentary fault setting of the late Palaeozoic there was an evolution towards the stable platform setting typical of the Mesozoic (e.g. Worsley et al. 1986; Worsley 2008). Subsidence persisted, though decreasing, in the Triassic, until tectonic stability was reached in the Late

Triassic/Middle Jurassic (Worsley 2008). Early to Middle Triassic sediments present evidence of downwarping along the abovementioned fault lineaments, especially in the Central Spitsbergen Basin where the thickest sequences are preserved (Worsley et al. 1986; Vigran et al. 2014).

Siliciclastics are the most common Early Mesozoic sediments. They were deposited in a relatively deep shelf environment, in some cases permitting the accumulation of high organic content. Svalbard was then mostly covered by the sea, but periods of uplift occurred and permitted alternation of marine and terrestrial deposition (e.g. Mørk et al. 1999a; Vigran et al. 2014).

The sediment input was mainly from the west (NE Greenland) (Fig. 2), but starting from the Late Triassic progradation from the east became increasingly more significant (e.g. Vigran et al. 2014). It should be mentioned though that many different basins, among which Svalbard was only one, were located in the Barents Sea Shelf and were divided by several highs (e.g. Sørkapp-Hornsund and Loppa Highs, among others). The progradation occurred then at a local scale from different areas, creating a very complex depositional pattern. Moreover, erosion and re-sedimentation occurred over a long time (Mørk et al. 1999a; Glørstad-Clark et al. 2010; 2011).

The Early and Middle Triassic deposits can be divided into eastern and western regions, which have different lithology and nomenclature (see Section 2.2.1 and Fig. 3). The western province, closer to the sediment source, is characterised by coarser sediments of coastal/shallow marine sandstones and shales, while the central and eastern areas are dominated by marine shales with minor siltstones and sandstones, as they were deposited in the more distal part of the basin (Hounslow et al. 2008a, b). Such palaeogeographic setting is visualized in Fig. 2, where the mentioned fining eastwards trend is clearly visible.

The Early Triassic lithological divisions will be now described briefly in more detail.

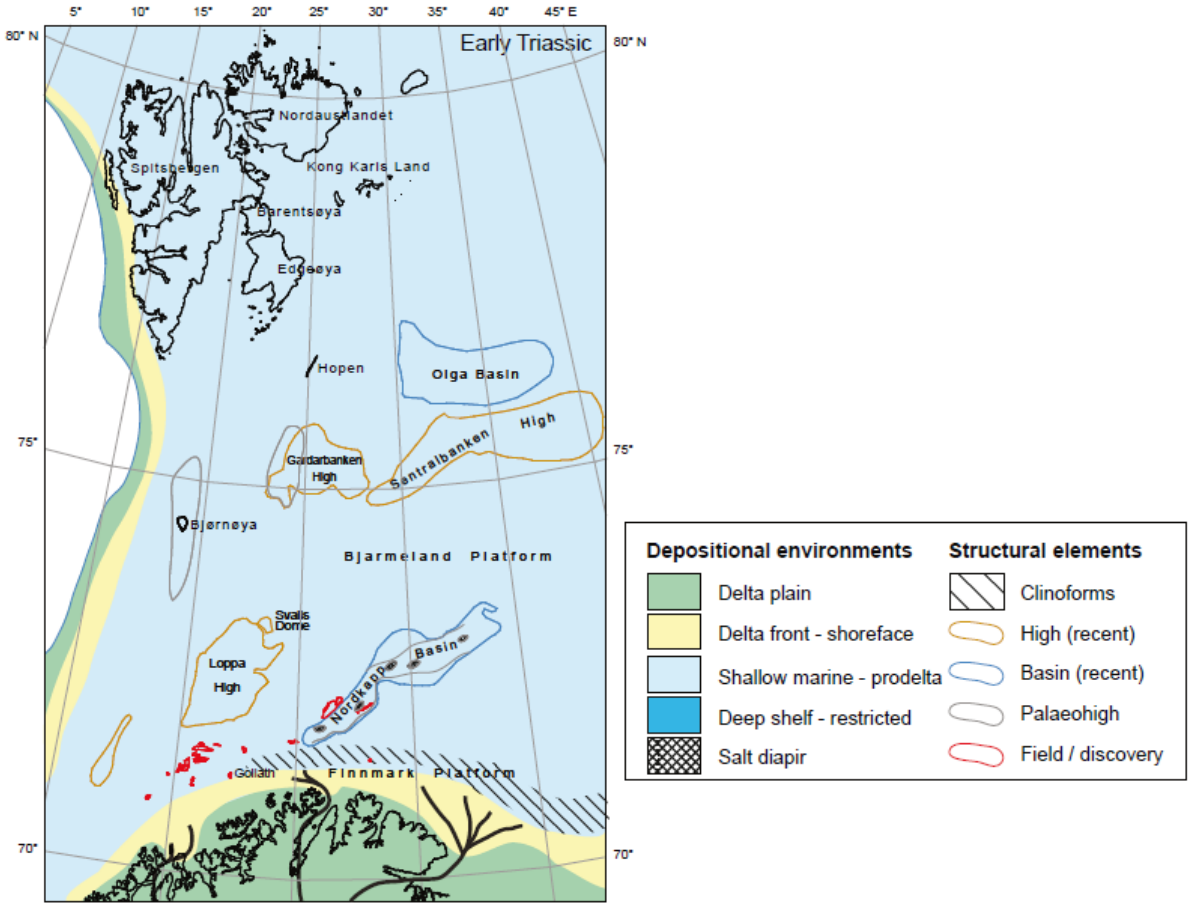

Fig. 2 Palaeogeographic setting during Early Triassic (from Lundschien, Høy & Mørk, 2014, fig. 10a).

2.2 Early and Middle Triassic deposits: the Sassendalen Group

The Sassendalen Group (~700 m thick) spans the Early and Middle Triassic and is exposed in western, central and eastern Spitsbergen, and on the islands Barentsøya and Edgeøya (see e.g. Fig. 4) (Vigran et al. 2014). The group can be divided into three main coarsening upward units, which reflect transgressive-regressive cycles that can be traced throughout the Boreal Triassic (Barents Sea Shelf, Arctic Canada and East Siberia) (Vigran et al. 2014). This repetitive pattern reflects periodical subsidence followed by progradation, as mentioned above, but on the whole transgression occurred. The fauna and sediments and the organic content indicate increasing depth and lower environmental energy with time (Mørk et al. 1982). The lithology varies greatly depending on the areas (Hounslow et al. 1996). The main lithologies are shales, siltstones and sandstones. Phosphatic nodules and very high organic content characterise the Middle Triassic part (Mørk et al. 1999a; Vigran et al. 2014). The depositional

environment is deltaic/coastal/shallow shelf in the west with gradation eastwards and southwards into deeper shelf mudstones (see Fig. 2).

2.2.1 Nomenclature overview

The Sassendalen Group was first defined by Buchan et al. (1965), who divided it into the Vardebukta (Induan), Sticky Keep (Olenekian) and Botneheia (Anisian - Ladinian) formations. The names were applied to all Svalbard areas. Many changes were proposed by other authors since then, though the most relevant revision was by Mørk et al. in 1982. They constructed a scheme accounting for the variations between western and central/eastern areas, and the current definition of the group was established. A single formation (the Barentsøya Formation), originally defined by Lock et al. (1978) for the eastern islands, was extended to eastern and central Spitsbergen. It kept the original threefold division from 1965, though as member subdivision. The Vardebukta Formation was limited to western areas, as the Deltadalen Member was established for eastern/central Spitsbergen and the islands (Mørk et al. 1982). Pčelina, in the 1980s, developed a similar nomenclature scheme using different criteria and efforts have subsequently been made to put together the Norwegian and Russian nomenclature systems (Mørk et al. 1999a, b). For a summary of the most important nomenclature changes and current names see Fig. 3.

As it can be understood from the brief overview above, the nomenclature is quite complex.
The central and eastern areas, including the islands, represent as mentioned the more distal sedimentation. Due to the difficulty in identification of the boundary between the Deltadalen and Sticky Keep members of central Spitsbergen (since this boundary is similar to another one within the Sticky Keep Member), the two lower units were united into one single formation, called the Vikinghøgda Formation (Mørk et al. 1999b). The Vikinghøgda Formation, as will be discussed in more details below, is divided into three units: the lowermost one, the Deltadalen Member, is unchanged, while the other two members, the Lusitaniadalen and Vendomdalen members, have replaced the Sticky Keep Member (Mørk et al. 1999a). The Botneheia Formation represents the Middle Triassic.
As for western Spitsbergen, the more proximal part of the basin, the formation names used are Vardebukta (Induan), Tvillingodden (Olenekian) and Bravaisberget (Anisian/Ladinian).

Fig. 3 Overview of the most important changes in the nomenclature of the Sassendalen Group, Svalbard (modified from Mørk et al. 1999a, b).

			Buchan et al. (1965)	Flood et al. (1971); Major & Nagy (1972)		Lock et al. (1978)		Mørk et al. (1982)		Pčelina (1983)		Mørk et al. (1999b)		
	Age	Stage	Svalbard	Spitsbergen, Barentsøya, Edgeøya		Barentsøya, Edgeøya		Western Spitsbergen	Central/Eastern Spitsbergen, Barentsøya, Edgeøya	Western Spitsbergen	Central/Eastern Spitsbergen, Barentsøya, Edgeøya	Western Spitsbergen		Central/Eastern Spitsbergen, Barentsøya, Edgeøya
Sassendalen Group	Middle Triassic	Anisian - Ladinian	Botneh. Fm.	Kongressfjellet Subgroup	Botneh. Fm.	Barentsøya Fm.	Oil shales Mbr.	Bravaisb. Fm.	Barentsøya Fm. Botneheia Mbr.	Van Keulenfjorden Fm.	Botneheia Fm.	Bravaisberget Fm.		Botneheia Fm.
										Bravaisb. Fm.	Hyrnef. Fm.			
	Early Triassic	Olenekian – Spathian	Sticky Keep Fm.		Sticky Keep Fm.			Tvilling. Fm.	Sticky Keep Mbr.	Pitnerodden Fm.	Wichebukta Fm.	Tvilling. Fm.	Ka. Mbr.	Vikinghøgda Fm. Vendomdalen Mbr.
		Olenekian – Smithian											Is. Mbr.	Lusitaniadalen Mbr.
		Induan – Dienerian	Vardeb. Fm.	Vardebukta Fm.		Vardebukta Fm.		Vardebukta Fm.	Deltadalen Mbr.	Vardebukta Fm.		Vardebukta Fm.		Deltadalen Mbr.
		Induan – Gries.												

Tvilling. Fm. = Tvillingodden Formation, Hyrnef. Fm. = Hyrnefjellet Formation, Ka. Mbr. = Kaosfjellet Member and Is. Mbr. = Iskletten Member

The Tvillingodden Formation was called Pitnerodden Formation by Pčelina (1983) (Mørk et al. 1999a).
The boundary between the two lower units of the Vikinghøgda Formation approximates to the Induan – Olenekian boundary, which corresponds to the Dienerian – Smithian transition (Mørk et al. 1999b).

2.3 The Vikinghøgda Formation

The Vikinghøgda Formation replaces thus in the central/eastern areas the Vardebukta and Sticky Keep formations previously defined by Buchan et al. in 1965 and the lower Barentsøya Formation of Lock et al. (1978), better defining the lithological variations (Mørk et al. 1999b).

The Vikinghøgda Formation is delimited by the Botneheia Formation above and the Permian Kapp Starostin Formation below (see Figs. 4-5). The type section localities are different for the various members: Deltadalen for the homonymous member (type section of Mørk et al. 1982); Vikinghøgda and Sticky Keep for the other members (Mørk et al. 1999b). The thickness is ~250 m in the type section, but diminishes eastwards. In particular, the three members are respectively 68 m (Deltadalen Member), 88 m (Lusitaniadalen Member) and 94 m (Vendomdalen Member) in the type section. The thicknesses are, however, variable (Mørk et al. 1999a).

As seen from the log in Fig. 6a (with associated legend on Fig. 5b), the formation is predominantly composed of silty shales with subordinate siltstones interbedded by fossiliferous carbonate beds and nodules (see below for more details on each member) (Mørk et al. 1999a, b; Lundschien et al. 2014). The limestones were formed in periods of oxygenation, while low-oxygen bottom conditions prevailed otherwise (Mørk et al. 1982; Nakrem et al. 2008). The formation can be divided into stacked transgressive-regressive cycles and the lower boundary of each member is defined by the onset of a transgressive episode, whose extent can be mapped throughout all Svalbard. All the members are dominated by shales and mudstones in their lower parts, but the sandstone/siltstone content increases upwards. Each member represents then a more distal environment than the underlying one and gets organic richer (Mørk et al. 1999a; Hounslow et al. 2008a).

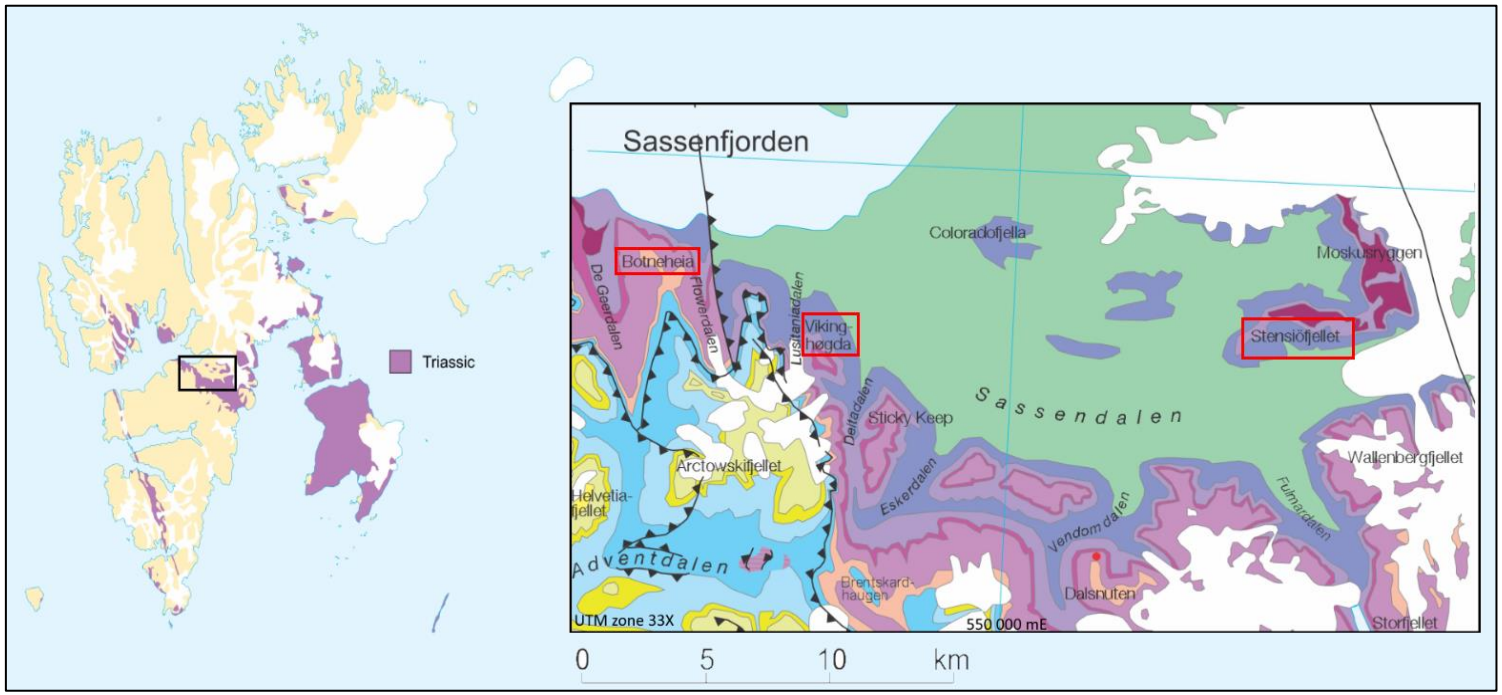

Fig. 4 Overview map over the Triassic sediments in Svalbard, with close up on the northern Sassendalen area. Stensiöfjellet, the locality from which the studied fossils were collected, and the other important localities mentioned in the text are highlighted (Maps modified from the Norwegian Polar Institute).

This formation is best dated by ammonoids (in addition to bivalves, conodonts and palynomorphs) and six zones are identified which can be correlated with other areas in the Arctic, though some intervals may be missing or condensed (Mørk et al. 1999b). The biostratigraphic divisions will be discussed in Chapter 4.

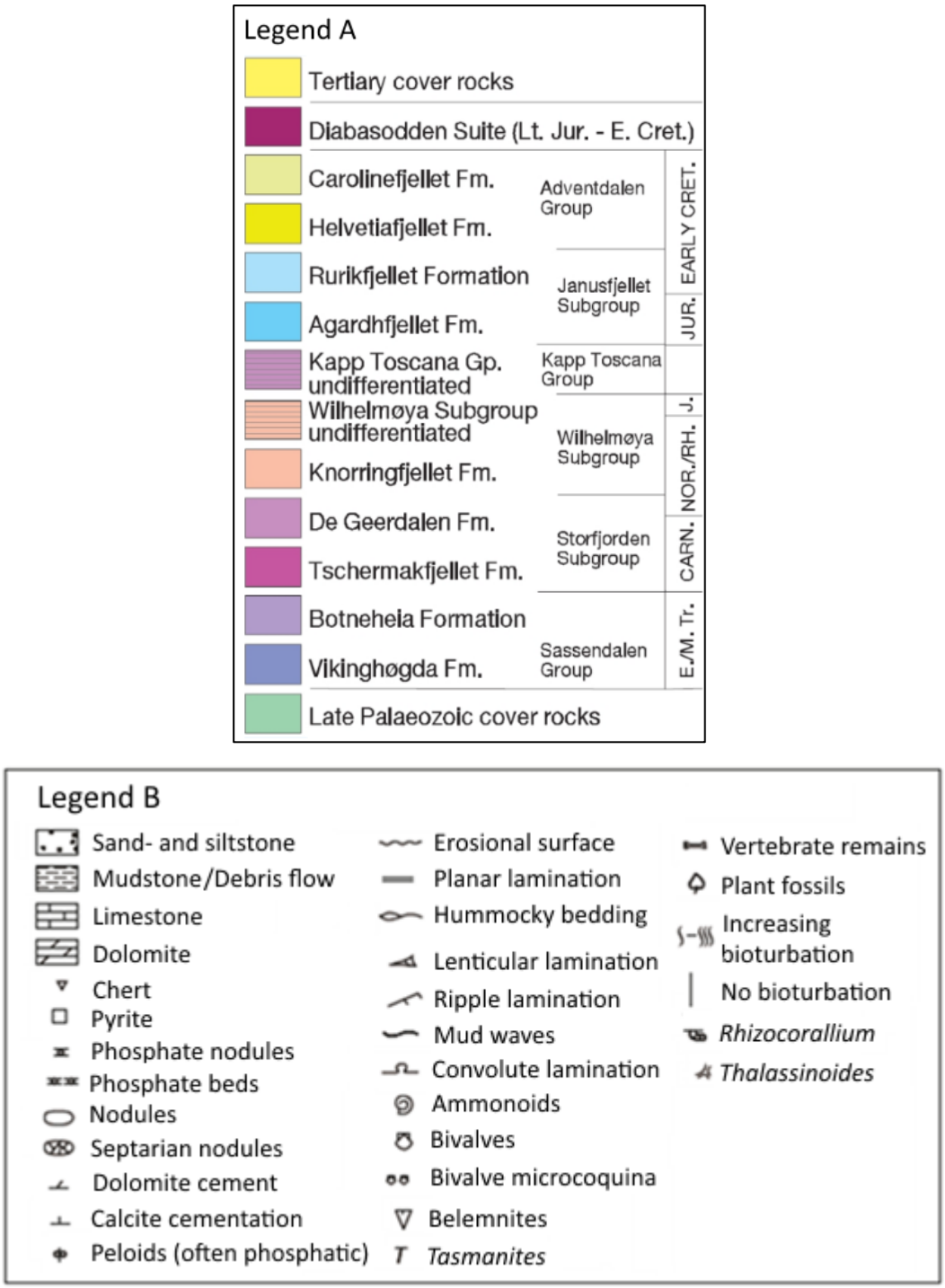

Fig. 5 Legends over the lithologies in the geological map (Legend A, modified from the Norwegian Polar Institute) and over the symbols used in the log (Legend B, modified from Vigran et al. 2014, fig. 18).

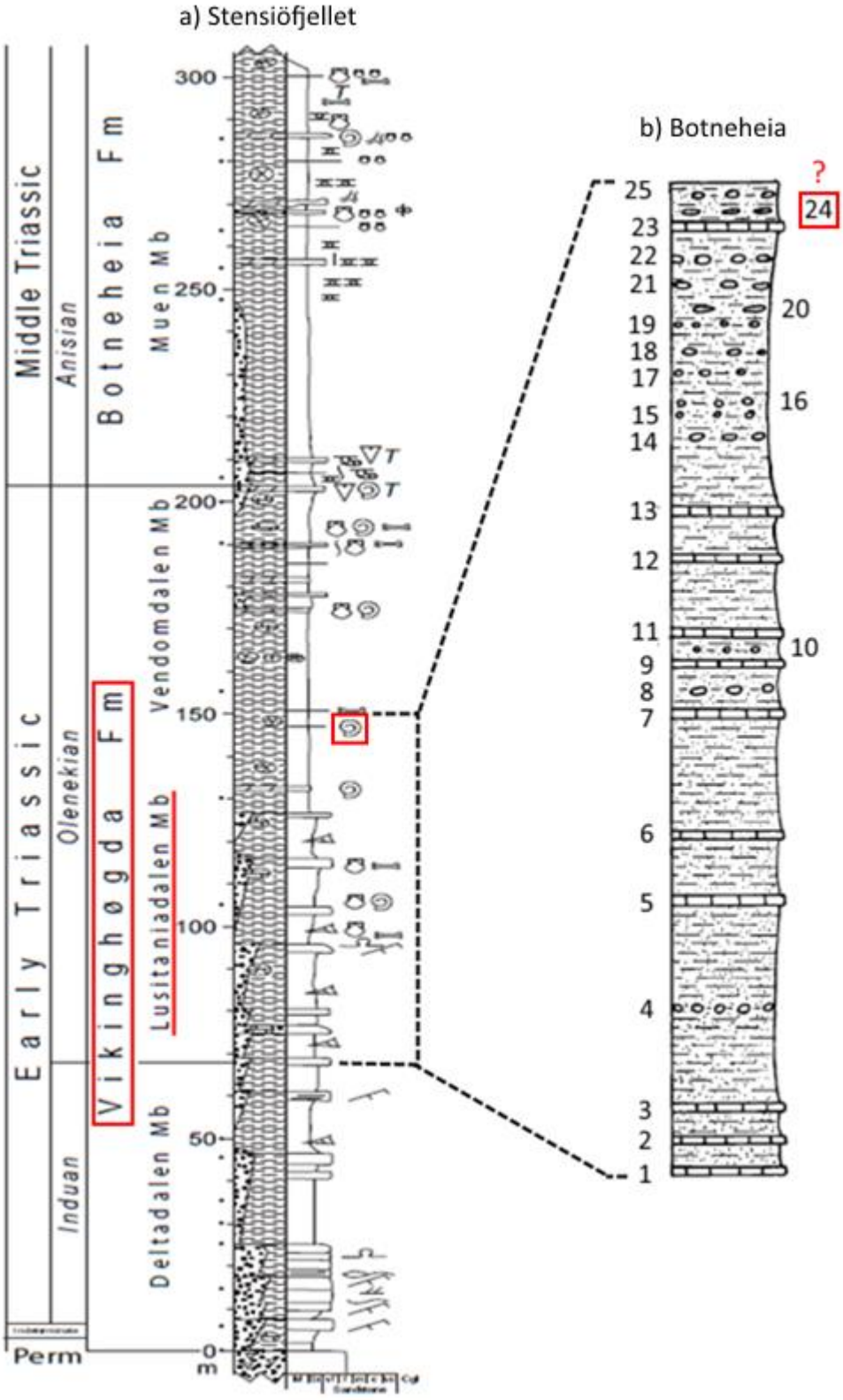

Fig. 6 Log sections of the Vikinghøgda Formation at Stensiöfjellet (a) and Botneheia (b). The limestone concretion to which the studied fauna may belong has been marked in the log from Botneheia by comparing the study material with the described fauna and hence the most likely correlation with log a) has been made (modified from Vigran et al. 2014, fig. 38a (log a), and Weitschat & Lehmann 1978, fig. 3 (log b)).

2.3.1 The Deltadalen Member

The Deltadalen Member is laterally equivalent to the Vardebukta Formation in the west (Fig. 3). It is mostly of Induan age, but the P-T boundary lies close to the base, still within the member (Vigran et al. 2014). The main lithologies are silty shales alternating with siltstones/fine hummocky-laminated sandstones (Fig. 6a). Carbonate concretions are also present. The member can be further divided into two coarsening-upwards units. The depositional environment is a shallow to moderately deep shelf. The transition to the Lusitaniadalen Member is defined by a reduction of the sandstone beds (Mørk et al. 1999a).

2.3.2 The Lusitaniadalen Member

The Lusitaniadalen Member is approximately the lateral equivalent of the western Iskletten Member (Tvillingodden Formation) and of the lower part of the former Sticky Keep Formation/Member (Mørk et al. 1999b) (Fig. 3). Using ammonoids, palynomorphs and bivalves the member has been assigned to the Smithian. The main lithologies are dark grey shales with sandstones, calcareous siltstones and limestone nodules/concretions (Mørk et al. 1999a; Lundschien et al. 2014) (Fig. 6).The lower part of this member is characterised by dark grey laminated silty mudstones interbedded with thin planar laminated sandstones/siltstones. The mudstone is on the whole finely laminated, with little bioturbation. Both sandstone and carbonate beds occur: the sandstones are hummocky and cross-laminated, while the carbonates get more prominent in the middle and upper parts. The carbonate concretions have most likely an early diagenetic origin, as indicated by the deformation of the shales around them and the good preservation of the fossils contained in such concretions. They are usually well defined and with a general thickness of 0.1-1 m. A ~0.9 m thick ferroan dolomitic silty-sandstone with mudstone interbeds is located in the uppermost part of the member (Hounslow et al. 2008a; Mørk et al. 1999a). The change from the Lusitaniadalen Member to the Vendomdalen Member is marked by a gradual shift from silty shales with sandstones to dark grey and uniform mudstones (Mørk et al. 1999a). The most abundant fossils are ammonoids and bivalves; they occur throughout the member except for the lowermost 30 m (Mørk et al. 1999b). A detailed description of the ammonoid faunal assemblages will be given in later chapters.

The depositional environment was a moderately deep shelf; the sequence is overall shallowing upwards (Mørk et al. 1999a). It is more distal with respect to the western source and to the underlying Deltadalen Member (Mørk et al. 1999b; Lundschien et al. 2014).

The Lusitaniadalen Member is the unit which this project focuses on, and the ammonoid fauna here studied was collected at Stensiöfjellet (see map on Fig. 4). This member corresponds to the formerly called "Fish-Niveau" (Wiman 1910), *Anasibirites* horizon and lower Posidonomya shales (Spath 1921), and *Goniodiscus nodosus* horizon (Frebold 1930) (see Section 4.2) (Buchan et al. 1965; Mørk et al. 1999a). The unit was also studied by Weitschat and Lehmann (1978), in the nearby locality of Botneheia. The most recent log (Fig. 6a) and the log Weitschat and Lehmann obtained (Fig. 6b) are compared. As mentioned previously, the section was not personally observed, but knowing that the studied collection comes from a limestone concretion from the uppermost part of the member, the faunal assemblages described by Weitschat & Lehmann (1978) were compared to the one here studied. As a result the limestone bed 24 (see Fig. 6b) was chosen as the most likely candidate source for the study material. Bed 24 contains in addition to ammonoids e.g. the nautiloid *Orthoceras* sp., and this genus is also present in the studied collection. The level marked in the Stensiöfjellet section (Fig. 6a) was hence identified with higher certainty.

2.3.3 The Vendomdalen Member

The Vendomdalen Member is equivalent to the upper part of the former Sticky Keep Formation/Member and to the Kaosfjellet Member (Tvillingodden Formation) in the west (Fig. 3). It corresponds approximately to the level of the *Arctoceras* horizon of Frebold (1930), the Lower Saurian and Grippia Niveaus (Wiman 1910) and the upper Posidonomya shales (Spath, 1921) (Buchan et al. 1965; Mørk et al. 1999a). Its depositional age is Spathian (Mørk et al. 1999b). This member is mainly composed of dark grey silty mudstones with medium/thick yellow-weathering dolomite beds (Lundschien et al. 2014). Large septarian nodules are located in the lower part, but small carbonate nodules are found throughout the whole member. A fossiliferous thick silty dolomite bed is found at the upper boundary. Also, in the uppermost part, phosphatic nodules appear indicating the transition to the overlying Botneheia Formation (Hounslow et al. 2008a). The depositional environment was a moderately deep to deep shelf (Mørk et al. 1999a).

3. Triassic palaeogeography: the faunal realms

The uniform palaeogeographic Triassic setting (Fig. 7), with the NS barrier represented by Pangea, is reflected by quite simple faunal patterns (Page 1996). Panthalassa was the main ocean surrounding the vast continent, while Tethys was a smaller equatorial ocean (Brayard et al. 2006).

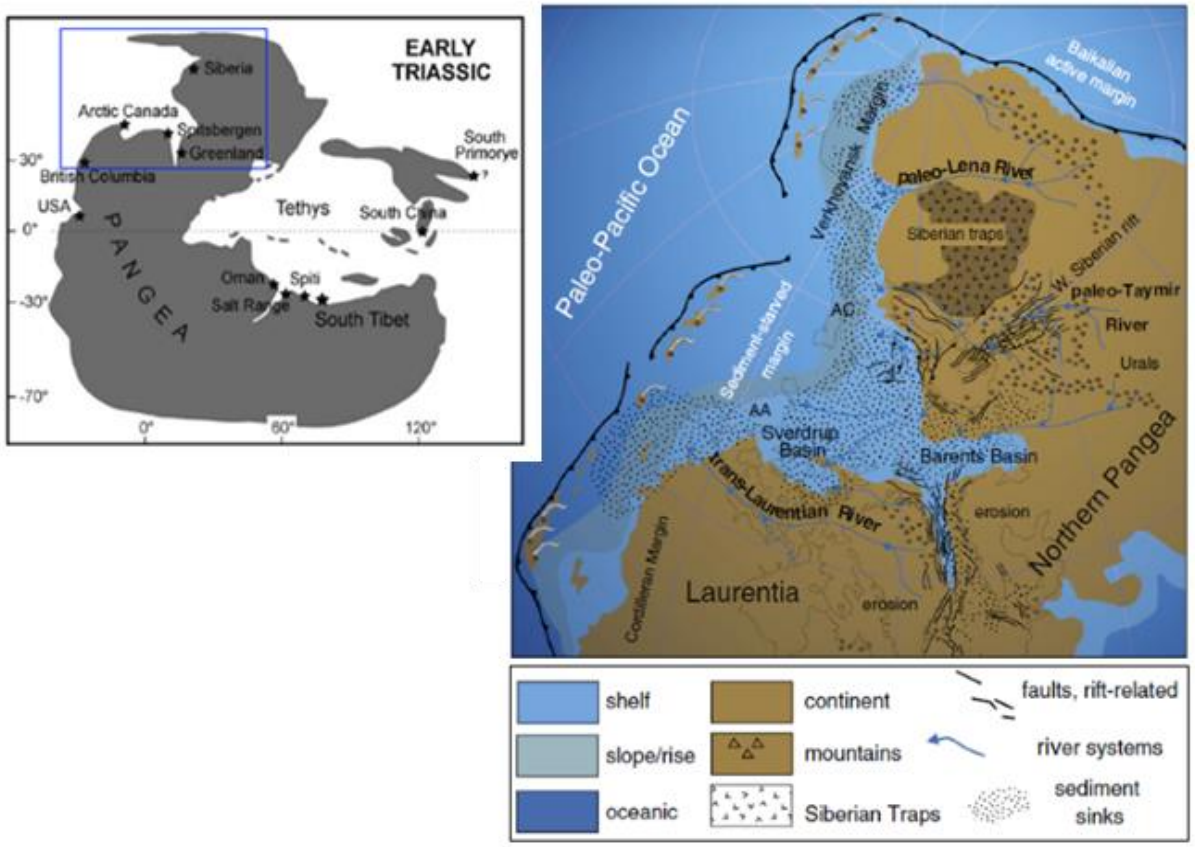

Fig. 7 Early Triassic palaeogeographic setting. Spitsbergen, as well as the other important Boreal and Tethyan localities, are marked in the map on the left (from Brühwiler et al. 2010, fig. 1). A close-up on the Arctic is shown in the figure on the right (from Miller et al. 2013, fig, 1).

First of all it is worth mentioning that faunal distribution patterns can be divided into specific categories: pandemic/cosmopolitan (taxa are globally widespread), latitude-limited (the diversity decreases towards higher latitudes) and endemic (taxa are restricted to specific provinces) (Page 1996). These patterns were all relevant during the Early Triassic (see Section 3.1). Fig. 8 shows for example ammonoid generic richness variations during the Smithian depending on the latitude: it is to be noted how the richest diversity is located at

lower latitudes. Moreover, the distribution can be influenced by geographic barriers and post-mortem processes (Page 1996).

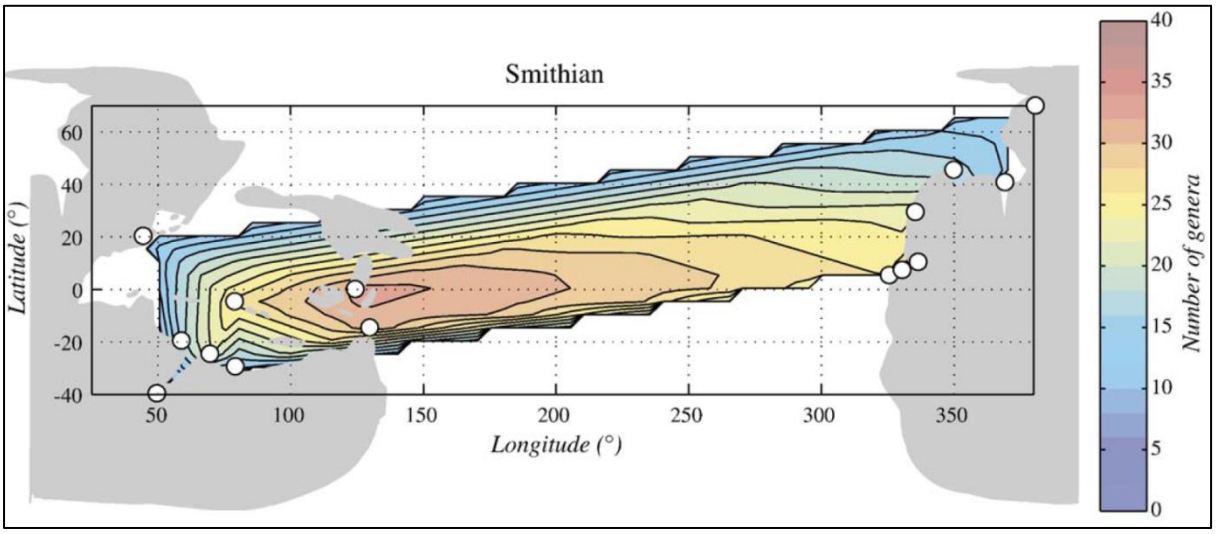

Fig. 8 Ammonoid richness (generic diversity) contour map for the Smithian (modified from Brayard et al. 2006, fig. 10).

The largest biogeographic areas into which ammonoids and marine fauna in general are divided are called realms. The Boreal and Tethyan Realms were the most important recognised throughout the Mesozoic. The Tethyan Realm extended to lower latitudes, while the Boreal Realm extended to northern latitudes (Page 1996).

The Boreal Realm included Svalbard in addition to Greenland, Canada (British Columbia and Arctic Canada) and Russia (Siberia). The faunas from these areas are characterised mainly by low diversity, high endemism and significant intraspecific variation (that is the morphological variety in same species/genus; see Chapter 5 for more details). It is estimated that just 1/5 of all Triassic genera are found in the Boreal Triassic, half of them being cosmopolitan genera. This may be indication of a stressed environment (Page 1996).

The Boreal Realm can be divided since the Early Triassic into western (Canadian) and eastern (Siberian) provinces according to taxonomic differences of the ammonoid assemblages. The Canadian Province was characterised by mixed faunas with Tethyan immigrants, as connections were present with the warmer Tethyan Ocean (Zakharov et al. 2002). In contrast, the Siberian Province was characterised by highly endemic taxa (Konstantinov 2008).

Svalbard was located somewhat in between these two big provinces and presents affinities to both of them. In the Early Triassic the faunal assemblages resembled more closely the Canadian faunas but such affinities were not constant. Due to these intermediate affiliations, the establishment of a Svalbardian province has been proposed (Weitschat & Dagys 1989).

3.1 Early Triassic ammonoid trends

The ammonoid diversity trend was variable during the Early Triassic. Such variability can give information about the sea-surface temperature (SST), which controls the latitudinal diversity gradient (defined by the latitudinal gradient of generic richness, LGGR). A steep SST gradient would indicate high global diversity (a steep LGGR) and more contrasted climatic conditions between the different latitudes. On the contrary, a flat SST gradient (corresponding to a flat LGGR) would indicate cosmopolitan and impoverished faunas, i.e. a homogeneous climate. So, a better understanding of geographic faunal distributions would give additional evidence about climatic changes (e.g. Galfetti et al. 2007).

As observed from Fig. 9, the recovery of Early Triassic ammonoids is characterised by episodes of cosmopolitanism alternating with periods of endemism. In general the trend was however inclined towards increasing endemism (Brayard et al. 2006).

The Smithian in particular represents the period of lowest provincialism (Weitschat & Dagys 1989) (see Fig. 9). The beginning of this stage is characterised by a short phase of cosmopolitanism with poorly contrasted SST/LGGR gradients and consequently low endemism. It is followed by an intensification of geographical differentiation with increasingly steeper SST/LGGR gradients until the end of the Smithian, corresponding to the *tardus* Zone and its low-latitude equivalent *A. pluriformis* Zone. The drop in diversity at the end of the Smithian is sharp and suggests a significant climatic event which caused a flattening of the SST and LRGG gradients. The Smithian/Spathian boundary represents a major faunal turnover in ammonoid evolution in the Early Triassic, with a renewed increase in the SST/LGGR gradients steepness during the Spathian (Brayard et al. 2006; Galfetti et al. 2007).

Tozer (1982) was the first to notice that an almost total extinction at the end of the Smithian occurred followed by a rapid radiation in the Spathian. The Late Smithian is characterised by low-diversity assemblages worldwide dominated by cosmopolitan prionitids (Galfetti et al. 2007).

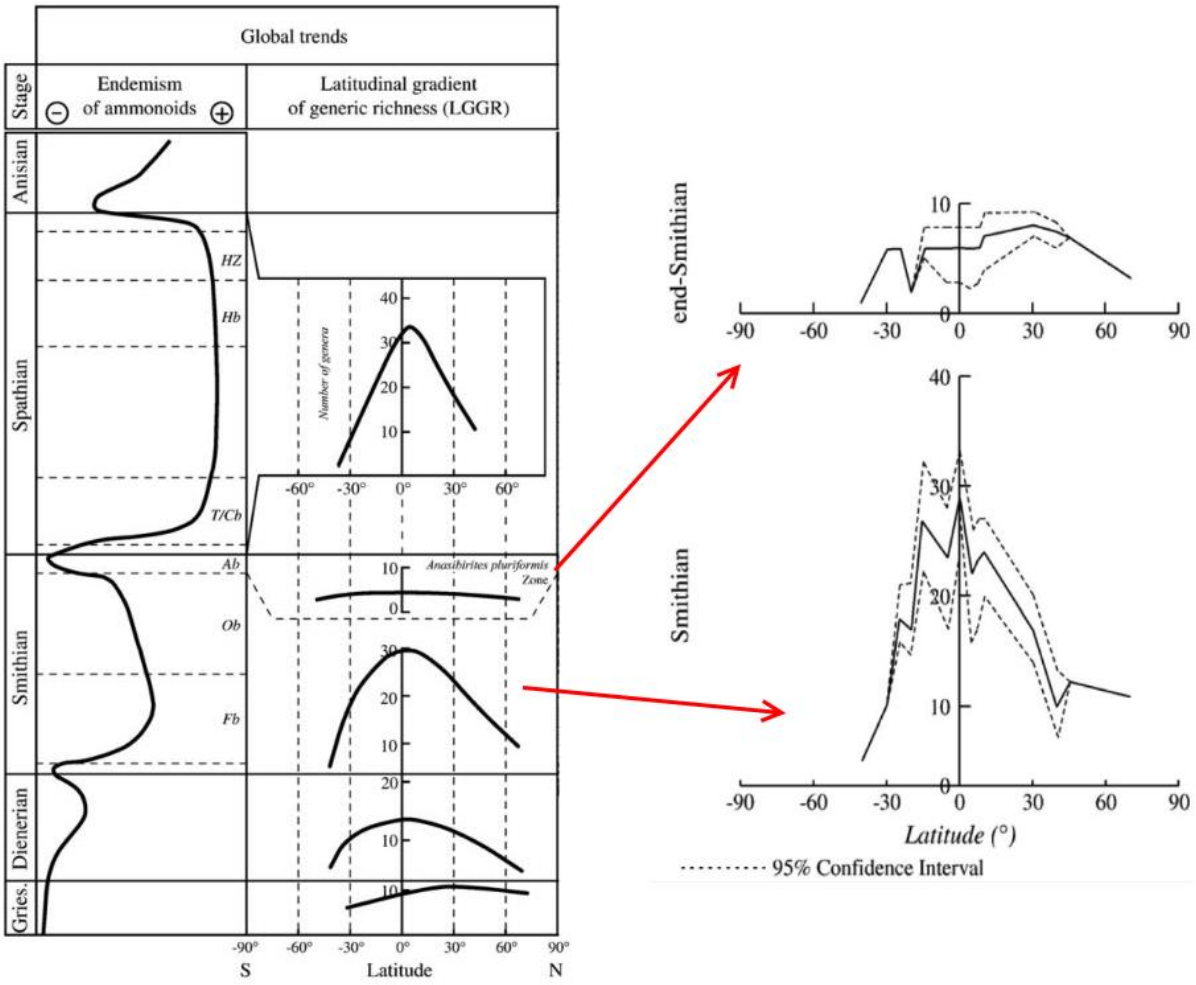

Fig. 9 Ammonoid endemic and latitudinal distributions during the Early Triassic, with focus on the genera abundance variation during the Smithian (modified from Galfetti et al. 2007, fig. 7 and Brayard et al. 2006, fig. 5).

The subdivision of the Boreal Triassic reflects therefore, as can be observed from Fig. 9, the major changes that occurred during ammonoid evolution. Trends such as the change from cosmopolitan faunas to more endemic ones have been identified not only in the Triassic and have been related to eustatic sea level changes by Enay (1980), who called them "faunal rhythms" after his studies on the Jurassic (Dagys 1994). Major transgressions occurred for example at the beginning of the Smithian and the beginning of the Spathian throughout the Boreal Realm. They correspond to faunal episodes, suggesting a correlation between ammonoid faunal turnovers and eustatic mechanisms (Mørk 1994).

3.2 Boreal ammonoid assemblages

Turning now more specifically to the Boreal regions, Triassic ammonoids occur mostly in carbonate or phosphate concretions (Weitschat 2008). Compared to assemblages in the Tethyan Realm, condensation is rare.

The faunal diversity, as already mentioned, is quite low (Dagys & Weitschat 1993b) and endemism on the contrary quite high. Different kinds of assemblages are recognised, which are usually mostly embedded *in situ*. They can be divided into (Dagys & Weitschat 1993b):

- Assemblages composed of adult individuals. Such assemblages may imply migration of adults into spawning areas with their subsequent death.
- Assemblages with only juveniles and subadult individuals, which imply that juveniles and adults may have lived separately.
- Assemblages composed mainly of one species, with all ontogenetic stages present and rare specimens of other genera.
- Assemblages composed mainly of several genera with all ontogenetic stages. This kind is rare especially on Svalbard.

The important characteristics of the intraspecific variation which characterises Boreal ammonoid assemblages will be treated and discussed separately in Chapter 5.

4. Early Triassic ammonoid biostratigraphy

Ammonoids have long been used as index fossils for biostratigraphic research due to their rapid evolution and relatively short range of each species. The provinciality of ammonoid taxa has however caused problems for correlation: taxa found in the Tethys are for instance not found in the Boreal Realm and vice versa. Moreover, as mentioned in the previous chapter, eastern Boreal faunas are different from the western ones. To solve this difficulty, integrative scales based on other fossil groups (e.g. bivalves, conodonts and nautiloids) have been used (Lucas 2010). A direct correlation can however be made for specific events, like eustatic episodes, which occurred over broad areas and imply an equalization of the fauna. The Late Smithian *tardus* Zone, with its cosmopolitan assemblages, is an example (Zakharov et al. 1997).

The development of a Triassic ammonoid biostratigraphic scale has therefore suffered due to the problems regarding the correlation between the Boreal and Tethyan Realms in addition to a (often unnecessarily) complicated taxonomy (Lucas 2010).

4.1 The Boreal Early Triassic

In the Mesozoic Svalbard was joined to North America, Greenland and Eurasia, as mentioned and shown in Chapters 2 and 3. This palaeogeographic setting explains the similarities between the different sections of Siberia, Greenland, Svalbard, Arctic Canada and British Columbia, making possible a Boreal correlation: the completeness of the record is variable depending on the considered region. Greenland presents the least complete record of all (Dagys & Weitschat 1993c): it will not be therefore considered in this work.

The Early Boreal Triassic ammonoid zones were first developed by Tozer in the 1960s in Arctic Canada (Sverdrup Basin) (Mørk 1994). All zones have their type localities in the Sverdrup Basin, except for the Early Smithian *hedenstroemi* Zone which has its type locality in Siberia (Nakrem et al. 2008).

Many of the best and most complete sections are from Siberia and North-eastern Asia (Konstantinov & Klets 2009). The sections in British Columbia are also very detailed and in

addition they contain mixed Tethyan and Boreal taxa, permitting a direct Tethyan-Boreal correlation (Zakharov et al. 1997), as mentioned in Chapter 3.

4.1.1 The *tardus* Zone in the Boreal Realm

The Boreal Smithian has been subdivided into three ammonoid zones (see Figs. 10 below and Fig. 11, Section 4.2): the *hedenstroemi* (not found in Svalbard and British Columbia), *romunderi* (called *kolymensis* in Siberia) and *tardus* zones. The *tardus* Zone will be discussed in more detail as it is most relevant for this project.

The Late Smithian *tardus* Zone (index species *Wasatchites tardus* (McLearn)) is characterised by prionitid genera such as *Wasatchites*, *Anasibirites* and *Hemiprionites*, in addition to the xenoceltitid *Xenoceltites*, which have a cosmopolitan distribution and facilitate correlation (Brühwiler et al. 2010). This zone has its type locality in north-eastern British Columbia (Toad Formation, Toad River) and can be tracked to the Barents Sea Shelf. It corresponds to a transgressive system tract of the Smithian/Spathian transgressive sequence (Vigran et al. 1998).

The faunas of British Columbia and Arctic Canada (e.g. Queen Elizabeth Islands) are more closely related to the faunal assemblages in Svalbard, as mentioned previously. They have in common for instance the genus *Arctoprionites*, which is not found in Siberia. The faunal assemblages of Siberia are characterised by the presence of more endemic and restricted genera/species that are not found in the other Boreal areas. Moreover it should be mentioned that in British Columbia *Xenoceltites* occurs in the beds above the ones containing *Wasatchites*/*Anasibirites* (Tozer 1994) while in Svalbard and Arctic Canada these genera occur together (Weitschat & Lehmann 1978; Tozer 1961).
The *Anasibirites/Wasatchites* fauna of the Boreal *tardus* Zone has been recognised in different areas worldwide, not only in the Boreal Realm. The correlations with the Tethyan Realm will be briefly described in the following section.

4.1.2 Comparisons with the Tethyan Realm

The Tethyan Smithian subdivision (Fig. 10) is much more complex and articulated than the Boreal one (Brühwiler et al. 2012b).
The Boreal *tardus* Zone can be correlated to the beds with *Wasatchites*/*Anasibirites* and *Xenoceltites* of many Tethyan localities (e.g. Tulong in Tibet, Oman, Spiti, Salt Range, Timor,

South China, Primorye in Russia and USA) (Brühwiler et al. 2012b). Moreover, in both the two realms the assemblages have in common the low diversity that is in contrast with older Smithian faunas. Such assemblages, both at low and higher latitudes, are, as already mentioned, dominated by prionitids (*Arctoprionites*, *Hemiprionites*, *Anasibirites* and *Wasatchites*) (Brayard et al. 2013).

Correlations within the USA are pretty straightforward (Brühwiler et al. 2010). Previously, the Smithian was divided into a lower *Meekoceras gracilitatis* and an upper *Anasibirites* zone, as recognised e.g. by Smith (1932), the latter considered by some authors a subzone of the *Meekoceras gracilitatis* Zone itself (Kummel & Steele 1962). After various revisions a more articulated biostratigraphic subdivision has been recently suggested that may improve correlation not only between eastern and western Panthalassa but also between the different palaeolatitudes. The *Anasibirites* fauna in the USA fauna is dominated by *Anasibirites*, *Wasatchites* and *Hemiprionites* and occurs above the beds with *Meekoceras gracilitatis* and *Arctoceras*. It corresponds then to the Boreal *tardus* Zone (Brayard et al. 2013).

There is however a marked difference between the late Smithian of Svalbard and other areas in the world, both Boreal and Tethyan. In Svalbard (as in Queen Elizabeth Island, Arctic Canada) the genus *Xenoceltites* occurs associated with *Anasibirites* and *Wasatchites*, as mentioned before (Weitschat & Lehmann 1978; Tozer 1961). But in the Tethys (e.g. in Tulong, Spiti, South China) it is associated with *Glyptophiceras sinuatum* above the prionitid faunas. This is evidence that the further subdivision of the uppermost Smithian into *Anasibirites* fauna followed by *Glyptophiceras*/*Xenoceltites* fauna cannot be extended to higher palaeolatitudes (Brühwiler et al. 2010). In Oman there is no evidence of *Xenoceltites*/*Glyptophiceras* above the *Anasibirites*/*Wasatchites* beds, while in Utah *Xenoceltites* have been found above the *A. kingianus* beds, suggesting a possible correlation with the *Glyptophiceras* beds (Brühwiler et al. 2010; Brühwiler et al. 2012a; Brayard et al. 2013).

Detailed correlation between the Tethyan and Boreal Realms is still uncertain due to incomplete knowledge of the ammonoid faunal assemblages and by the endemic distribution that is particular especially for higher-latitude assemblages (Brühwiler et al. 2010).

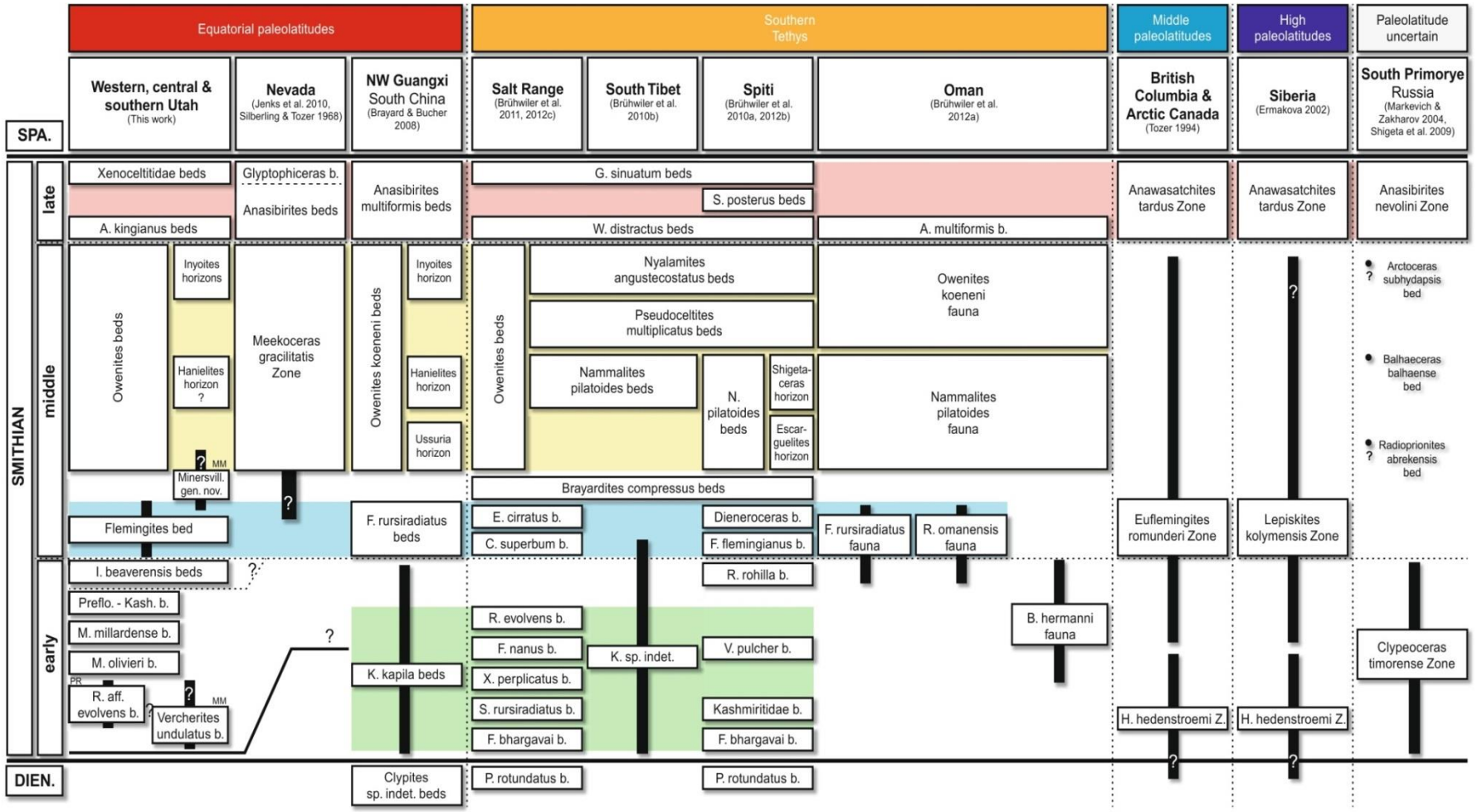

Fig. 10 Biostratigraphic correlations between the most important Tethyan and Boreal localities (from Brayard et al. 2013, fig. 14). It is mentioned that in South China Xenoceltites does occur above Anasibirites but is is included in the A. multiformis beds. The location of the Tethyan localities mentioned can be viewed in Fig. 7.

4.2 Smithian ammonoids from Svalbard

This chapter describes in more detail the Smithian faunas of Svalbard, with focus on the *tardus* Zone, reviewing briefly the main results that have been obtained through the years.

4.2.1 Previous research

Triassic fossils have been known in Svalbard for more than ca. 140 years (e.g. Öberg 1877). The Smithian strata, to which the studied section belongs and previously known as "Fish-Niveau" or "*Posidonomya* beds", were first studied by Frebold (1930) and Spath (1921, 1934). They defined two different faunal zones: an upper *Arctoceras* fauna and a lower prionitid fauna (corresponding to either *Goniodiscus nodosus* or *Anasibirites* horizon) (e.g. Buchan et al. 1965).

Later results have however contradicted such conclusions, proving that the identification of two faunas is correct but their order is actually reversed.
Kummel (1961) and Tozer & Parker (1968), for example, compared the *Arctoceras* and prionitid faunas of Spitsbergen with the *Meekoceras* and *Anasibirites* beds of Western United States and Northern Canada respectively, pointing out the strong similarities between them but the reversed order: the *Meekoceras* beds, to which the *Arctoceras* faunas is compared, lies in fact below the *Anasibirites* beds, which in turn correspond to the prionitid fauna of Spitsbergen. Kummel (1961) also suggested that the genus *Arctoceras* ranges up to the Late Smithian, though being more common in older strata.
As illustrated in the paper by Tozer & Parker (1968), two faunal zones are distinguished in Svalbard (as in British Columbia, see Fig. 11): the lower *romunderi* Zone and the upper *tardus* Zone. The genus *Arctoceras* occurs, according to Tozer & Parker (1968) and Kummel (1961), in both zones in Spitsbergen.
Improvements were made by Korčinskaja (e.g. 1970, 1973) and Weitschat & Lehmann (1978). Weitschat & Dagys in 1989 compared the Svalbard biostratigraphic zones to the ones in Eastern Siberia.
In her papers from the 1970s Korčinskaja maintains a double zonation of the Smithian in Svalbard, with a lower *Arctoceras blomstrandi* and an upper *Anasibirites* zone (e.g. 1973). In a later paper from 1986, on the other hand, the Smithian in Svalbard is represented by just one biostratigraphic zone, the *Arctoceras blomstrandi* Zone, which is subdivided into the lower *Euflemingites* and upper *Wasatchites* zones. The reason for such different division is the

believed vertical range of *A. blomstrandi* up to the uppermost Smithian, as suggested already e.g. by Kummel (1961) (Weitschat & Dagys 1989).

Such subdivisions were not confirmed by Weitschat & Lehmann (1978) and Weitschat & Dagys (1989). Instead they confirmed the classical double zonation for the Smithian in Svalbard: the lower arctoceratid fauna is correlated to the *romunder*i Zone, while the upper prionitid fauna corresponds to the *tardus* Zone. In the paper from 1978 it is however stated that *Arctoceras* does range up to the *tardus* Zone, while in the one from 1989 the presence of arctoceratids in the *tardus* Zone is not confirmed.

4.2.2 Ammonoid faunal zonations

Now, the two Smithian faunas of Svalbard will be described in more detail, with focus on the *tardus* Zone, as the studied assemblage belongs to that interval. Some of the most important biostratigraphic divisions of the Smithian in Svalbard and the correlations with the other Boreal areas cited are shown in Fig. 11.

The *romunderi* Zone

The *romunderi* Zone fauna (Middle Smithian) of Svalbard corresponds to the *Arctoceras* fauna of Frebold (1930) and Spath (1934) and is correlated to the Tethyan *Meekoceras* beds (see Fig. 10). It is characterised by large arctoceratids (Mørk et al. 1999b) that are typical in the Sverdrup Basin and in Spitsbergen. The index species *E. romunderi* is rare, while *Arctoceras blomstrandi* is more common (Hounslow et al. 2008a). *A. blomstrandi* is a long ranging ammonoid that is thought to occur throughout the whole Smithian stage, as mentioned above. It is usually more restricted to the *romunderi* zone, though on Ellesmere Island (Arctic Canada) it actually does occur with *Wasatchites* (Weitschat & Lehmann 1978).

The *tardus* Zone

The Late Smithian is defined in Svalbard as in the other areas of the Boreal Realm by the *tardus* Zone, which is dominated by prionitids. It corresponds to the *Goniodiscus*/*Anasibirites* horizon of Frebold (1930) and Spath (1934). When this fauna was first described many species were established that are no longer valid, creating confusion in taxonomy and biostratigraphy. The reason is that the high intraspecific variation of prionitids was not taken into account.

In their investigation of sections at Botneheia, Weitschat & Lehmann in 1978 described an assemblage composed of abundant *Xenoceltites* with rare *Wasatchites*, *Arctoprionites* and *Pseudosagaceras multilobatum.* In addition, the bivalve *Posidonia mimer* and the nautiloid *Orthoceras* sp. were found in one of the uppermost carbonate concretions (bed 24, see Fig. 6b). *Arctoceras blomstrandi* is restricted to the lower part of the section. It is worth mentioning that the whole section was assigned to the *tardus* Zone, since no typical ammonoids of the *romunderi* Zone were found (Weitschat & Lehmann 1978).
In a similar fashion in various sections in the Isfjorden area (see the map in Fig. 4, Chapter 2), Weitschat & Dagys (1989) found the following ammonoid species in the *tardus* Zone: *Wasatchites tardus, Wasatchites tridentinus, Arctoprionites nodosus*, *Anasibirites*. sp. nov., *Xenoceltites subevolutus*, *Pseudosagaceras* sp. nov., and the bivalve *Pseudomontis occidentalis*.
In the type section of Vikinghøgda the following species have been collected: *Wasatchites tardus*, *Xenoceltites subevolutus*, *Arctoprionites nodosus*, *Anasibirites* spp. and *Pseudosagaceras* sp., in addition to the bivalve *Pseudomontis occidentalis* (Mørk et al. 1999b).

The Svalbard fauna is consistent with the faunal assemblage from British Columbia (although there *Wasatchites* is abundant while *Xenoceltites* is rare) and Arctic Canada (Weitschat & Lehmann 1978). The genus *Arctoprionites* seems to be restricted to Arctic Canada and Svalbard. The other important prionitid genera (e.g. *Wasatchites* and *Anasibirites*) are found also in Siberia (Weitschat & Dagys 1989).

Fig. 11 Table with a review of the most important changes in ammonoid biostratigraphic zonation of the Smithian in Svalbard and correlation with the other Boreal regions.

			High-palaeolatitude						**Mid-palaeolatitude**
	Spitsbergen lithostratigraphy (Hounslow et al. 2008b)		**Svalbard**				**Siberia (Boreal Standard)**	**Sverdrup Basin (Arctic Canada)**	**British Columbia**
	West	Central - East	(Korčinskaja 1973)	(Lock et al. 1978)	(Korčinskaja 1986)*	(Dagys & Weitschat 1993c)	(Dagys & Weitschat 1993c; Konstantinov et al. 2007)	(Dagys & Weitschat 1993c)	(Tozer 1994)
Lower Olenekian (Smithian)	Iskletten Mbr. (lower Tvillingodden Fm.)	Lusitaniadalen Mbr. (upper Vikinghøgda Fm.)	Anasibirites	Wasatchites tardus	Arctoceras blomstrandi: Wasatchites tardus	Wasatchites tardus	Wasatchites tardus	Wasatchites tardus	Wasatchites tardus
			Arctoceras blomstrandi	Euflemingites romunderi	E. romunderi	Euflemingites romunderi	Lepiskites kolymensis	Euflemingites romunderi	Euflemingites romunderi
							Hedenstroemia hedenstroemi	Hedenstroemia hedenstroemi	

**As mentioned in Weitschat & Dagys 1989.*

5. Intraspecific variation and the Buckman's law of covariation

The term intraspecific variation refers to the morphological variability within one species and/or genus. It has been observed at various degrees in many ammonoid groups from the Triassic and is fairly common in Boreal taxa (e.g. Dagys & Weitschat 1993a; Weitschat 2008) (see Chapter 3). A great variation in involution and compression degree, whorl shape and ornamentation is reported in several scientific publications. Compression refers to the lateral variation (more compressed individuals are flatter) while depression refers to the ventro-dorsal variation (more depressed individuals are thicker). Both are determined by the whorl height/whorl width ratio (De Baets et al. 2012).

A pattern can be observed that relates shell shape and ornamentation: the ornamentation strength is negatively related to compression and involution degree (Hammer & Bucher 2005). So, involute compressed shells are less ornamented and grade into more evolute, thicker and more heavily ornamented ones (Figs. 12 and 13). A great variety of intermediate shell shapes, which are more common, exist in between these extremes (De Baets et al. 2012). Moreover, the higher the compression, the more the umbilical width is reduced. This has been interpreted not only as an effect of Buckman's law but also a mechanism to maintain the centre of gravity of the shell (Checa et al. 1997).

This covariation had already been described by Buckman in 1892 but it was not until 1966 that the "Buckman's law of covariation" was named by Westermann, who understood the taxonomical and biological implications (Guex et al. 2003).

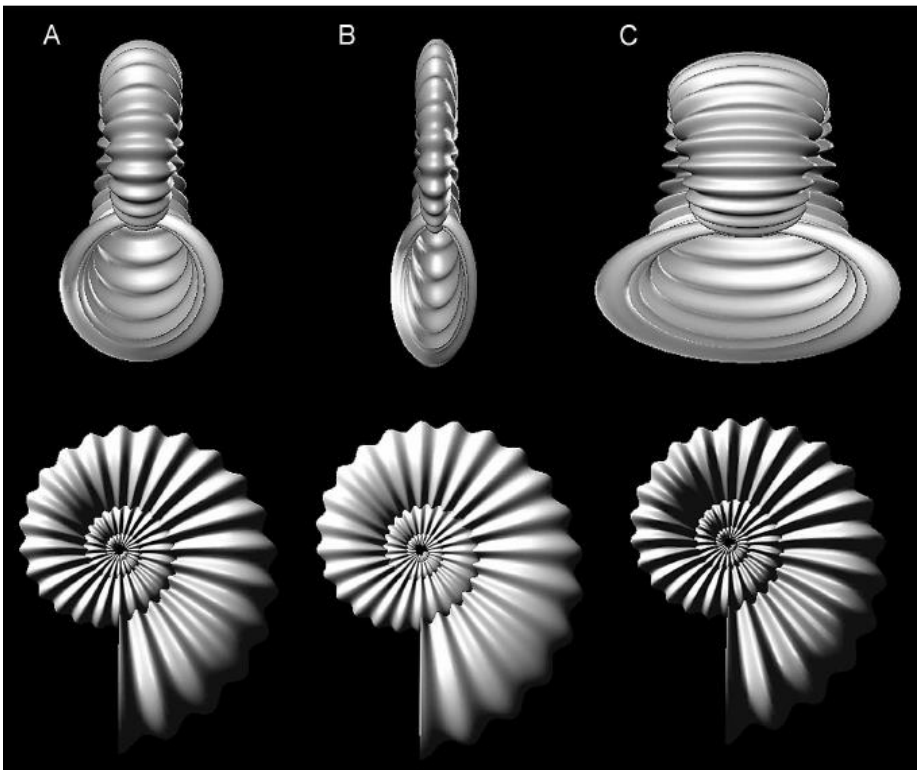

Fig. 12 Graphical model illustrating the Buckman's law of covariation: a hypothetical shell A has been compressed (B) and depressed (C). As a result the lateral ornamentation is weaker in case B but more enhanced in case C, as expected (from Hammer & Bucher 2005, fig. 3).

So, Buckman's law simply defines formally the proportionality between the various elements of the ammonoid shell. Originally this law referred only to stronger lateral ornamentation on more depressed specimens and vice versa. The implication that ventral ornamentation (including keels) is stronger on more compressed specimens was discussed by Hammer & Bucher (2005). This can be noted for example on the venters of the ammonoids shown in Fig. 13.

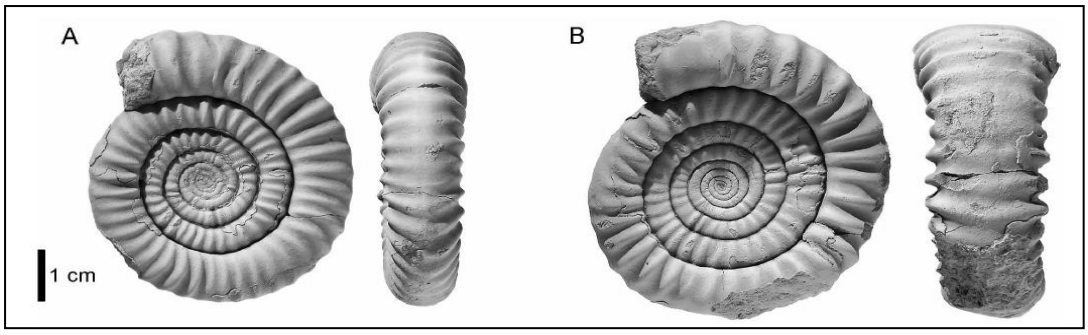

Fig. 13 Comparison between two specimens of Pseudodanubites halli (Mojsisovics) from the Middle Triassic of Nevada. Note how the ornamentation of the more compressed specimen A is slightly more subtle compared to the more depressed and more markedly ornamented specimen B (from Hammer & Bucher 2005, fig. 5). Note also how the ventral ornamentation is still evident in specimen A.

In this way the deformation that the internal soft tissues go through with compression/depression can be explained. The lateral extent of the soft parts decreases with increasing compression. As such the lateral ornamentation would be small in response, since its formation is controlled by the soft tissues (see Section 7.3). The inverse is also true as depression would "squeeze" the soft tissues laterally, making ornamentation stronger in that direction. This law would, however, be inverted for the venter: in compressed specimens the soft tissue would be thicker in the ventral direction, permitting strong ornamentation, and vice versa (Hammer & Bucher 2005). This concept is visualised in Fig. 14.

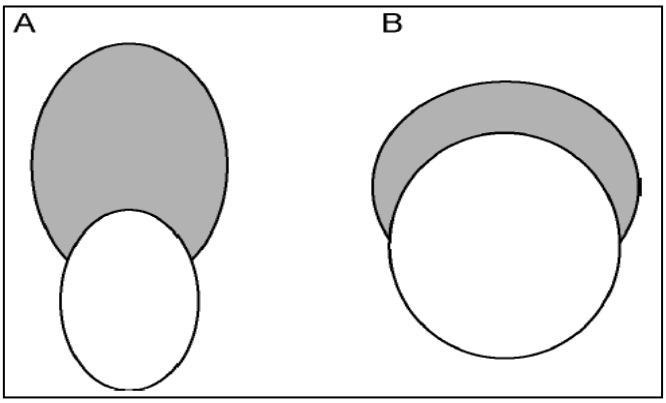

Fig. 14 Variation in extension of the soft tissue (grey areas) in evolute (A) and involute (B) ammonoids. In case A the soft tissue is thicker ventrally, so the ornamentation would be thicker on the venter in response. The contrary is true is case B (from Hammer and Bucher 2005, fig. 4).

Still, exceptions to Buckman's law exist.

Other studies, as discussed by Yacobucci (2004), have for example suggested that ornament growth may be controlled by genetic factors while shell shape is more influenced by the environment: this is a point of view very different from the Buckman's law of covariation, leading to the so-called Buckman's paradox. In many ammonoid groups this law is evident, in others it is not. This paradox is evidence that much is still unclear about ammonoid morphogenesis (Yacobucci 2004). Though, this apparent non-correlation between whorl shape and ornamentation may be related as the amount of intraspecific variation is variable from species to species (Hammer & Bucher 2005).

It may be interesting to mention that there is another law for intraspecific variation: The second Buckman's law of covariation (Westermann 1966). This law relates the ornamentation and compression degree to the complexity of the suture lines. It is discussed in Section 7.2 that sutures change during the ontogeny of an individual and look different between

individuals of the same species. The sutures are more elongated and frilled in more compressed specimens, though exceptions are to be found (Hammer & Bucher 2005).

A result of intraspecific variation/Buckman's laws is that specimens belonging to the same taxon may look very different from each other, with the consequence of having often erroneously been assigned to different species or genera (Dagys & Weitschat 1993a). This high morphological variability has caused problems for taxonomical identifications and hence for stratigraphic and ecologic interpretations (Weitschat 2008). The recognition of this variation has generally permitted simplifications in taxonomical classifications.

Different shell morphologies can then be found in the same environment, making it difficult to explain the relationship between morphology, environment and shell function that has been assumed by many authors (Dagys & Weitschat 1993b). How these different forms lived together is still not clear, but it has been suggested that selection pressure on the conch morphology was not significant (Dagys & Weitschat 1993a).

6. Data collection and methods

Working on this project gave the opportunity to experiment with different techniques common in palaeontological research. In this chapter a brief description of such techniques is given, with references to the recommendations of my supervisors and the specialised staff, as well as the theoretical guidelines provided by the manual "Paleotechniques" (1989).

6.1 Working with the specimens: a group division as a start

At the beginning of the study of this fauna, the specimens were split into groups according to the ornamentation degree: from the more compressed and smoother ones to the more depressed and coarser ones. Notes were also made if in the same group specimens were present with a similar ornamentation, but e.g. with a different kind of venter morphology. This group division was not kept when the identification of the species/genera became clearer, but it helped as a starting point to recognize trends and similarities between the different genera/species. A group division was however kept for *Wasatchites* (both adults and juveniles), as this genus shows the highest variability in ornamentation and morphology.

6.2 Measurements

The basic parameters for ammonoid morphological studies (see e.g. Korn 2010) were measured using a digital calliper.
These basic parameters are the following (see Fig. 15 for a visual representation):

D (or dm) = Maximum conch diameter measured.

W (or ww) = Maximum whorl width.

H (or wh) = Whorl height.

U (or uw) = Umbilical width.

From these parameters ratios could be calculated:

CWI = W/D = Conch Width Index. It describes the conch shape.

UWI = U/D = Umbilical Width Index. It is used to classify the umbilical width.

WWI = W/H = Whorl Width Index. It describes the shape of the whorl cross section.

While taking the measurements, the largest diameter available was recorded. It does not necessarily represent the maximum possible diameter, since the specimens may be broken. This imaginary diameter has to cross the centre of the umbilicus.

It was not always possible to measure all the parameters for each specimen due to preservation; in such cases all the possible measurements were done, but they were not included in the statistical and graphical representations to avoid having zero values in the plots.

Various kinds of statistical analyses and plots could be made using just these few parameters, as presented in Chapter 8. They were obtained by using Microsoft Office Excel 2007 © and Past 3.05 (Hammer et al. 2001).

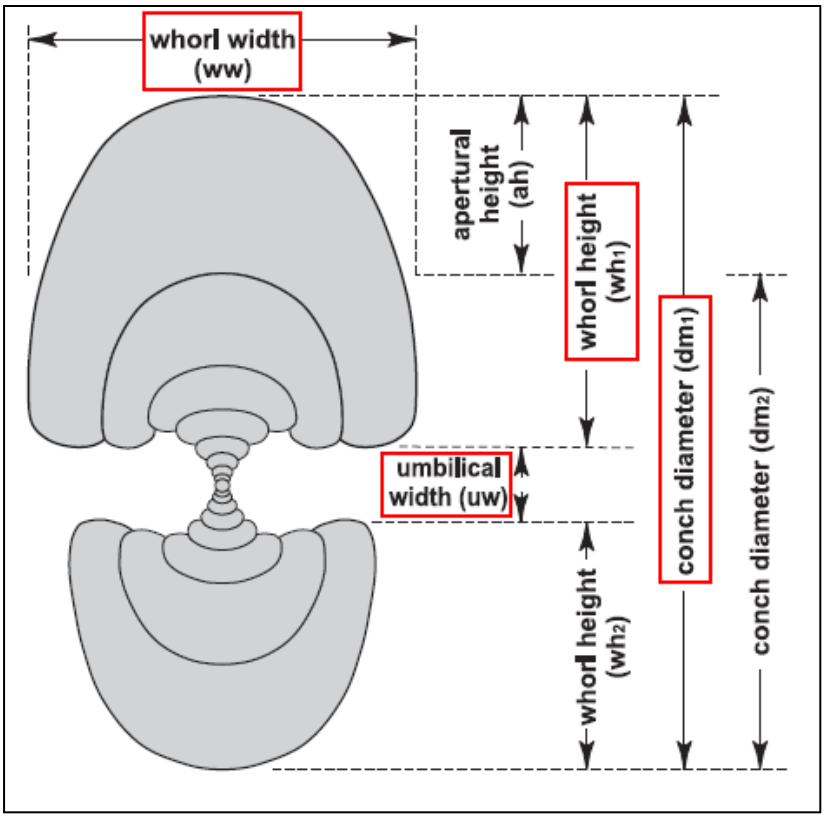

Fig. 15 Terminology for ammonoid conch morphology. The red boxes highlight the parameters used in this project (modified from Korn 2010, fig. 1).

6.3 Preparation of the specimens

Most of the specimens of the collection did not need any chemical or physical preparation. The only specimens which were prepared were the ones that were assigned to the two new yet unnamed taxa (Gen. et sp. nov. and *Arctoceras* sp. nov., see descriptions in Chapter 8).

For the purpose of a more detailed description, the vibro-hammer was used in order to clean the umbilici of the specimens as well as was possible.

The vibro–hammer (also called pneumatic tool or air scribe) (Fig. 16) is a compressed air-driven instrument which can remove matrix quite efficiently. Care must be taken since the vibrations may damage and/or break the fossil. While using this instrument it is important not to put too much pressure on the area that is supposed to be treated. It is good practice to work on small areas towards the centre of the fossil and check for loosened matrix pieces and cracks. Different needle sizes are available depending on the purpose: the smaller sizes are more suitable for delicate preparations and the bigger ones for larger fossils (Chaney 1989).

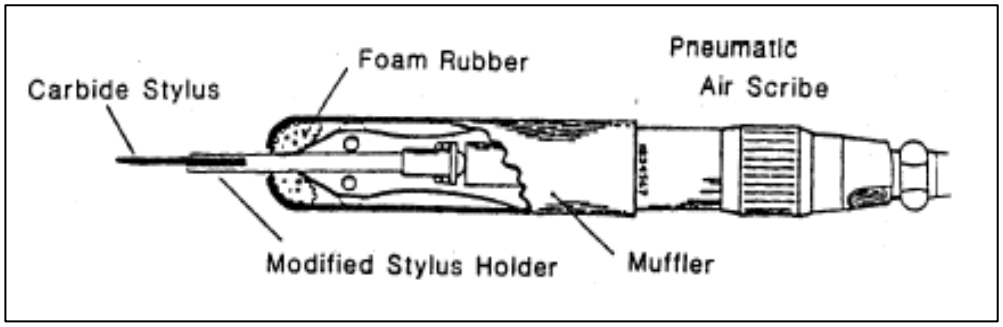

Fig. 16 Illustration of a pneumatic air scribe with an overview of its internal structure (modified from Chaney 1989, fig. 5).

Especially when cleaning umbilici, and when their morphology is not known, it may be necessary to destroy part of them to get an idea of the umbilical depth and of the shape of the innermost whorls. However, it can be impossible to clean completely the umbilici and in that scenario the best preparation possible was done, in order to clean at least the umbilical shoulder and walls.

6.4 Photography

The most representative specimens were chosen for photography in order to show the most important features of each species. Prior to photography they were cleaned, painted and whitened. All the steps are illustrated in the following sections below.

6.4.1 Whitening

The first step prior to whitening was cleaning the specimens. Cleaning was done in order to prevent dust and other dirt particles to stick on the surface in the process. Then the specimens were painted black, being careful that the colour was not too thick to cover e.g. any suture lines or other details. The purpose of painting is to get a uniform cover that helps enhancing the relief (Feldmann 1989b). The paint was left to dry completely for one day before the whitening.

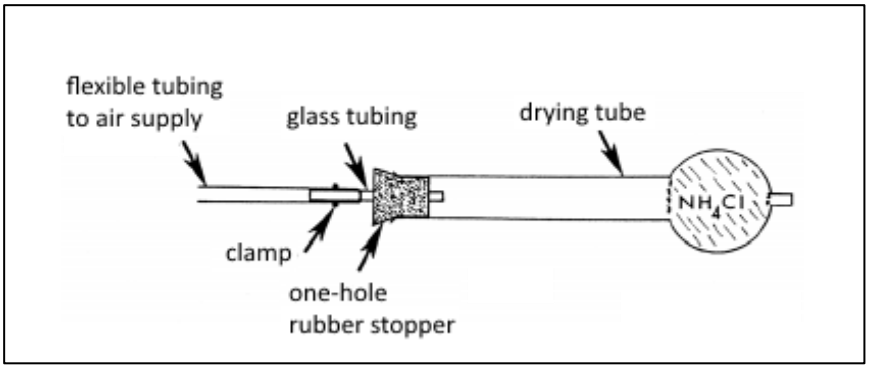

Fig. 17 Structure of a whitening apparatus, similar to the one used for the project (from Feldmann 1989b, fig. 2).

Whitening is a preferable method for photography since it enhances the morphological features as topographic relief: the white cover provides a uniform surface that reduces the effects of the original colour pattern. This coating is obtained by heating ammonium chloride (NH_4Cl) powder, which sublimates and is deposited on the chosen surface. Additional advantages are that the cover can be easily removed and reapplied, and it is therefore not a destructive technique. However, it is tricky to get the right amount of sublimate on the surface of the fossil in order to have it not too white or not too subtle, as well as uniform on the entire surface. Moisture moreover would cause the whitening to disappear faster (Feldmann 1989b).

The equipment used for whitening (Fig. 17) includes a glass pipe, a rubber pump attached to it, ammonium chloride supply and a Bunsen burner. The proper amount of ammonium chloride (too much will occlude the pipe) is put in the glass pipe before attaching it to the rubber pump and heated. In the process a lot of smoke is produced, so it is good advice to work in a fume hood (Feldmann 1989b).

Once the sublimate starts to flow through the aperture of the pipe, the whitening process can be started. The pipe has to be heated several times since it tends to cool. While whitening, it was tried to keep the pipe low angled and to whiten the fossil surface from a single direction.

6.4.2 Photographic setup

The photographic setup mainly consists of a copy stand (a black plane on which to lay the specimens for photography and a vertical rod on which the camera is mounted), and lights. The camera can be moved up- and downwards depending on the magnification needed: more distance is required for bigger specimens and vice versa.
Attention was paid to placing and keeping the specimens horizontal to avoid unwanted contrasts between shadow and light. Light is a very important factor, and a correct light setup is necessary to highlight the contrasts and details (Feldmann 1989a). For this purpose, in addition to a halogen indoor light, a smaller light on the upper left corner was used, pointing towards the lower right corner.
The camera was arranged with special settings. A long exposure time was chosen in order to get the proper exposure while the ISO (photographic sensity to light, or "film speed") was kept low to avoid grainy images. As for the aperture, which controls the amount of light through the lens, a large number (= small aperture) was chosen to get a good depth of field.

Photos were taken of one side mostly, but also of the venter in the more interesting instances. In those cases, the specimens were mounted on small rubber pieces to hold them in place and whitened again before having them photographed.
The best photos were finally assembled to prepare the plates with the graphic software Paint.Net © (dotPDN LLC 2014). The photos were adjusted to get uniform brightness and colours.

6.5 Drawing the suture lines: the camera lucida

To draw the suture lines a camera lucida technique was used (Fig. 18). This is a simple optical instrument that is attached to the microscope and allows seeing and drawing a small object at the same time. As it can be seen in Fig. 18 an oblique mirror is mounted on the side of the microscope. In this way, not only the specimen can be seen but also the sheet of paper and the hand of the observer. To improve the visibility of both the specimen and the reflections of the hand and pencil a set of lights is added. One is attached to the microscope itself and another is pointed from the upper right corner towards the paper sheet.
The advantage is that it is possible to draw without looking away from the specimen. The degree of distortion represents however a limitation. In case of ammonoids, for example, the suture lines are present on the venter, or may be crossed by prominent ornamentation, so that

they do not lie on a flat plane. The specimen would need to be turned for the suture lines to become visible. This implies that actually the correct real proportions are not maintained.

The minimum magnification of x6.4 was used for all specimens.

The drawings such obtained were improved with the graphic software Paint.Net © (dotPDN LLC 2014).

Fig. 18 The setup of the camera lucida, microscope, lights and mirror.

7. Terminology of ammonoid morphology: an overview

Before proceeding with the proper systematic descriptions, a short introduction is given about the morphology of ammonoids together with an overview of the most recurrent terms used.

7.1 Shell morphology

The ammonoid shell (or test) is divided into protoconch (the larval shell), phragmocone and body chamber (Fig. 19b-c). The phragmocone is the part of the shell divided into chambers, whose succession reflects the forward movement of the animal during growth. Such chambers are delimited by the septal walls, which are secreted by the mantle, the soft tissue that secretes the shell. These walls are attached to the shell through the septal edges, defining the suture pattern (see Section 7.2 below). The phragmocone is followed by the body (or living) chamber which on the contrary has no septa and represents the last chamber in which the animal lived (Arkell et al. 1957; Benton & Harper 2009b).

Most of the ammonoids of the faunal assemblage here described are involute (Fig. 20b-c), while only one species is evolute (Fig. 20a). The difference is that in involute shells the younger whorls cover, partly or completely, the older ones. In evolute shells, on the contrary, there is no such overlap and all the whorls are visible. Evolute forms have generally wider umbilici than the involute types (Arkell et al. 1957).

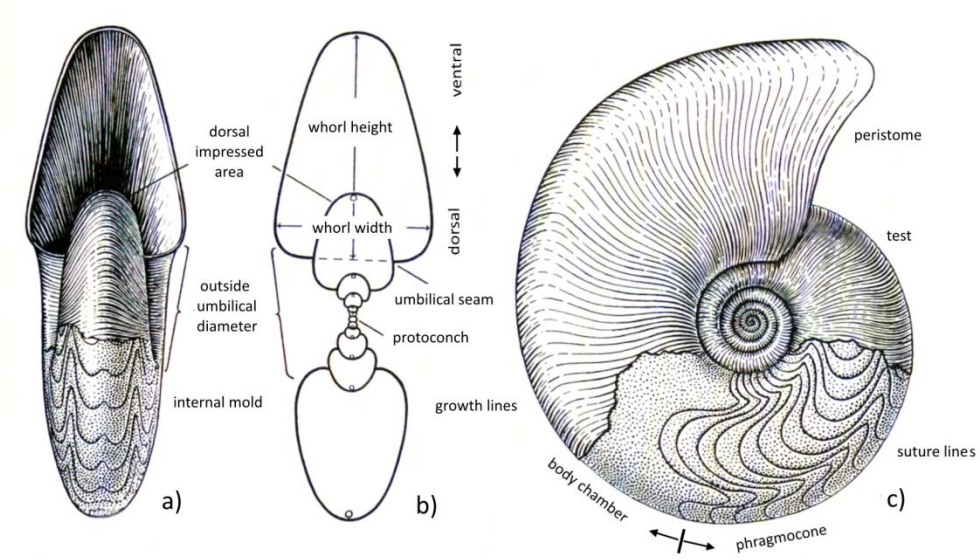

Fig. 19 Overview of the main ammonoid external morphological features (modified from Arkell et al. 1957, fig. 1).

Ammonoids present also a very wide range of conch shapes, which can be estimated by looking at the external morphological characteristics such as the kind of coiling and the compression degree (see e.g. Arkell et al. 1957). The shapes common in the studied assemblage are shown in Fig. 20. Such descriptive terms are however only indicative, as a high number of intermediate forms are to be expected due to the effects of intraspecific variation (see Chapter 5).

In the studied assemblage most of the species are platycones (Fig. 20b-c) and a few serpenticones (Fig. 20a).

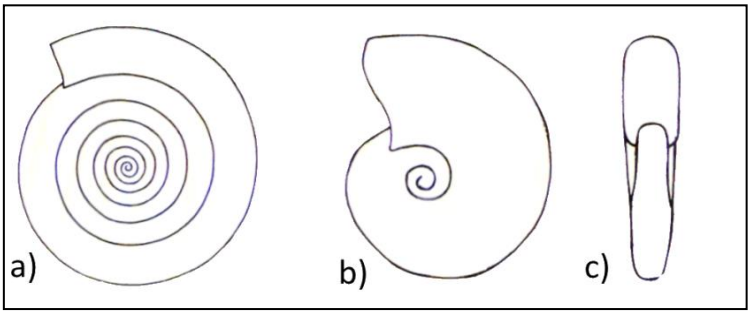

Fig. 20 The main conch shapes considered in the project (modified from Arkell et al. 1957, fig. 125): a) represents an evolute and serpenticone shell; b) and c) represent a typical platycone and compressed shell (lateral view and cross section).

An estimation of the conch shape and its features (umbilicus, cross section, diameter etc.) can also be obtained through the measurements of the basic conch parameters (see Section 6.2). In particular the conch shape and the involution degree can be estimated in a plot that relates

whorl and umbilical widths. Such a plot was originally presented in a paper by Korn (2010) about Palaeozoic ammonoids, but many of the elements described were considered valid also for Mesozoic forms. It is shown in Chapter 8, Fig. 25, where the measurements obtained in this project, excluding the species with few values available, were inserted.

The shape of the cross section (whorl section) can give even more information. It can change through growth, defined in that case as allometric growth, or be constant, in that case being isometric growth. The shape can range from being rounded to almost rectangular. The most common forms in the assemblage are shown in Fig. 21a, c, e.
In a similar fashion the venter can be defined as arched (as in Fig. 21c, e for instance), tabulate (Fig. 21b) or keeled (Fig. 21d).

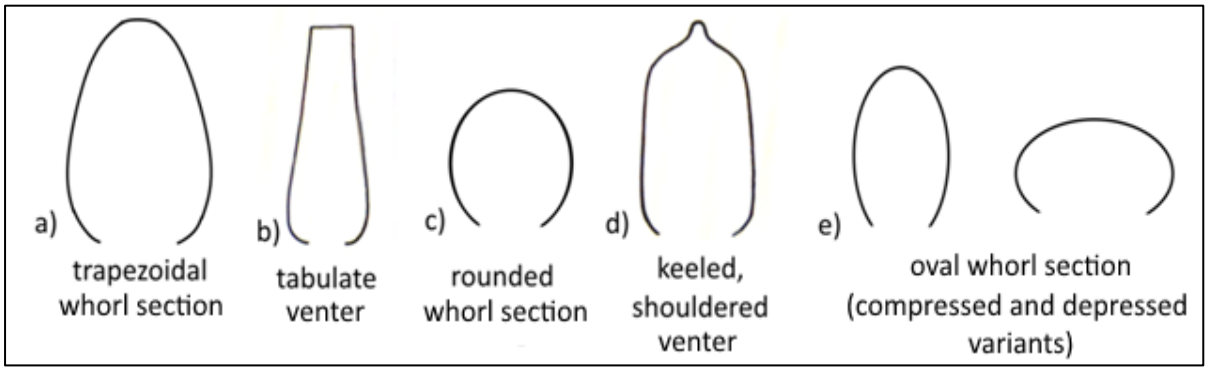

Fig. 21 Overview of the most common venter and whorl section shapes (modified from Arkell et al. 1957, fig. 127).

7.2 Suture lines

The ceratitic suture line is typical for the ammonoids here considered and for the Triassic in general. This kind of suture is characterised by denticulated lobes and rounded saddles. The terminology is explained in Fig. 22.
Suture lines represent the junctions between the external shell and the septa and are therefore visible only on internal moulds or polished shells. When the growth has slowed down at maturity, the suture lines get closer together and the length of the lobes increases (Arkell et al. 1957), as it is observed on some specimens in this study with the whole phragmocone preserved.
Suture lines are useful for ontogenetic studies, as they develop from simpler to more complicated forms with growth, and for taxonomy, as relationships between different ammonoid categories can be discerned. In addition, suture lines may also present a high degree of intraspecific variation (as mentioned in Chapter 5) as their structure is closely

linked to the mantle shape and deformation. Therefore it should not be a surprise if individuals of the same species present different sutures, but despite the apparent differences the main suture features (e.g. number and shape of the lobes) should be the same (Arkell et al. 1957).

The nomenclature of suture lines is different from country to country and in some instances from author to author, but in this project no further discussion on the topic is introduced.

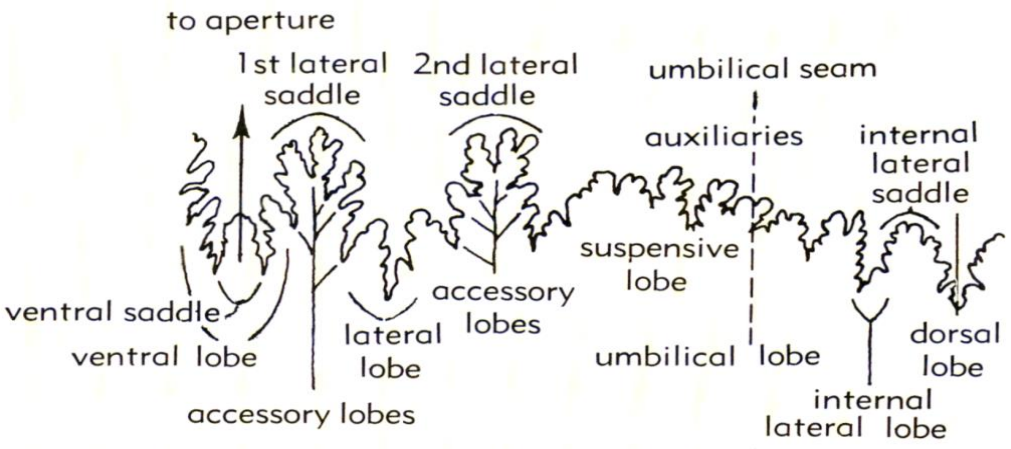

Fig. 22 Overview of the terminology of the suture lines. The black arrow on the left marks the middle of the venter, the dashed line on the right marks the position of the umbilical seam and the unbroken line in the far right marks the middle of the dorsum. As it can be seen, lobes point away from the aperture while saddles point towards it (from Arkell et al. 1957, fig. 141).

7.3 Ornamentation

The specimens here described are mostly internal moulds, but in few cases parts of the shell are preserved. An important consequence is that the ornamentation visible is actually only an internal reflection of the original external appearance: it can be deduced that specimens with e.g. a weak ornamentation would have been more prominently ornamented if the shell had been preserved.

Ammonoid ornamentation terminology is very rich and many terms have been coined according to the size and morphology of the sculpture.

Growth lines are the smallest ornaments of an ammonoid, found on the surface of the shell (Fig. 19c). They mark the migration of the peristome or apertural margin.

As regards the ribbing, different styles are defined, as shown in Fig. 23.

Ribs represent folds of the shell wall and their formation is controlled by the mantle (Bucher et al. 1996).

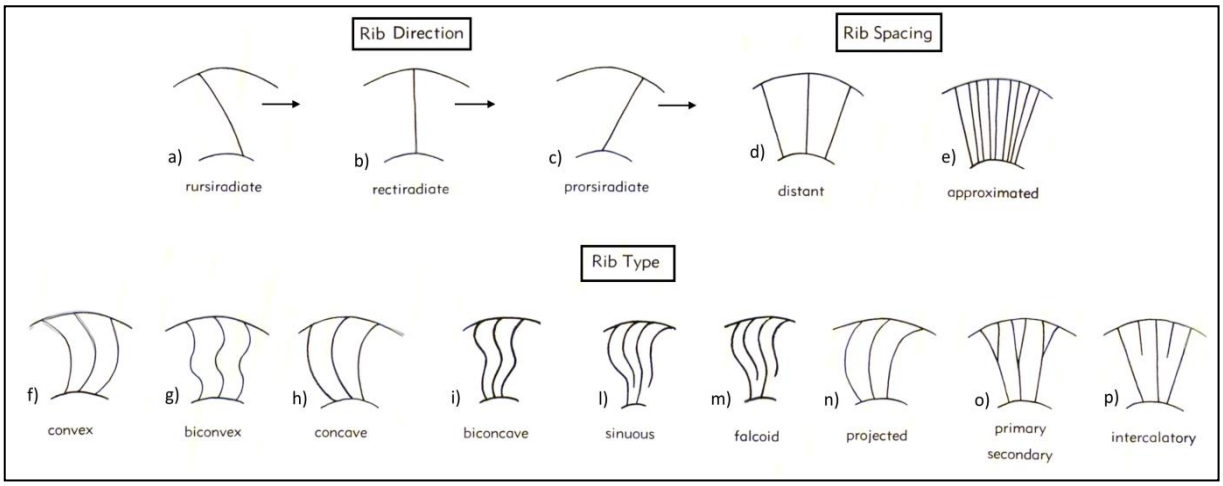

Fig. 23 Overview of the most common terms regarding ammonoid ribbing (modified from Arkell et al. 1957, fig. 132).

On the ribs, or independently of them, tubercles may occur (Fig. 24a-c). Elongated tubercles in particular are named bullae (Fig. 24a). Tubercles on the internal mould may represent spines on the test (Arkell et al. 1957).

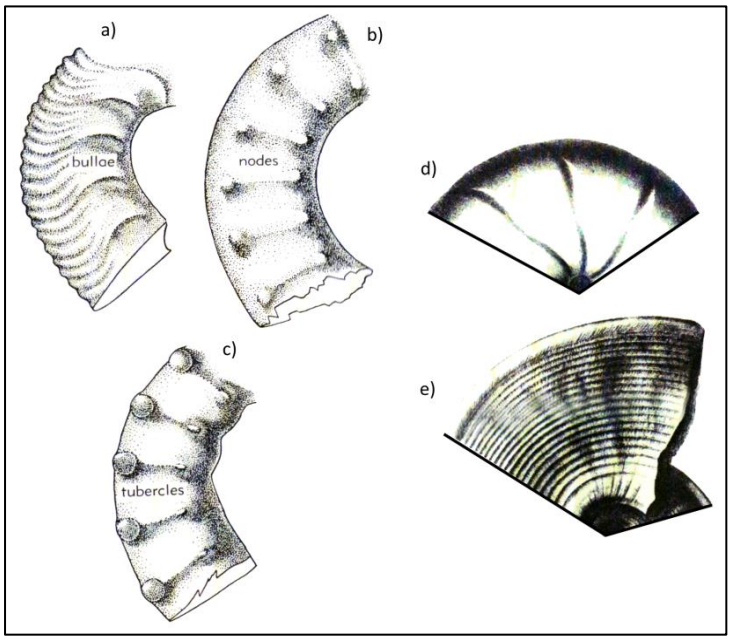

Fig. 24 Explanatory figures for bullae (a), nodes (b), tubercles (c), constrictions (d) and strigations (e). Modified from Arkell et al. 1957, fig. 133-134-139).

During the taxonomical process of identification of the species, it was very important to understand the distinction between ribs and megastriae.

Megastriae are asymmetric ridges with a wide and low-angled side that points in a rursiradiate direction (away from the aperture) and a steep side in a prorsiradiate direction (towards the

aperture). They are usually well defined and feel sharp at touch. Ribs on the contrary can be faint and feel smooth and are more symmetric (Jattiot 2014, personal communication).
The megastriae mark the halts and starts of continuous growth episodes. These features though are more common in early ontogenetic stages as they tend to disappear at mature stages. Megastriae can be associated with ribs, indicating a relation between rib formation and growth breaks (Bucher et al. 1996).
The importance of recognising megastriae from ribs lie in their morphological difference. The formation of the ribs involves a deformation of the mantle, as mentioned before, and involves folding also of the deeper mantle layers. The megastriae on the contrary are superficial features that involve deformation of the most external layers (Jattiot 2014, personal communication).
Megastriae occur in various taxa but ribs are the most common morphological feature. Of the prionitids, for example, only *Anasibirites* presents megastriae and this was a key factor in the distinction between true *Anasibirites* and juveniles of *Wasatchites* with *Anasibirites*-like ribbing (Jattiot et al., *in prep*.).
Some specimens may look the same but the distinction between ribs and megastriae may permit correct classification (Jattiot 2014, personal communication).

Also constrictions (Fig. 24d) are enhanced on the internal mould. Constrictions are grooves on the shell surface that are caused by internal thickening of the shell and can appear as depressions on the internal mould or on both the shell surface and the internal mould (Korn 2010). Ridges on the shell may be associated with internal constrictions.
They also represent growth discontinuities, and appear usually at later stages and strengthen the shell (Arkell et al. 1957; Bucher et al. 1996).

The keel is a particular structure that runs longitudinally on the venter, most commonly in a central position. A keeled venter occurs in only one instance (see Fig. 21d) and it will not be discussed further. The same specimen presents also strigations on the venter (Fig. 24e), which are longitudinal ridges (Arkell et al. 1957).

8. Results

In this chapter the results of the study are presented, starting with the systematic descriptions of the fossil assemblage followed by the statistical analyses of the data obtained through the measurements.

Before proceeding, it is shown how the conch shapes of the studied ammonoids fall into the range of discoidal (low umbilical and conch widths) with sub-involute to sub-evolute coiling (Fig. 25); this makes it difficult to distinguish the different genera/species just by considering the conch shape. As mentioned previously, such estimation was obtained by plotting the measurements in the graph elaborated by Korn (2010).

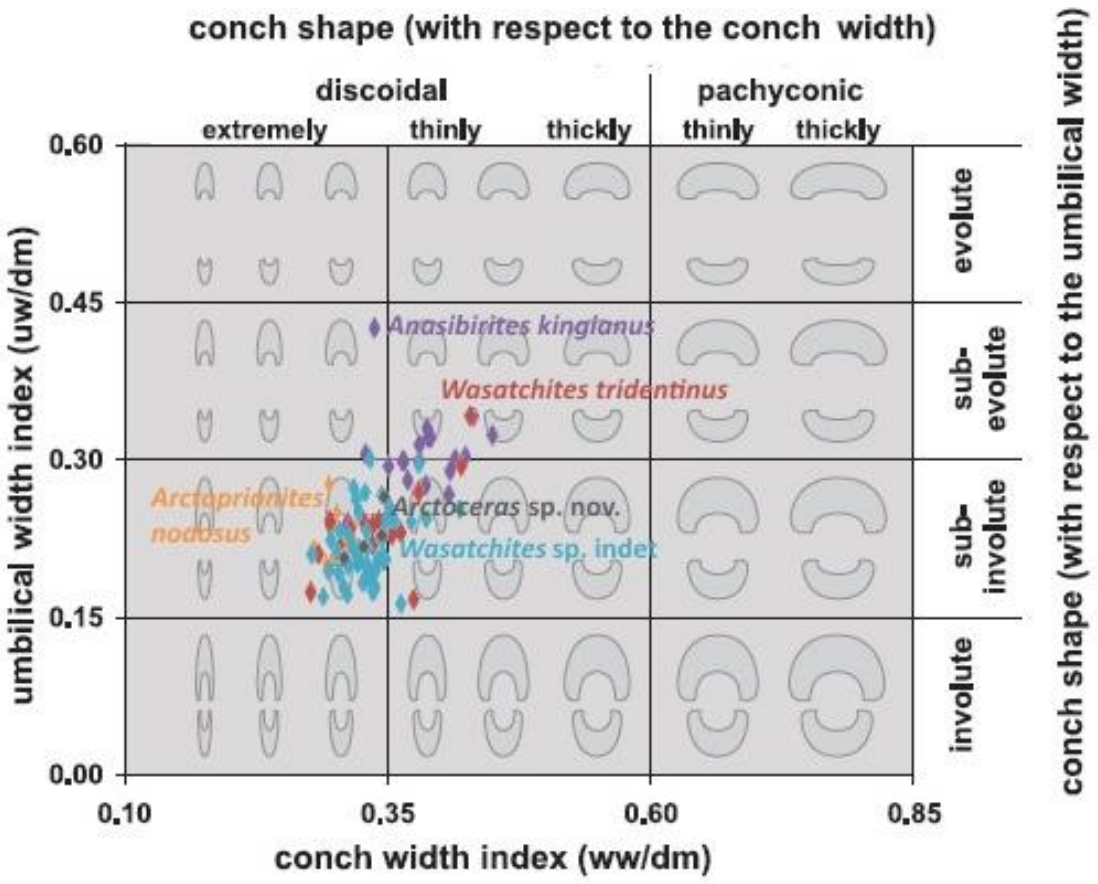

Fig. 25 Conch shape defined by the conch and umbilical widths (plot modified from Korn 2010, fig. 2, with added Spitsbergen data).

8.1 Systematic descriptions

In the following chapter the systematic descriptions are presented. The morphology of the species treated here is described using the classical geometrical parameters as introduced in Section 6.2. Both the absolute values H, W and U and the ratios H/D, W/D, U/D and W/H have been plotted on scatter diagrams as functions of D, when at least four measurements could be obtained. Repository of labelled specimens is abbreviated as PMO (Palaeontological Museum Oslo). The taxonomical work was conducted with reference to the manual "Procedure in Taxonomy" (1956). In the synonymy lists the abbreviations used are: cf. = confer = to be compared to; ? = doubtful identification, which may be considered valid, but the author is unsure; partim = the reference cited is considered valid only in part. In the descriptions below, *N* = total number of specimens assigned to a genus/species and *n* = number of measured specimens. The scale bar used for the suture lines is 25 mm.
Each species is discussed and compared with other described taxa, and reasons for the here presented classification are given.

Class Cephalopoda Cuvier, 1797

Subclass Ammonoidea Zittel, 1884

Order Ceratitida Hyatt, 1884

Superfamily Xenodiscaceae Frech, 1902

Family Xenoceltitidae Spath, 1930

Genus ***Xenoceltites*** Spath, 1930

Type species. *Xenoceltites subevolutus* Spath, 1930 = *Xenodiscus* cf. *comptoni* (*non* Diener), Frebold 1930

Xenoceltites subevolutus Spath, 1930

Pl. I, Figs. a-c

1930 *Xenoceltites subevolutus* Spath; p. 12.
1930 *Xenodiscus* sp. cf. *X. comptoni* Diener; Frebold, p. 14, pl. III, figs. 1-3.
1930 *Lecanites* sp. cf. *L. ophioneus* Waagen; Frebold, p. 12, pl. III, figs. 4, 4a, 5.
? 1932 *Xenodiscus rotula* Waagen; Smith, p. 45, pl. 79, figs. 5, 6 (After Mathews, 1929, pl. I, figs. 38, 40).
1934 *Xenoceltites gregoryi* sp. nov. Spath; p. 129, pl. V, fig. 3; pl. VI, figs. 4, 5; pl. XI, figs. 3, 4, 6.
1934 *Xenoceltites spitsbergensis* sp. nov, Spath; p. 128, pl. IX, figs. 1, 2; pl. XI, figs. 5, 7, 8.

1934 *Xenoceltites subevolutus* Spath; Spath p. 130, pl. II, fig. 2; pl. VIII, fig. 2; p1. IX, fig. 4; pl. XI, fig. 2.
1961 *Xenoceltites subevolutus* Spath; Tozer p. 53, pl. XVI, fig 1.
1978 *Xenoceltites subevolutus* Spath; Zakharov, pl. XI, fig. 17.
1978 *Xenoceltites subevolutus* Spath; Weitschat & Lehmann, p. 95, pl. 11, figs. 1a-b, 2, 3a.
1978 *Xenoceltites spitsbergensis* Spath; Weitschat & Lehmann, p. 94, pl. 11, figs. 3b, 4a-b, 5.
1990 *Xenoceltites subevolutus* Spath; Dagys & Ermakova, p. 23, pl. V, fig. 4.
1994 *Xenoceltites subevolutus* Spath; Tozer, p. 52, pl. 36, figs. 3-8.

Occurrence. This species occurs throughout the Boreal Realm (Arctic Canada, British Columbia, Siberia) and USA. It is rare in the sample from Stensiöfjellet (N = 8), but common in other sections in Spitsbergen, e.g. Botneheia, W-Spitsbergen (Weitschat & Lehmann 1978).

Description. The shell is compressed, evolute, serpenticone and discoidal. The whorl section is poorly preserved, but when visible it looks oval. The umbilicus is wide and shallow. The umbilical wall increases slightly on the body chamber; the umbilical shoulder is rounded. The flanks are slightly convex. The ornamentation is variable: some specimens have a smooth shell (Pl. I, Fig. c), while others have constrictions on the venter that extend to the ventral shoulder and partly to the sides (Pl. I, Figs. a-b). The inner whorls look smooth.
The suture lines are poorly preserved and can be well seen on only one specimen (Pl. I, Fig. b). They are ceratitic with broad and rounded saddles and elongated, weakly denticulated lobes.

Measurements. See Appendix 2. The estimated maximum diameter is ~ 17 mm.

Discussion. This species is rare in the faunal assemblage and it occurs here together with *Wasatchites* and *Anasibirites* as in other areas of Spitsbergen. In other Boreal and Tethyan localities, however, it occurs above *Anasibirites* and they do not overlap (see Chapter 4 on biostratigraphic correlations). This difference will be also discussed in the interpretation chapter.
The specimens here studied can be divided into two groups, one with smooth shell and the other with constrictions on the venter, as described above. This was at first interpreted as evidence for the presence of two different species, *X. subevolutus* (more compressed and smoother) and *X. spitsbergensis* (more evolute and ornamented), following the description of Weitschat & Lehmann (1978). Spath (1934) described three species of *Xenoceltites: X. gregoryi*, X. *spitsbergensis* and *X. subevolutus*. According to his observations, *X. gregoryi* is a smoother and thinner variant of *X. spitsbergensis* with constrictions on the venter, with immature forms very similar to both *X. spitsbergensis* and *X. subevolutus*. *X. subevolutus* is

also similar to *X. gregoryi* but it is more compressed and involute (Spath 1934). These differences can however be considered quite minor. If related to the concept of intraspecific variation, they could actually be viewed as variable characters within the same species, *X. subevolutus*. Therefore *X. spitsbergensis* and *X. gregoryi* would be considered junior synonyms, as suggested already by Dagys & Ermakova (1990).

Superfamily Meekoceratoidea Waagen, 1895

Family Prionitidae Hyatt, 1900

This family is very widespread worldwide and is characterised by tabulate/sub-tabulate venters, sub-involute shells, narrow umbilici with rounded shoulders and variable ornamentation degree (e.g. Weitschat & Lehmann 1978). The genera *Wasatchites* and *Anasibirites* were previously placed in the family Sibiritidae (e.g. Spath 1934), but subsequently moved to the Prionitidae (e.g. Tozer 1961). Due to the high rate of intraspecific variation, the taxonomy is quite challenging. As for what concerns the suture lines, they are quite similar in all prionitids, so it is hard to distinguish the different species just by considering the sutures.

Genus ***Arctoprionites*** (Frebold, 1930)

Type species. *Goniodiscus nodosus* Frebold, 1930.

Arctoprionites nodosus (Frebold, 1930)

Pl. II, Figs. a-d

1930 *Goniodiscus nodosus* sp. nov. Frebold; p. 8, pl. I, figs. 1-7; pl. II, fig. 2.
1934 *Arctoprionites nodosus* (Frebold); Spath, p. 340, pl. XVI, fig. 5; pl. XVII, fig. 1.
? 1934 *Arctoprionites tyrrelli* sp. nov. Spath, p. 342, pl. XIV, fig. 5; pl. XVII, fig. 6.
? 1934 *Hemiprionites garwoodi* sp. nov. Spath, p. 336, pl. XVI, figs. 1, 3; pl. XVII, figs. 3, 5.
1978 *Arctoprionites nodosus* (Frebold); Weitschat & Lehmann, p. 93, pl. 10, figs. 1a-b.
1994 *Arctoprionites nodosus* (Frebold); Tozer, p. 83, pl. 34, figs 5, 6.

Occurrence. This species is quite common in our sample (N = 20). The genus was established for specimens from Spitsbergen, but it has been documented also in Arctic Canada (Tozer 1994).

Description. The shell is sub-involute, extremely discoidal, platycone and compressed. The whorl section is trapezoidal, with convergent ventral shoulders at a high angle, so that a weak concavity near the venter is discernible in some cases. The umbilicus is narrow, moderately

deep; the umbilical shoulder is rounded and quite high-angled. The venter is tabulate and mostly smooth or faintly ribbed. The flanks get slightly more convex on the body chamber. The ornamentation is mostly limited to the flanks and the intensity is variable. The ribs are sinuous/biconvex, although in some specimens they are poorly defined. In some cases the ribbing intensity is slightly stronger closer to the umbilicus and decreases towards the venter (e.g. Pl. II, Fig. d). The inner whorls are smooth.

The suture lines are nicely preserved in some specimens. They are ceratitic with two elongated lateral lobes and rounded saddles (Fig. 26).

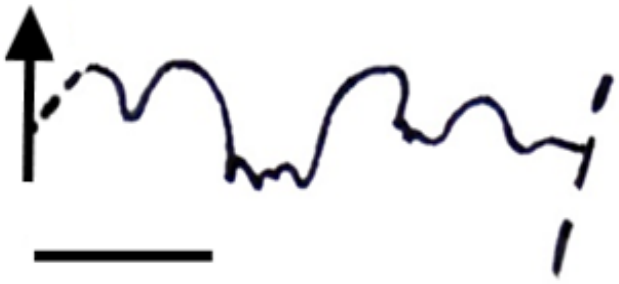

Fig. 26 Suture line from specimen PMO 227.992.

Measurements. See Fig. 27 and Appendix 2. The estimated maximum diameter is ~ 28 mm.

Discussion. As mentioned in the description, this species was originally described and named by Frebold (1930), who illustrated specimens from Spitsbergen with prominent ventral bullae and tabulate venter. Interestingly, the specimens here assigned to *A. nodosus* present quite weak ornamentation (a character that may be enhanced by the lack of the shell), and are closer to the specimen illustrated by Weitschat & Lehmann in fig. 1a, b (1978). They may be considered juvenile/immature individuals.

The identification of this species was quite challenging due to the similarities to the related genus *Hemiprionites* and the not always good preservation of the specimens.

Attention was paid to the presence or absence of concavity on the ventral shoulder, very common in *Hemiprionites*. But, since the specimens are still immature forms, the similarities between these two genera are strong and a weak depression close to the venter may also be observed in *Arctoprionites*.

Actually Spath (1934) described the species *Hemiprionites garwoodi* from Spitsbergen. It has been mentioned to be present in Late Smithian assemblages e.g. by Weitschat & Lehmann (1978), but Tozer (1994) considered it to be more likely immature forms of *A. nodosus*. Then, since also *A. nodosus* has already been described from Spitsbergen, and the studied specimens

look indeed similar to the juveniles of *Arctoprionites*, it has been considered more natural to assign these specimens to *Arctoprionites* instead of *Hemiprionites*.

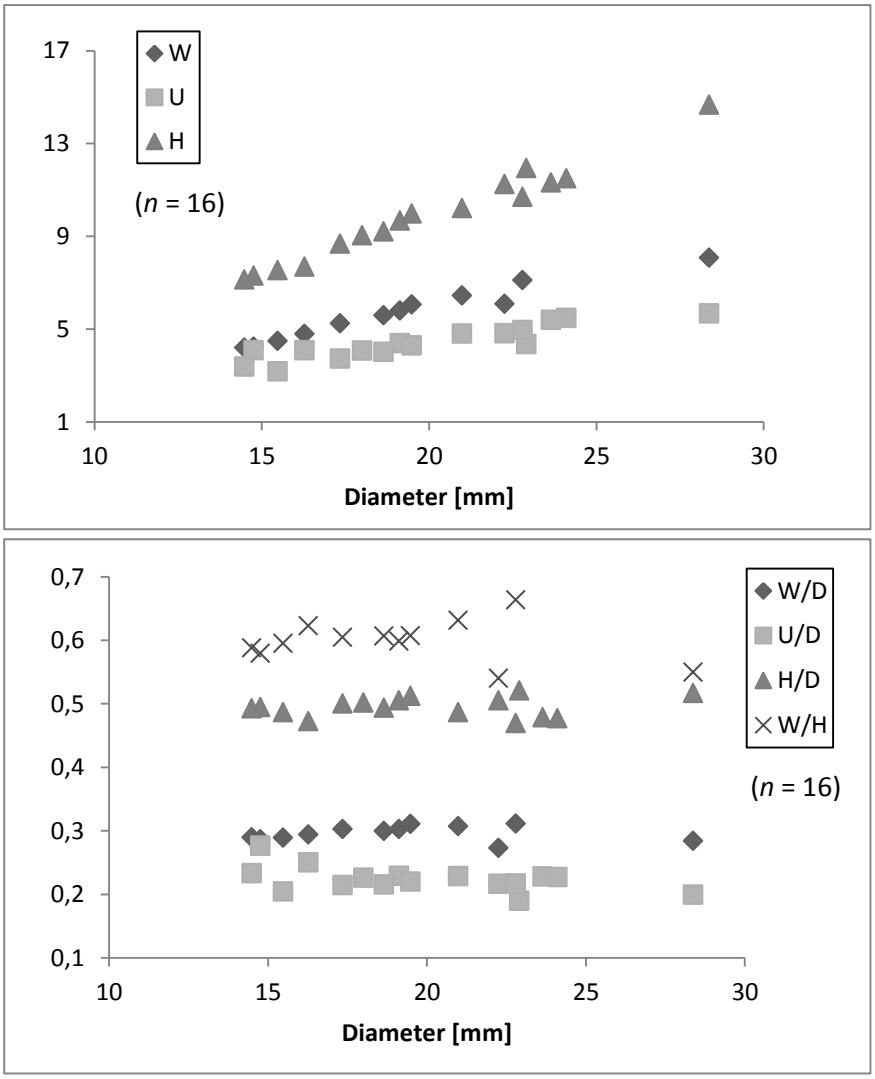

Fig. 27 Scatter diagrams of W, U, H (above) and W/D, U/D, H/D and W/H (below) for A.nodosus.

Arctoprionites resseri (Mathews, 1929)

Pl. II, Figs. e-g

1929 *Kashmirites resseri* n. sp. Mathews; p. 38, pl. VIII, figs 4-7.
1932 *Kashmirites resseri* Smith; p. 67, pl. 81, figs. 9, 10.
1962 *Arctoprionites* sp. indet. Kummel & Steele; p. 699, pl. 101, fig. 2.
1994 *Arctoprionites williamsi* n. sp. Tozer; p. 83, pl. 34, figs. 1–4.
2013 *Arctoprionites resseri* Brayard et al.; p. 198, figs. 67a-e.

Occurrence. This species has originally been described from Late Smithian beds of USA, and in the Boreal Realm it has been found also in the *Wasatchites* beds of British Columbia/Arctic

Canada (Tozer 1994). This is the first documented occurrence of this species from Spitsbergen, although it is very rare ($N = 2$).

Description. Involute, discoidal and platycone shell. The whorl section is not very well preserved in either of the two specimens although it looks rectangularly trapezoidal. The umbilicus, as seen only on one specimen (PMO 228.002, Pl. II, Figs. e-f) is narrow and moderately deep (although the preservation is not good), with a high-angled rounded umbilical shoulder. The venter is tabulate to slightly arched and crossed by faint straight horizontal ribs. The flanks are flat, slightly convex on the body chamber. Two different ornamentation stages can be viewed in the two specimens. PMO 228.001 (Pl. II, Fig. g), more compressed, has fainter ornamentation limited to the flanks. There are no bullae and the folds fade towards the umbilicus. They are biconcave/sinuous. PMO 228.002, more ornamented, has well developed ventral nodes and umbilical bullae, whose position gets more medial approaching the body chamber (their orientation also changes). Very fine radial lines are visible in between the bullae. No suture lines are preserved.

Measurements. No valid measurements could be obtained due to the incompleteness of the specimens.

Remarks. Both specimens are crushed on one side. The specimen PMO 228.001 looks asymmetrically compressed, but such asymmetry may indicate diagenetic compression.

Discussion. As mentioned, this is the first report of this species from Spitsbergen. The strongly tabulate venter was the key factor in the assignation to the genus *Arctoprionites*, and comparisons with the specimens illustrated in Brayard et al. (2013) confirmed even more the designation as *A. resseri*.

Compared to the described specimens of *A. nodosus*, the ornamentation of this species is more intense, both on the venter and flanks. As mentioned above however, *A. nodosus* can also present heavy bullae – *A. resseri* differs by their more umbilical position (Brayard et al. 2013). Moreover, the size of the specimens is greater than the average size of *A. nodosus*. Unfortunately the specimens are both broken, but they show a different ornamentation style (see description and Pl. II) which may be explained by intraspecific variation.

Tozer (1994) described the species *A. williamsi* from the *Wasatchites* beds of British Columbia. The specimens he assigned to this species are ornamented by prominent bullae, allowing comparisons with *A. resseri*. He claims that the difference lies in the elevation and prominence of the bullae, which is less in *A. resseri*. This slight difference can be viewed as

intraspecific variation. Therefore *A. williamsi* can be considered a synonym of *A. resseri*, extending its occurrence also to the Boreal Realm. With the assignation of the studied specimens to this species, its record is extended also to Svalbard.

Genus ***Anasibirites*** Mojsisovics, 1896

Type species. Sibirites kingianus Waagen, 1895

Anasibirites kingianus (Waagen, 1895)

Pl. III, Figs. a-g

1895 *Sibirites kingianus* n. sp. Waagen; p. 108, pl. VIII, figs 1a-c, 2a-c.
1895 *Sibirites chidruensis* n. sp. Waagen; p. 109, pl. VIII, figs 3a-c, 4a-c.
1895 *Sibirites inaequicostatus* n. sp. Waagen; p. 113, pl. VIII, figs 7a-b, 8a-b.
? 1895 *Sibirites ceratitoides* n. sp. Waagen; p. 115, pl. VIII, fig. 10a-c.
? 1905 *Sibirites noetlingi* sp. nov. Hyatt & Smith; p. 49, pl. IX, figs. 1–3.
1909 *Sibirites spiniger* v. Krafft & Diener; p. 131, pl. XXXI, figs. 2a-b, 7.
? 1909 *Sibirites robustus* v. Krafft &Diener; p. 132, pl. XXXI, fig. 1a-b.
? 1909 *Sibirites* sp. indet. ex aff. *robusto* Krafft & Diener; p. 133, pl. XXXI, fig. 6.
? 1909 *Sibirites spitiensis* v. Krafft & Diener; p. 136, pl. XXXI, fig. 8.
? 1909 *Sibirites* sp. indet. Krafft & Diener; p. 138, [partim.] pl. XXXI, figs. 4, 5 (not pl. XXVIII, figs. 4a-c).
1929 *Anasibirites kingianus* (Waagen); Mathews, p. 8, pl. VII, figs. 14–22.
1929 *Anasibirites perrini* n. sp. Mathews; p. 18, pl. III, figs. 34–36.
1932 *Anasibirites kingianus* (Waagen) var. *inaequicostatus* Waagen; Smith, p. 72, pl. 79, figs. 16, 17. (After Mathews, 1929; pl. III, figs. 34, 36).
1964 *Anasibirites inaequicostatus* (Waagen); Bando, p. 70, pl. 1, figs. 19a, b.
1978 *Anasibirites kingianus* (Waagen); Guex, pl. 3, figs. 2, 9; pl. 4, fig. 6.
? 2007 *Anasibirites kingianus* (Waagen); Lucas et al., p. 104, [partim.] figs. 3H-J (not figs. 3D-G); figs. 4A-B, E-H, J–L.
2010 *Anasibirites kingianus* (Waagen); Stephen et al., fig. 7A-B.
2012b *Anasibirites kingianus* (Waagen); Brühwiler et al., p. 101, figs. 84A–U.
2012c *Anasibirites kingianus* (Waagen); Brühwiler et al., p. 155, figs. 31O, 32AA–BD.
2013 *Anasibirites kingianus* (Waagen); Brayard et al., p. 195, figs. 62a-k.

Occurrence. Anasibirites kingianus occurs worldwide and has been described e.g. from USA, China, Salt Range (Pakistan), Primorye (Russia), Siberia, British Columbia. It has been mentioned in descriptions for the Late Smithian in Svalbard (e.g. Mørk et al. 1999b) but not properly described. In the assemblage it is one of the most common species ($N = 36$).

Description. Sub-involute to sub-evolute, thinly discoidal, platycone shell. The whorl section is trapezoidal, but in the most depressed specimens it becomes almost rounded/quadrate. The umbilicus is relatively shallow and narrow, but it gets deeper and wider in more depressed and more ribbed specimens (as according to Buckman's first law of covariation). The

umbilical wall is oblique and high-angled. The umbilical shoulder is rounded. The venter is tabulate to slightly arched. The flanks are slightly rounded and become more convex on the body chamber. The ornamentation consists of megastriae spreading on the whole shell or fading towards the body chamber. The megastriae are generally projected/sinuous but also straight. They cross the venter, on which they seem to thicken. The megastriae are more pronounced and thicker on the more depressed specimens and finer (feeling sharper at touch) and more approximated in the more compressed specimens. In the more mature specimens, with decreasing ornamentation towards the body chamber, the distance between the megastriae increases. In many specimens there is in addition an alternation of thicker and thinner (1 to 3) megastriae (see e.g. Pl. III, Fig. b). The thinner megastriae seem to be intercalary. The inner whorls are ribbed.

The suture lines are ceratitic with two elongated lateral lobes, smaller auxiliary lobes and broad rounded saddles (Fig. 28).

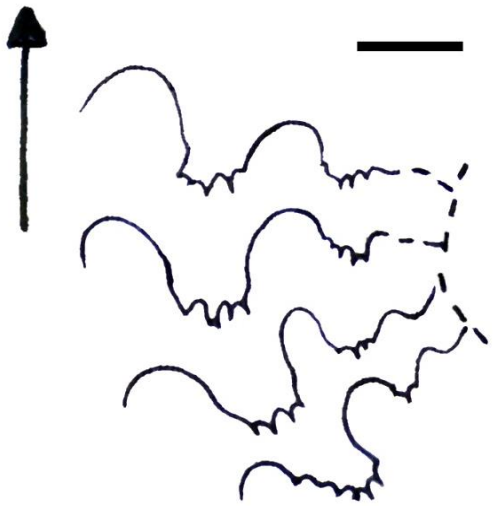

Fig. 28 Suture lines from the specimen PMO 227.998, Pl. III, Fig. e All the visible sutures were drawn.

Measurements. See Fig. 29 and Appendix 2. The estimated maximum diameter is ~ 20 mm.

Remarks. The body chamber is not always preserved; it occupies ca. half a whorl in the specimens with the better preservation.

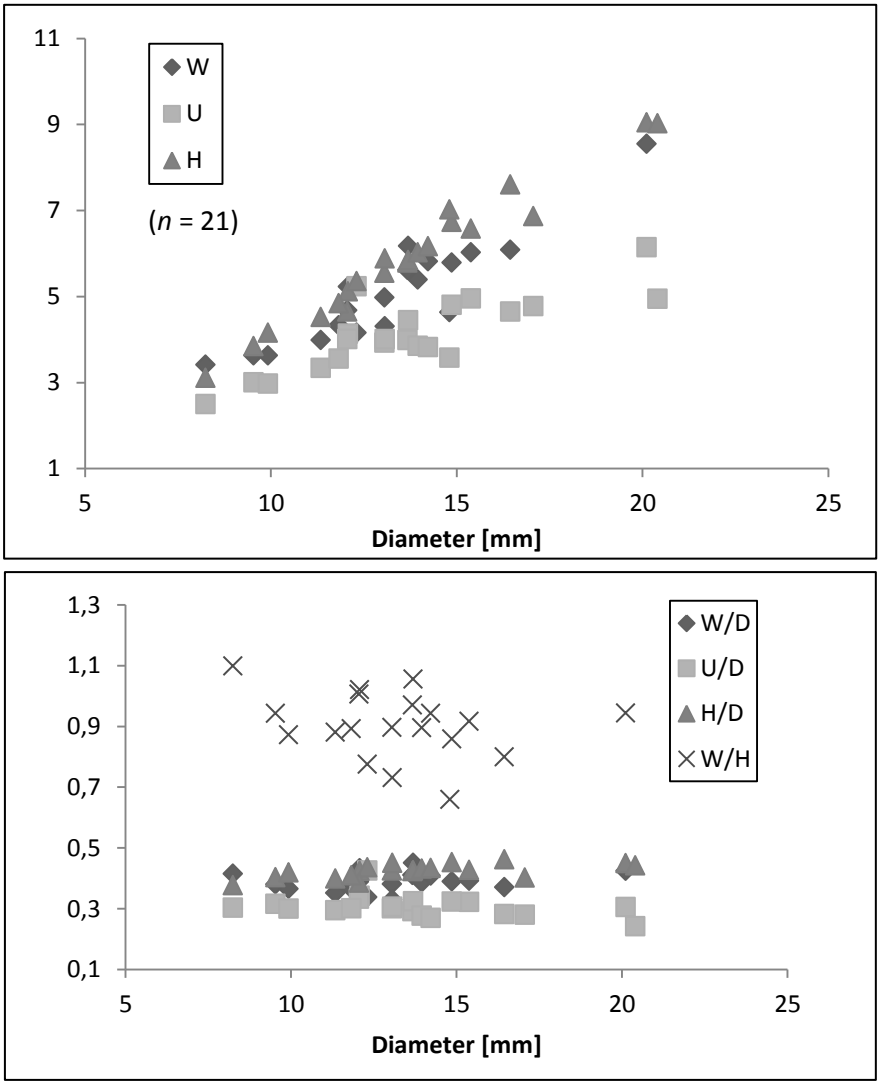

Fig. 29 Scatter diagrams of W, U, H (above) and W/D, U/D, H/D and W/H (below) for A.kingianus.

Discussion. Anasibirites is a cosmopolitan genus in the *tardus* Zone. As in the studied assemblage, also in other localities it occurs associated with *Wasatchites* and other prionitids, including USA, Salt Range, and China in the Tethyan Realm (e.g. Brayard & Bucher 2008; Brühwiler et al. 2012b; Brayard et al. 2013) and Arctic Canada (Tozer 1994) in the Boreal Realm just to name a few. In literature about Spitsbergen *Anasibirites* has been mentioned various times (e.g. Spath 1921 and 1934; Korčinskaja 1973; Weitschat & Lehmann 1978; Mørk et al. 1999b) but not described in detail.

The genus has gone (and is still) going through a systematic revision (e.g. Brayard & Bucher 2008; Brühwiler et al. 2012b; Jattiot et al., *in prep*.). Of the many species described in the literature, just a few would be considered valid as most of the names were assigned without considering the high intraspecific variation of the genus (Brayard et al. 2013)**.**

The species names kept are then *A. kingianus* and *A. multiformis*. *A. nevolini* and *A. angulosus* are considered junior synonyms of *A. kingianus* (Jattiot et al., *in prep*.).

For the identification of *Anasibirites* it was fundamental to check for the presence of megastriae (see Section 7.3). The distance between the megastriae increases towards the adult stage (as it is observed in *A. kingianus*, see e.g. in Brayard et al. 2013), as expected with mature ornamentation.

The ornamentation at immature stages often reflects the alternation of thicker and thinner closely packed megastriae, which can be observed in many of the studied specimens. This alternation is clearly observed in *A. nevolini*, to which the specimens here described may be assigned. However, if the inner whorls of *A. kingianus* are compared to specimens of *A. nevolini*, it can be noted that they look very similar. For these reasons it has been suggested by Jattiot et al. (*in prep.*) that *A. nevolini* represents the individuals of *A. kingianus* that kept the juvenile features longer and in this sense it can be considered a juvenile synonym of *A. kingianus* (Jattiot et al., *in prep*.).

This statement is supported by the plots shown in Fig. 30. The basic morphological parameters (U, W, H) and ratios are plotted on separate scatter diagrams. The data from Spitsbergen are the ones previously shown, but they are here plotted together with data from Timor which have been kindly shared by Jattiot (Jattiot et al., *in prep.*). As observed, the specimens from Spitsbergen are located in a well-defined area, represented by juvenile and more depressed specimens – adult individuals tend in fact to be more compressed. This fits with the observations.

Based on these measurements and ratios the specimens here studied were assigned to *A. kingianus*, though they clearly are juveniles and are identical to *A. nevolini*.

A. angulosus presents a more angled whorl shape, especially at younger stages, which was not observed in any of the studied specimens.

As for *A. multiformis*, it was not identified in the assemblage as it is mainly distinguished by its isometric growth (Brayard & Bucher 2008). *A. kingianus* (and its synonyms *A. nevolini* and *A. angulosus*) have allometric growth (Jattiot et al., *in prep*.).

Since the specimens in the studied assemblage are mostly small, with high prominence of juvenile stages of *A. kingianus* (= *A. nevolini*), a detailed work on intraspecific variation was not possible. Additional statistical analyses will be provided in the next chapter.

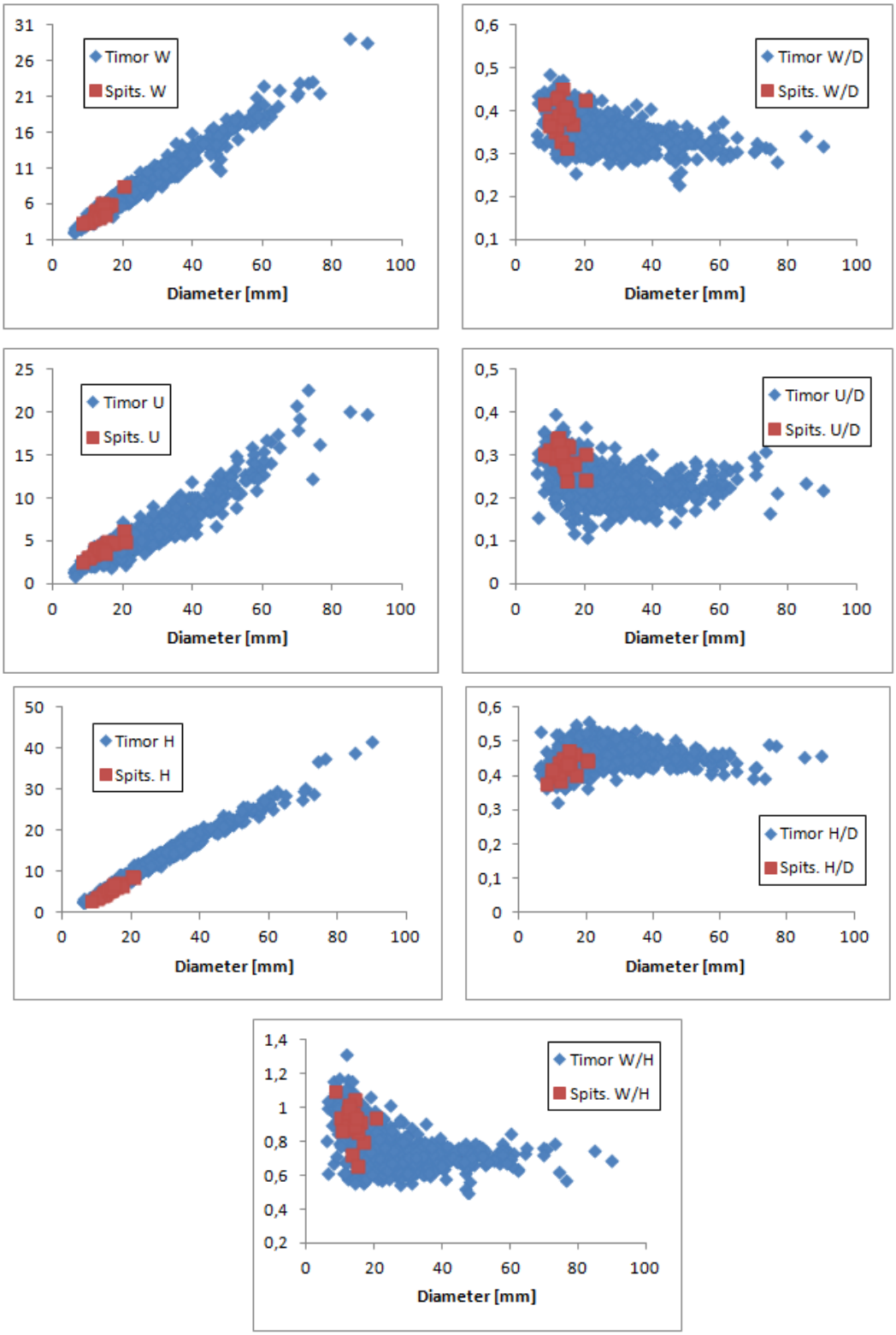

Fig. 30 Scatter plots of the Anasibirites kingianus specimens from Spitsbergen (red points) and Timor (blue points). The measurements from Timor belong to the unpublished results of Jattiot et al., in prep.

Genus ***Wasatchites*** Mathews, 1929

Type species. *Wasatchites perrini* Mathews, 1929.

Wasatchites* cf. *distractus (Waagen, 1895)

Pl. IV, Figs. a-d

cf. 1895 *Acrochordiceras distractum* n. sp. Waagen; p. 94, pl. III, fig. 4a-c.
cf. 1895 *Acrochordiceras coronatum* n. sp. Waagen; p. 96, pl. III, fig. 5a-c.
cf. 1895 *Acrochordiceras* cf. *damesi* Noetling; Waagen, p. 97, pl. IV, fig. 5a-b.
cf. 1895 *Acrochordiceras compressum* n. sp. Waagen; p. 98, pl. IV, fig. 4a-c.
cf. ? 1909 *Sibirites* sp. indet. Krafft & Diener; p. 138, [partim.] pl. XXVIII, fig. 4a-c (not pl. XXXI, figs. 4, 5).
cf. ? 1978 *Stephanites corona* Waagen; Guex, pl. 5, fig. 2.
cf. 2010 *Wasatchites distractus* (Waagen); Brühwiler et al., p. 423, fig. 15(1a-b).
cf. 2012b *Wasatchites distractus* (Waagen); Brühwiler et al., p. 97, fig. 81M-U, 82A-X.
cf. 2012c *Wasatchites distractus* (Waagen); Bruhwiler et al., p. 152, fig. 32A-Z.

Occurrence. This species has mainly been documented from Late Smithian beds in the Tethyan Realm (Salt Range, Spiti and Tibet) but not from Svalbard or other areas of the Boreal Realm. In the section it is rare, as $N = 9$.

Description. Involute and discoidal shell, which is thickest in the middle of the flanks. The whorl section looks rounded/quadrate, but the preservation is not good in any of the specimens. The umbilicus is relatively deep, but it looks wider and shallower in the biggest and thickest specimens. The umbilical shoulder is rounded and the wall high-angled. The flanks are rounded and convex, especially towards the body chamber. The venter is arched but it can be more tabulate in the compressed specimens (e.g. Pl. IV, Fig. e). The ornamentation consists of straight, quite distanced ribs which cross the flanks and venter. The venter can be smooth/faintly ribbed (e.g. Pl. IV, Fig. d) to crossed by straight ribs (e.g. Pl. IV, Fig. b). The ribs bifurcate from prominent tubercles, and intercalary ribs seem also visible in between them. The degree of ornamentation is variable: it ranges from smoother variants with no tubercles or bifurcations (Pl. IV, Fig. c) to heavily ornamented specimens with large tubercles (Pl. IV, Figs. a-e). The inner whorls are in some cases ornamented, but the smoothness may be due to preservation. No suture lines are preserved.

Measurements. The only specimen that was possible to measure (PMO 228.004, Pl. IV, Figs. a-b) presents a diameter of ~ 42 mm (see Appendix 2 for the measurements obtained), but the size of the specimens is variable.

Remarks. Shell remnants are found which show growth lines and reflect heavier ornamentation.

Discussion. The specimens that have been assigned to this group are distinguished by their generally larger size, strongly arched venter, convex flanks and most importantly by their prominent tubercles on the middle of the flanks. This is quite interesting as tubercles in the boreal *Wasatchites* species are usually located in an umbilical position, as observed e.g. in *W. tridentinus* (see below).

Comparing different literature sources it was noticed that there are similarities with *W. tardus*. *W. tardus* also presents bullae extending towards the middle of the flanks, as it can be observed in e.g. fig. 8F in Mørk et al. (1999b). As described by Tozer (1994), the bullae in *W. tardus* appear at the end of the phragmocone, which is mostly smooth. This parameter for identification is considered here not to be the most useful, being hard to estimate especially in cases when the specimens are broken. The specimens here studied are in fact all incomplete, making it difficult to determine whether and how much of the body chamber is preserved. The smaller, immature specimens in particular present similar bullae, but their position is still not umbilical and the overall ornamentation is stronger than in the juveniles of *W. tardus* illustrated by other authors (e.g. Dagys & Ermakova 1990 and Tozer 1961).

The most important factor that prevented the assignation of the specimens of this group to *W. tardus* is the morphology of the venter and flanks. As mentioned above, the specimens here treated have a markedly arched venter and convex flanks, but *W. tardus* has generally a subtabulate venter and flatter flanks.

The closest and most similar equivalent has therefore been found in *W. distractus*, which is characterised by tubercles on the flanks and similar morphology and ornamentation. This species has however never been described from Spitsbergen or other areas of the Boreal Realm, as it is more typical for the Tethyan Realm (*W. distractus* beds), so it was decided to leave a margin of doubt in the taxonomical assignment here presented. Findings of this species on Svalbard may indicate that the geographic range of *W. distractus* can be extended also to the Boreal Realm. Further studies may be able to confirm such a statement.

As for the other *Wasatchites* species, also this one shows intraspecific variation (see Pl. IV), ranging from smooth variants with fainter bullae to heavily ornamented specimens.

Wasatchites tridentinus Spath, 1934

Pl. V, Figs. a-i

1934 *Wasatchites tridentinus* sp. nov. Spath; p. 352, pl. XV, figs. 2a-c; pl. XVI, figs. 2a-b, 4.
? 1934 *Wasatchites orientalis* sp. nov. Spath; p. 350, fig. 118, p. 352
1978 *Wasatchites tridentinus* Spath; Weitschat & Lehmann, p. 94, pl. 10, figs. 3-5.

Occurrence. This species has been described/mentioned frequently from the *tardus* Zone of Svalbard (e.g. Spath 1934; Weitschat & Dagys 1989), and it occurs also in other areas of the Boreal Realm such as British Columbia (Tozer 1994). In the sample this is a very common species (N = 53).

Description. Mostly sub-involute, platycone, discoidal shell. The whorl section is trapezoidal, although in more depressed specimens it gets more rounded/quadrate. The umbilicus is narrow and moderately deep, but it gets shallower and wider with increasing depression. The umbilical wall is quite high-angled and the umbilical shoulder is rounded. The flanks are sub-rounded and get more convex on the body chamber. The venter is occasionally tabulate (although less than for *Arctoprionites*) but is most commonly arched. It is ornamented by straight or arched ribs whose intensity range from faint to high. The variation in the ornamentation degree is in fact very large. The ribs are mostly straight (e.g. Pl. V, Fig. g) but also projected (e.g. Pl. V, Fig. d), and their thickness and height are variable. When the ribs are more defined it is common to see an alternation of stronger and weaker ribs with intercalary ribs (as seen e.g. in Pl. V, Fig. g). Diverse combinations of ornamentation elements are possible. Some specimens present small tubercles close to the umbilicus but no or very faint ribbing on the shell (e.g. Pl. V, Figs. a-b, c), others have more defined ribbing with faint umbilical bullae which give rise to 2-3 ribs (e.g. Pl. V, Figs. d, e). The ribbing and the tubercles become increasingly more prominent and thicker. The venter also becomes increasingly more ribbed (e.g. Pl. V, Figs. f-h). The tubercles are more or less prominent depending on the specimens and the biggest ones are closer to the aperture. At maturity the specimens present fainter ribbing on the shell but prominent tubercles, as well as small nodes on the ventral shoulder (e.g. Pl. V, Fig. i). The inner whorls are ribbed in the more ornamented specimens, but not in the smooth ones (see Pl. V, Fig. a vs. Fig. f).
The suture lines are ceratitic with two elongated lateral lobes and rounded saddles (see Fig. 31a-b). The auxiliary lobes were not preserved. In some cases, as in Fig. 31a, the ventral lobe is bifurcated. The morphological variation is evident.

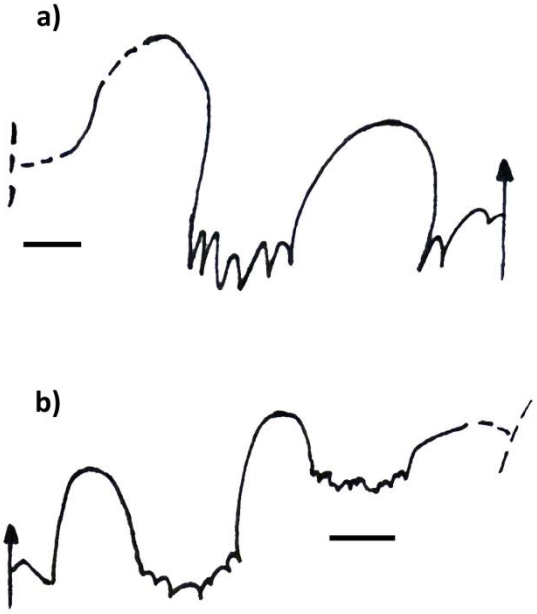

Fig. 31 Two different suture lines as drawn from specimens PMO 228.010 and PMO 227.981.

Measurements. See Fig. 32 and Appendix 2. The estimated maximum diameter is ~ 41mm.

Remarks. This taxon can be subdivided on the basis of morphology, which reflects a large intraspecific variation. The size range is very variable, much more than for the other specimens/genera. Some of the largest specimens belong to this species. The preservation ranges from excellent to quite poor.

Discussion. Wasatchites is a cosmopolitan genus that occurs both in the Tethyan and Boreal Realms. It is very useful therefore for biostratigraphic correlations between the various areas as it is a very common representative of the Late Smithian. It is in fact one of the most prevalent genera in the *Anasibirites kingianus* beds and in the *tardus* Zone in general (Brayard et al. 2013).

The specimens belonging to this group have been assigned to the species *W. tridentinus*, in accordance with most of the works regarding *tardus* Zone faunal assemblages in Spitsbergen.

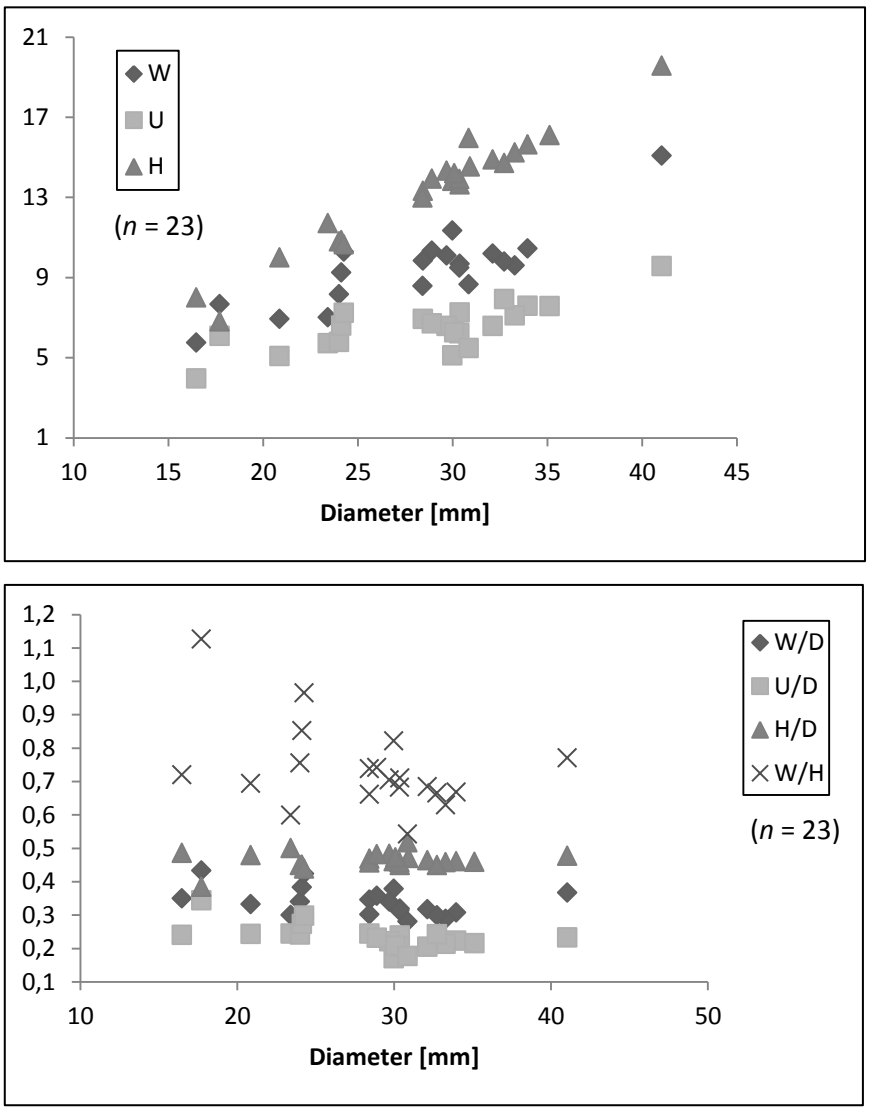

Fig. 32 Scatter diagrams of W, U, H (above) and W/D, U/D, H/D and W/H (below) for W. tridentinus.

The assignation to this species was quite problematic. Comparisons with previous literature revealed similarities between the species *W. perrini*, *W. tridentinus* and *W. tardus*. They are all closely related and differ only in ornamentation degree and style.

Spath (1934) described four species of *Wasatchites* from Spitsbergen: *W. orientalis*, *W. meeki*, *W. tridentinus* and *W. magnus*. Of these species, *W. meeki* and *W. magnus* have been synonymised by Brayard et al. (2013) with *W. perrini*, which then has a record also from Spitsbergen and not only from eastern Panthalassa.

W. orientalis is quite similar to *W. tridentinus*; but differs by its narrower venter, closer and thicker ribs and smaller size. Such differences can be seen in the light of the intraspecific variation, and *W. orientalis* could be considered a synonym of *W. tridentinus*.

W. tridentinus is distinguished from *W. perrini* by strong tubercles developed only on half a whorl of the phragmocone, from a diameter of 25 mm, and by being less inflated (Spath 1934; Tozer 1994). *W. perrini*, on the contrary, has tubercles at least on a full whorl of the phragmocone. These differences were considered to be not clear enough, as in incomplete specimens it may be difficult to estimate the length of the body chamber/phragmocone and therefore determine the species. An unpublished note by Brüwhiler (shown by Jattiot 2014, personal communication) on Spath's "Catalogue of the fossil Cephalopoda, Part IV (1934) suggests that *W. tridentinus* may be a synonym of *W. perrini*.

In a similar fashion, also *W. tardus* has been compared, by Dagys & Ermakova (1990), to *W. perrini*. They recognise a strong closeness between the two species, being *W. tardus* with smoother inner whorls and more involute. In addition they discussed that this species is very common on Spitsbergen, where it had been described as *W. tridentinus* e.g. by Weitschat & Lehmann 1978. They suggested therefore that a revision of this genus may be needed.

The material available for the current project permitted to recognize the similarities between these species pointed out by these authors, but it was regarded as insufficient to reject or confirm Brüwhiler's hypothesis or whether all these three species are actually conspecific. Further future work may however permit a better discussion on the matter.

The intraspecific variation shown by the specimens is considerable (see e.g. the illustrations on Pl. V), making the classification even more challenging. Studying the specimens, questions also arose regarding the combinations of ornamentation characters. Specimens were in fact observed which had tubercles but almost no ribbing, others showed intense ribbing but no tubercles, and others both. A suggestion could be that it is an effect of both ontogenetic degree and intraspecific variation.

***Wasatchites* spp. indet.**

Pl. VI, Figs. a-h

Occurrence. This group is the most common in the faunal assemblage, as $N = 86$.

Description. Sub-involute, discoidal, platycone shell. The whorl section is generally trapezoidal. The umbilicus is narrow and moderately deep, but wider in the thicker specimens. The umbilical shoulder is rounded and the umbilical wall is high-angled. The flanks are generally convex but can be flatter in more compressed specimens (e.g. Pl. VI, Figs f-h). The venter is most commonly arched but it can also be tabulate. It is variably ribbed and varies from smooth/slightly ribbed (e.g. Pl. VI, Fig. b) to clearly ribbed (e.g. Pl. VI, Fig. e). There is

a high variation in ornamentation, from faint (e.g. Pl. VI, Figs. a-c) to more intense on the whole shell (e.g. Pl. VI, Figs. d-h). The ribs are straight/slightly sinuous to projected, and in many cases they are stronger closer to the umbilicus. The rib spacing is usually regular, though the ribs become more distant on the phragmocone. There are no tubercles as seen in more adult specimens, although there are in some cases faint elongated umbilical thick ribs that may have originated tubercles at later growth stages. From the better preserved specimens it can be seen than the inner whorls are ribbed.

The suture lines are ceratitic, with elongated denticulated lobes and broad rounded saddles, similar to the ones observed in specimens of *W. tridentinus*.

Measurements. See Fig. 33 and Appendix 2. The estimated maximum diameter is ~ 33 mm.

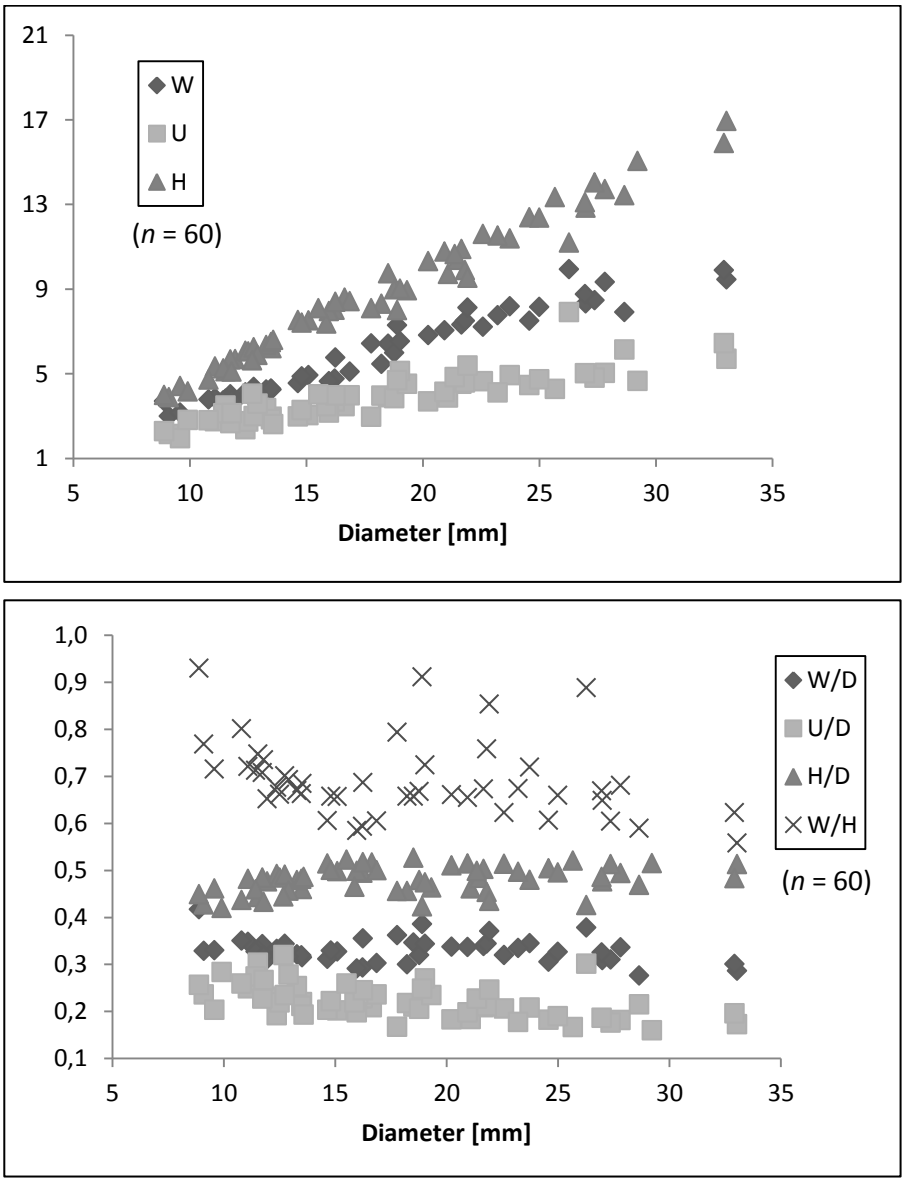

Fig. 33 Scatter diagrams of W, U, H (above) and W/D, U/D, H/D and W/H (below) for Wasatchites spp. indet.

Discussion. The specimens assigned to this group are generally small and hard to identify at the species level. They were assigned to *Wasatchites* as they present evident and regular ribbing and commonly arched/subtabulate venter which are typical for the genus. They are immature as they still do not display tubercles. The fact that they have heavy ribbing is further evidence of their immaturity, as can be compared in the illustrations of Weitschat & Lehmann (1978). Heavy ornamentation tends to fade in adult specimens.

The identification has therefore been particularly hard, and the question remains whether they are juveniles of the same species or of more than one. The juveniles of different *Wasatchites* species (as well as of different prionitid genera) look very similar and it was considered to be the most sensible decision to only refer these specimens to the genus *Wasatchites*, since a more detailed identification cannot been trusted.

The measurements obtained for this group were plotted together with the ones for *W. tridentinus* in the same scatter diagrams (Fig. 34), while they have been presented separately in the previous chapter. It can be observed that there is quite a degree of overlap. This may either suggest that the specimens belong to different *Wasatchites* species or that the overlap area is occupied by the specimens belonging to both the groups of *W. tridentinus* and *Wasatchites* spp. indet. that are neither juveniles nor adults. This hypothesis will be discussed in the next section on statistical analyses.

The specimens illustrated on Pl. VI, PMO 228.000 (Figs. f-g) and PMO 228.011 (Fig. h), deserve particular mentioning. They differ from the other specimens assigned to the genus *Wasatchites* for their tabulate venter and flat flanks. They may be compared to *W. quadratus* (Mathews, 1929) and *Gurleyites freboldi* (Spath, 1934) instead.

W. quadratus is now considered to be a synonym of *W. perrini*, as illustrated in the paper by Brayard et al. (2013), while *G. freboldi* was erected by Spath (1934). Spath compared *G. freboldi* with the also newly erected *W. tridentinus*, as they seem to present the same *Anasibirites*-like inner whorls, but he recognised also the similarities with *Arctoprionites* concerning the flatness of venter and flanks. In other words it could be considered a transitional immature form closer to *W. tridentinus* (Spath 1934).

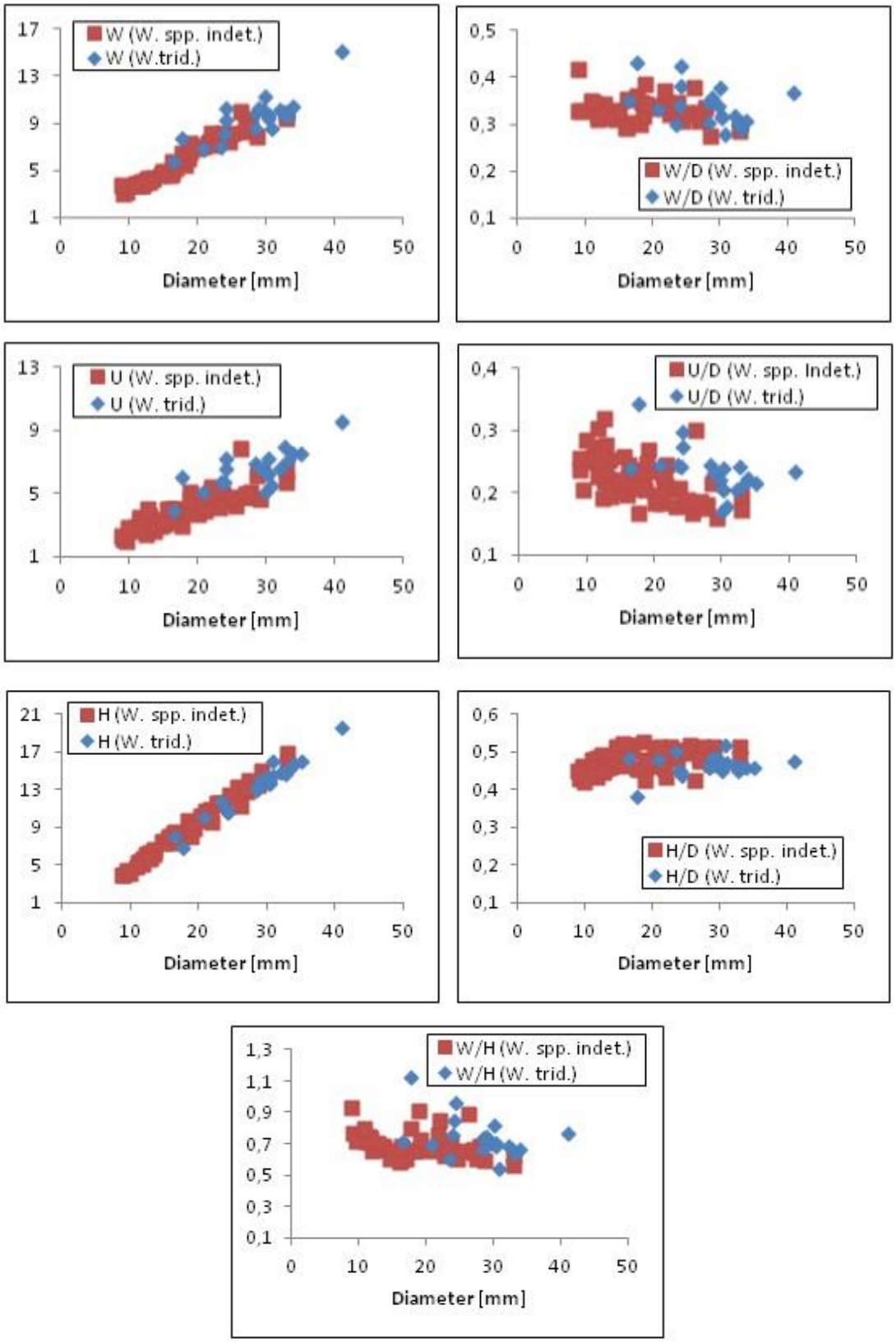

Fig. 34 Scatter diagrams for all the Wasatchites specimens in the studied assemblage (the blue points being W. tridentinus and the red points the immature individuals Wasatchites spp. indet.).

The presence of specimens such as the ones in Pl. VI, Figs. f-h, which are clearly different and may be compared to juvenile synonyms of *W. perrini*, and the fact that actually other *Wasatchites* species already described from Spitsbergen (see Spath 1934) have been synonymised with *W. perrini*, as discussed above, suggest at least that *W. perrini* may be present in the assemblage, but more similar specimens should be collected to confirm this idea. For now it was decided to keep these specimens as *Wasatchites* spp. indet.
This degree of uncertainty is proof enough of the confusion and difficulty that still persists when it comes to taxonomical studies of immature ammonoid forms.

Gen. nov.
Type species proposed. Gen. et sp. nov.

Composition of the genus. The species here described. *Anasibirites ochotensis* (Bytschkov, 1976) may also be included.

Diagnosis. Prionitid with fairly smooth shell, ornamented only by faint sinuous regularly spaced ribs, and arched venter. A constriction is observed on the specimen PMO 227.988, Pl. VII, Fig. b.

Discussion. See below for a detailed discussion.

Gen. et sp. nov.
Pl. VII, Figs. a-d

Holotype suggested. PMO 227.988 (see discussion below).

Diagnosis. As for the genus.

Occurrence. The specimens assigned to this group are rare in the whole assemblage, as their total number $N = 6$.

Type locality and horizon. Stensiöfjellet, northern Sassendalen, Svalbard. The stratigraphic level is the uppermost Lusitaniadalen Member ("Fish Niveau", Vikinghøgda Formation), *tardus* Zone ammonoid fauna (Late Smithian, Early Triassic).

Description. The shells are involute, discoidal and sub-platycones. The whorl section seems oval, but the preservation is poor on most of the specimens. The venter is commonly arched. It is smooth or very slightly ribbed, as can be seen e.g. on Pl. VII, Fig. c. The ribs crossing the venter are slightly arched to straight. The flanks are convex, especially on the body chamber.

The more depressed specimens seem to present a slightly more tabulate venter and flatter flanks. The umbilicus is moderately deep and narrow, and it gets wider and deeper in the more depressed and bigger specimens. The umbilical shoulder is rounded, with a fairly high-angled umbilical wall, whose height increases towards the body chamber. The ornamentation consists of sinuous ribs, visible mostly on the flanks and regularly spaced. A constriction on the body chamber is observed on the specimen PMO 227.988 (Pl. VII, Figs. b-c): this is the only occurrence of constrictions in the whole collection. The inner whorls look smooth/slightly ribbed. The shell is partly preserved on some of the specimens (e.g. Pl. VII, Figs. a, d) and growth lines are discernible: they are straight on the flanks and slightly arched on the venter.

The suture lines are poorly preserved and never completely visible. They are ceratitic, with elongated lobes and broad rounded saddles. The ventral lobes are also denticulated.

Measurements. Just a few specimens (n = 3) could be measured and the maximum diameter is ~ 27 mm. See Appendix 2.

Discussion. The specimens belonging to this group were assigned to the family Prionitidae, as they present characters that were observed also in the other prionitids here described. These typical prionitid features are the compressed shell, the narrow umbilicus with rounded umbilical shoulder, and the high-angled oblique umbilical wall increasing towards the body chamber.

The specimens were first compared to known prionitids (*Anasibirite*s, *Wasatchites*, *Arctoprionites* and *Hemiprionites*). They differ from the latter two by their lack of tabulate venter/flanks and from the first two by the ornamentation style: *Anasibirites* presents megastriae (Jattiot et al., *in prep.*), while *Wasatchites* is typically characterised by tubercles at maturity and regular ribbing especially at immature stages. None of this characterises the specimens.

In addition they differ from other prionitid genera mainly by the morphology of the venter, which is clearly arched. In other prionitid genera it is generally tabulate/subtabulate (such as in the genera *Prionites*, *Stephanites*, *Lucasites*) or sulcate (such as in *Meekoceras*).

The constriction observed, moreover, may be peculiar for this prionitid. It appears only on the body chamber of one specimen (PMO 227.988, Pl. VII, Figs. b-c). Since constrictions tend to appear at a later stage, it may indicate that the specimen is older than the others. If the whole shell of this specimen and of the other ones would have been preserved, it may have been possible to observe more of them.

Constrictions have not been mentioned in other descriptions for prionitids, so the erection of a new genus and new species is here proposed. The holotype suggested is the same constricted specimen mentioned above, which is the best preserved and most likely the more mature specimen of all, while the other specimens illustrated in Pl. VII (Figs a, d) would be possibly part of the paratype series.

As suggested by Bucher (2014, personal communication), the genus may also include *Anasibirites ochotensis* (Bytschkov, 1976), described by Dagys & Ermakova (1990) on pg. 47 and illustrated in pl. XIII, figs. 2-5. The ornamentation of this species is different from what would be expected of a true *Anasibirites*, and their specimen resembles the specimens here discussed.

These suggestions are however still informal and further research is required to officially confirm them and continue with a formal description and designation of types.

Family Arctoceratidae Arthaber, 1911

Genus ***Arctoceras*** Hyatt, 1900
Type species. *Ceratites polaris* Mojsisovics, 1896

***Arctoceras* sp. nov.**
Pl. VIII, Figs. a-d

Holotype suggested. PMO 210.489 (see below).

Diagnosis. Arctoceratid with arched venter and slightly convex flanks. The ornamentation consists of irregularly spaced, radial/gently sinuous folds that cross the flanks but not the periphery. Ventral strigations present only on the specimen PMO 210.489.

Occurrence. The age range of *Arctoceras* has long been uncertain, although the genus is currently considered to be of Smithian age, below the *Anasibirites*/*Wasatchites* assemblages. The genus *Arctoceras* is known from Spitsbergen, Arctic Canada, USA and Timor (Tozer 1961). The species is rare in the assemblage, as $N = 4$.

Description. Sub-involute, platycone and extremely discoidal shell. The whorl section looks rectangularly trapezoidal. The umbilicus is narrow and fairly deep. The umbilical wall is high and very steep (ca. 90°) – and it gets higher towards the body chamber. The umbilical shoulder is sharply angled. The venter is arched. The specimen PMO 210.489 (Pl. VIII, Figs.

c-d) has a keeled/bottle-neck venter on the terminal part of the preserved body chamber. It has no ornamentation but strigations are visible, at least on most of the venter. The flanks are flatter on the smaller and more compressed specimens and more convex on the more depressed ones. The specimen PMO 210.489 has a partially crushed body chamber, making it impossible to tell the original shape of the flanks. The preservation of the two smaller specimens is poor so it is hard to make comments regarding the ornamentation. However, the best preserved specimens, which are shown on Plate VIII, present folds on the flanks. Their shape is radial/gently sinuous. They are more pronounced on the specimen PMO 227.985 (Pl. VIII, Figs. a-b). The same specimen seems also to present finer striae in between the folds. The folds become also more distanced at the end of the phragmocone and on the body chamber. The preservation of the inner whorls does not allow to estimate whether they present ornamentation or not.

Only the specimen PMO 227.985 has very well preserved suture lines (Fig. 35), with two elongated, prominently denticulated lateral lobes and rounded saddles. The denticulation is very pronounced and the ventral lobe is bifurcated. The body chamber is missing but the last sutures are more approximated, so they could represent the more mature stage.

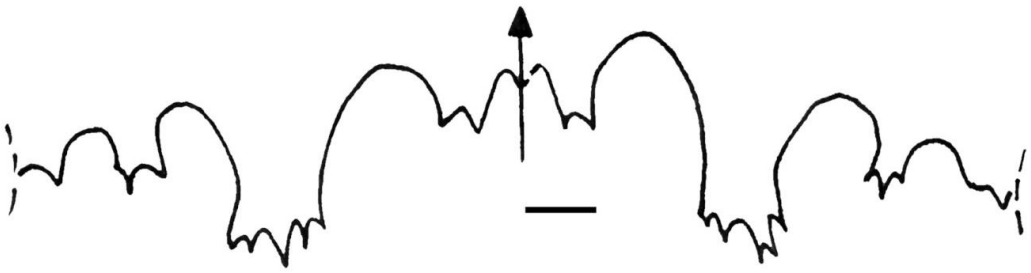

Fig. 35 Drawing of the next youngest suture line visible on the specimen PMO 227.985 (Pl. VIII, Figs. a-b) from both sides. Noted the small differences between the two sides.

Measurements. See Fig. 36 and Appendix 2. The estimated maximum diameter is ~ 32 mm.

Remarks. The specimen PMO 210.489 (Pl. VIII, Figs. c-d) seems to contain a smaller ammonoid in the body chamber just under the „keel“.

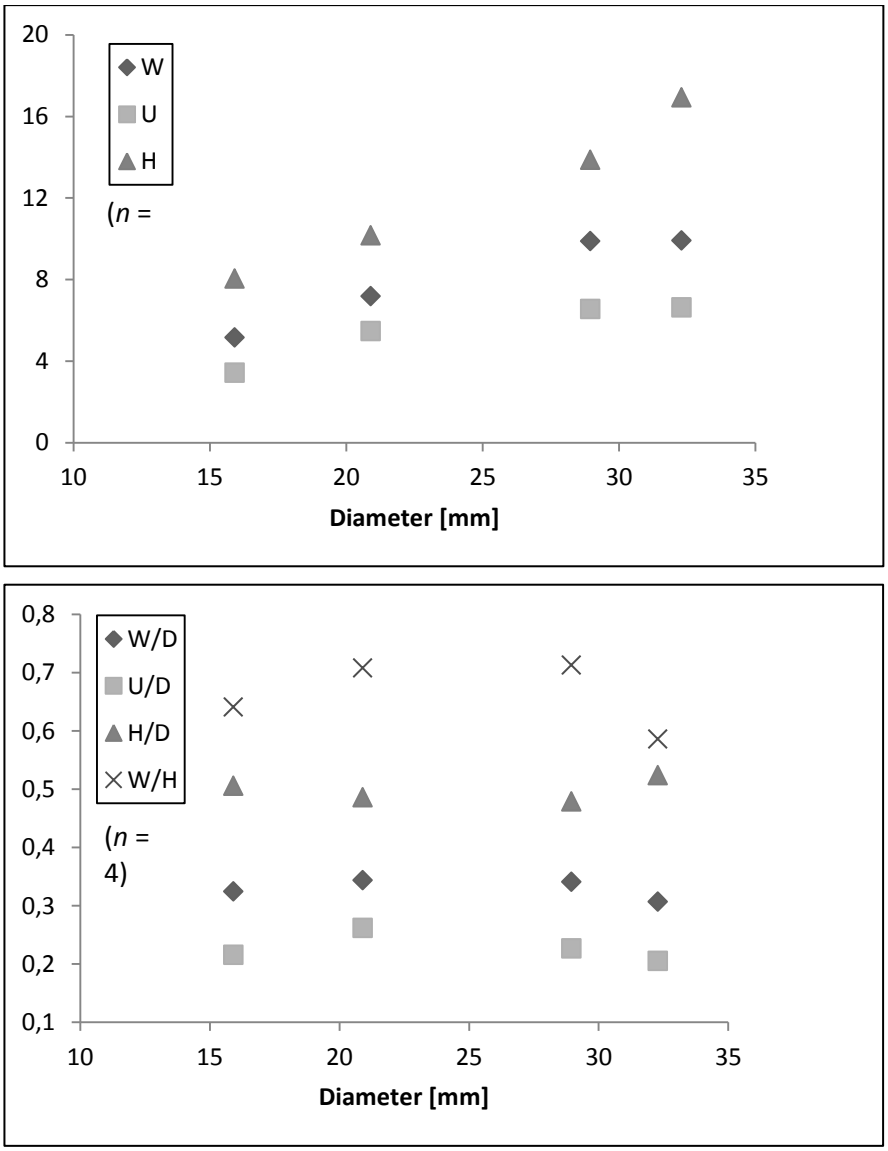

Fig. 36 Scatter diagrams of W, U, H (above) and W/D, U/D, H/D and W/H (below) for Arctoceras sp. nov.

Discussion. Arctoceratids are easily distinguished by very steep (close to 90°) umbilical walls and distanced, well defined ribs. The specimens here discussed are then assigned to this family according to the umbilical morphology, and to the genus *Arctoceras* mainly due to the shape of the venter and whorls. The erection of a new species is suggested because the specimens here studied differ from the other described species by some morphological features.

The specimen PMO 210.489 (Pl. VIII, Figs. c-d) presents ventral strigations and a partly keeled venter. Strigations are not a new feature in the genus, as seen e.g. in *A. strigatus* (Brayard & Bucher 2008), where they are most prominent on the flanks. *A. tuberculatum* also presents some weak strigations, but it is characterised by umbilical tuberculation which is clearly not present in the specimens here studied. They can be compared also with *A.*

blomstrandi, which is the main arctoceratid recorded from the Smithian beds of Spitsbergen. *A. blomstrandi* presents defined and regularly distanced ribs and umbilical tuberculation (Tozer 1994, 1961) that are not here observed. The ornamentation of the studied specimens is weaker, and the distance between the ribs is more irregular and less prominent than in *A. blomstrandi*. This species (and its synonyms) was never mentioned to develop a keel at maturity.

Keels, as constrictions, are features developed at more mature stages. Moreover, as predicted by the Buckman's law of covariation, they would be enhanced in compressed specimens and "levelled down" in depressed ones. The same specimen discussed above is therefore suggested as possible holotype for this new species, while the other specimen illustrated in Pl. VIII, Figs. a-b could be the paratype. The specimens here classified as *Arctoceras* sp. nov. are however very few and only the two illustrated are well preserved. As pointed out above in the case of the new genus, these are just informal suggestions that require further research to be officially accepted.

The finding itself of an arctoceratid at this level is very interesting. Arctoceratids are in fact more typical for Middle Smithian faunas below the *Anasibirites*/*Wasatchites* beds, and in Spitsbergen they are considered to be mainly restricted to the *romunderi* Zone. The age range has however been long uncertain, as the genus *Arctoceras* was thought previously to be much younger. Mojsisovics (1886), for example, assigned it to the Anisian while Spath (1934) and Frebold (1930) assigned it to the uppermost Early Triassic (see further information on the topic in Chapter 4 on biostratigraphy). In one locality on Ellesmere Island (Arctic Canada) *Arctoceras* is indeed associated with *Wasatchites* (Tozer 1961). The presence of arctoceratids up to this level may then indicate a vertical range of *Arctoceras* up in the *tardus* Zone, a suggestion that is actually not new in previous biostratigraphic researches of Smithian faunas in Svalbard (see Section 4.2).

8.2 Statistical analyses

Scatter plots of W, U, H and their ratios with the diameter were already presented in the systematic descriptions. In the following pages they will be briefly commented on and further statistical analyses introduced and discussed.

8.2.1 Linear regressions (RMA) and histograms

The RMA (reduced major axes regression) is a bivariate linear model which studies the relationship between two variables, trying to minimize the error ranges in both directions (Hammer & Harper 2006). The reduced major axis represents the mean estimate of the growth trajectory. This kind of plot is very common in palaeontology (Harper & Owen 1999).

The regression equation is expressed by the general formula for a straight line $y = ax + b$, where a = slope and b = intercept. When plotting RMA diagrams, these values are usually given together with standard errors and bootstrapped confidence intervals. The correlation, or the strength of the relationship between the considered variables, is measured by the coefficients r (linear correlation coefficient) and its square value r^2 (coefficient of determination). The coefficient r can range from -1 (complete correlation with negative slope) to +1 (complete correlation with positive slope). As for r^2, the closer the value is to +1, the stronger is the correlation and the residual error is smaller. In both cases, the closer these values approach 0, the lower the correlation (Hammer & Harper 2006).

All values are presented for each plot in Appendix 3. It is mentioned in particular that all the statistical analyses have given very low p values, which give further evidence that the correlations are significant.

When enough measurements were available, the variation of the whorl shape (W vs. H) of each of the identified species has been investigated in a RMA plot. This gives information about the kind of growth: isometric or allometric. Allometry mainly means that one variable changes at a different pace than the other during ontogeny. In such case the measurements do not fall on a straight line, or a sharp change in the slope of the obtained curve (called knickpunkt) is observed. If the curve is linear, then the growth is isometric (Hammer & Harper 2006).

Working with the data, a simple RMA linear regression was used. A log-log transformation is in fact recommended when the relationship is clearly nonlinear. But this process is an extra step that requires (sometimes unnecessarily) a further transformation of the data set that may

complicate the interpretation (Hammer & Harper 2006). Anyway, such a step was performed to check for possible variations in the curve shape and/or correlation coefficient. No significant changes were observed in most of the cases, so a simple regression was used and discussed. In a few instances, though, an evident increase in r^2 was obtained, indicating a better fit for the measurements than the untransformed RMA regression. In log-log diagrams, when $a \neq 1$ the growth is allometric (Harper & Owen 1999). Those instances are mentioned below when relevant.

Histograms for each measured parameter (D, U, W, H) were also plotted, and their trend compared to the normal distribution. They are useful in studying each species e.g. from a palaeoecological point of view (e.g. Hammer & Harper 2006). Knowing for example if the assemblage is mainly composed of adults or juveniles can give an idea of the environment. The palaeoecological interpretations will be presented in the next chapter.

Arctoprionites nodosus

Despite the quite few measurements, it is possible to observe a trend already in the RMA diagram (Fig. 37). At a first glance the curve seems to follow a sort of step-like trend. But, since the number of measurements is low, this trend could just be sampling noise. Therefore the increases of the curve slope at a whorl height values of 7.5 mm and 10 mm may not be true knickpunkte. Instead a very possible knickpunkt can be observed close to H = 8 mm, after which the curve slope generally decreases. While the points in the interval 8-10 mm plot almost on the axis, they seem to be random scatter around the regression line from 10 mm and up, as expected since r^2 is very high (~0.91).
What the plot surely shows is that the growth is allometric. This conclusion fits with the scatter diagram in Fig. 27: the measurements do not plot on a straight line but are more irregularly distributed; this would not be the case for isometric growth.

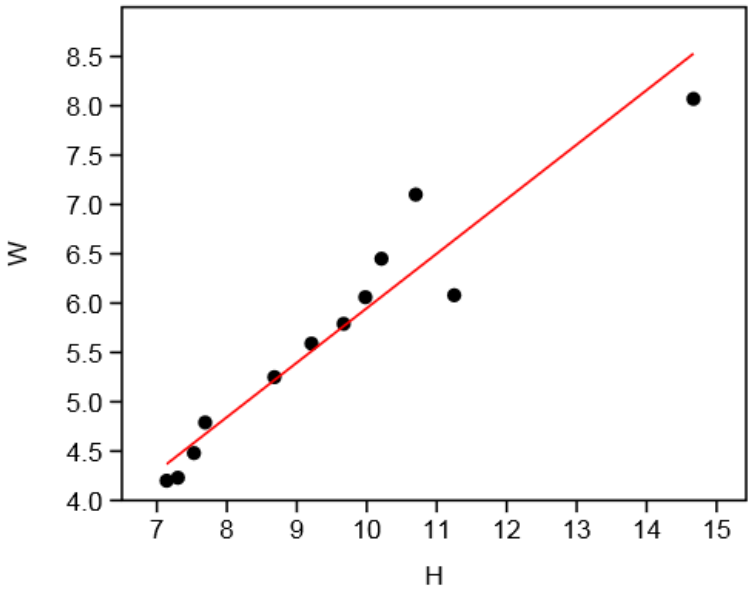

Fig. 37 RMA linear regression of A. nodosus.

An interesting variation is observed also in the histograms (Fig. 38). All of them are skewed to the right, a trend that suggests infant mortality (Hammer & Harper 2006).

From the size-distribution histogram for the diameter, it is observed in fact that there are no individuals representing the smallest sizes and quite few representing the biggest sizes. The peak is reached quickly at 18-20 mm and then there is a gradual drop. This may indicate a population where the true juveniles and adults are missing. Most of the individuals of this group have reached a certain size and very few have reached a more mature stage. As observed from the other histograms, the shell becomes progressively more involute and compressed, as it is expected from increasing maturity. The trends of H and W are very similar, though for the corresponding W values the H measurements are higher – hence a more compressed whorl section.

This conclusion regarding the immaturity of these specimens fits with the observations made on the ornamentation, which is very weak compared to the ornamented and bigger specimens of *A. nodosus*. And also it can be observed already from the scatter diagrams in Fig. 27, that there is a lack of very small and bigger shells.

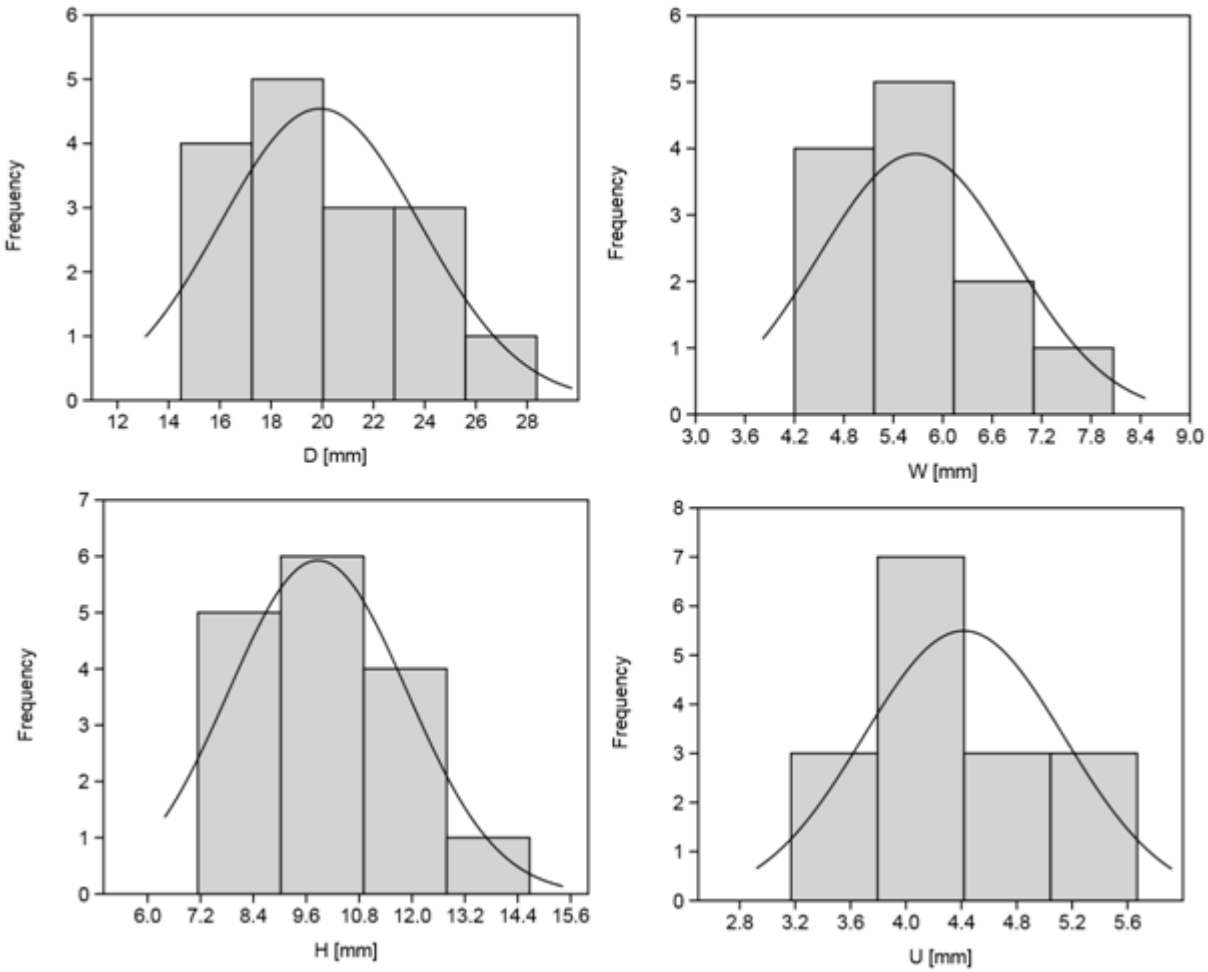

Fig. 38 Size distribution histograms for A.nodosus.

Anasibirites kingianus

As before, the RMA plot (Fig. 39) can give an indication of the kind of growth of this species, together with the scatter plot in Fig. 29. The points in this case are more widely scattered around the RMA axis (r^2 = ~0.75) and, as it is also observed in the W, U and H scatter diagrams, there seems to be no marked change in the slope. Therefore the growth trend seems quite uniform.

Considering the scatter diagrams in Fig. 30, where the data from Timor are included, it is possible to see some allometry. This sounds contradictory as it is not observed in either Fig. 39 or Fig. 29, as mentioned above. A possible explanation is considered below.

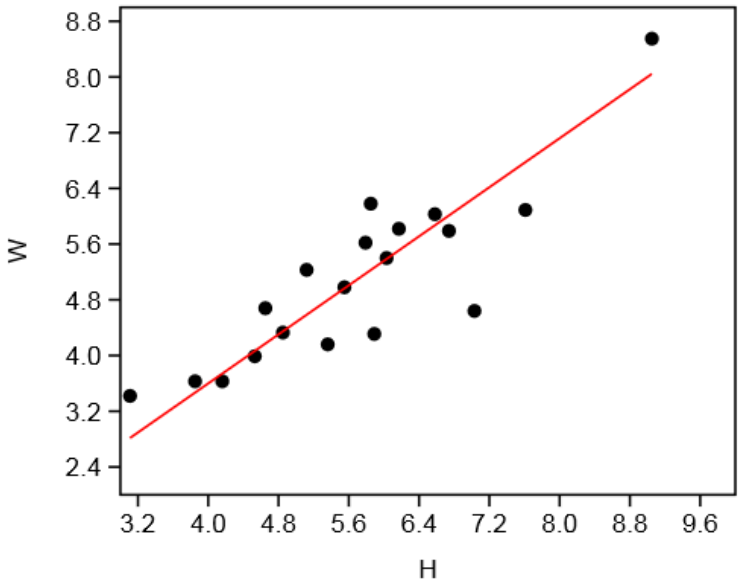

Fig. 39 RMA linear regression for A. kingianus.

As for the histograms (Fig. 40), three of them show a skewing to the right, but H and D show a quite symmetrical trend. The truly juvenile individuals are again here under-represented and the same is true for the fully adult forms. Most of the specimens in fact belong to the group with a diameter range of ~11-16 mm.

As mentioned above, the size-distribution histogram for D is closer to a symmetrical trend compared to the others. Putting together the results of the scatter plots of Fig. 29 and the RMA plot, it can be confirmed that the *A. kingianus* assemblage here studied then represents a juvenile population with a quite regular size distribution. The specimens may represent individuals from the same year class, although the size range is quite large. This explanation would account for the lack of allometry in the studied *Anasibirites* population, when allometric growth in this genus is been documented with other data.

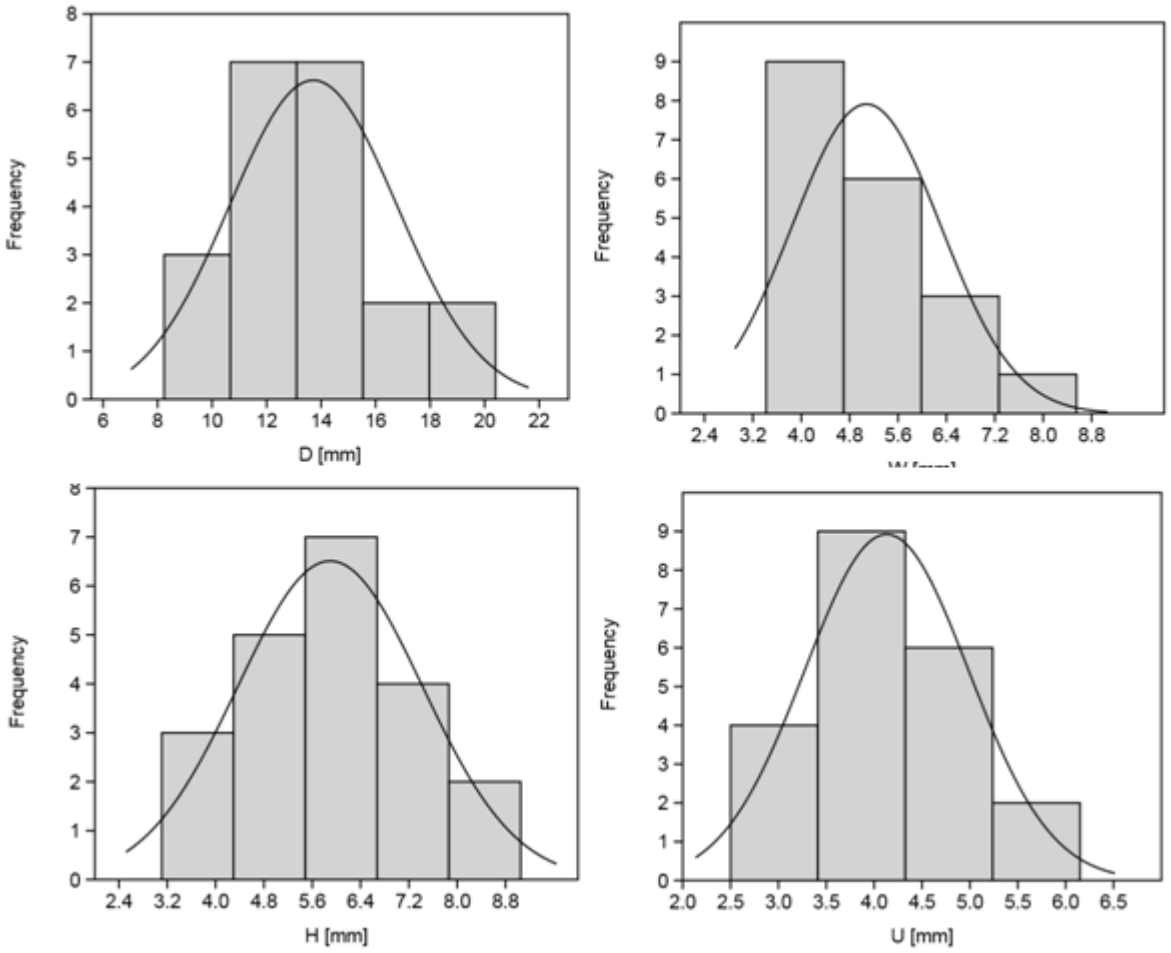

Fig. 40 Size distribution histograms for A.kingianus.

Wasatchites tridentinus

As mentioned in the previous chapters, the specimens assigned to this group are the ones considered to be more mature and adults.

The RMA regression (Fig. 41) does not show any particular slope change as observed in the previous instance. The points are quite scattered, as r^2 = 0.61, and no particular trend is observed. The data look therefore isometric, despite the fact that, checking in addition the log-transformed curve, the slope is less than 1. This could be an effect of the lack of more measurements. Allometry may be more likely observed in juveniles that were not included in this sample: at adult stage the conch shape becomes more regular (as can be observed also in the previous regression plots) and that would explain the more isometric trend of this data set. In Fig. 32, there seems to be a change in the relation between W and H – the smaller specimens have a higher W/H ratio (more marked depression), which decreases in the bigger

specimens (further compression). But again there are too few points to support with certainty such change, and the growth looks on the whole quite constant.

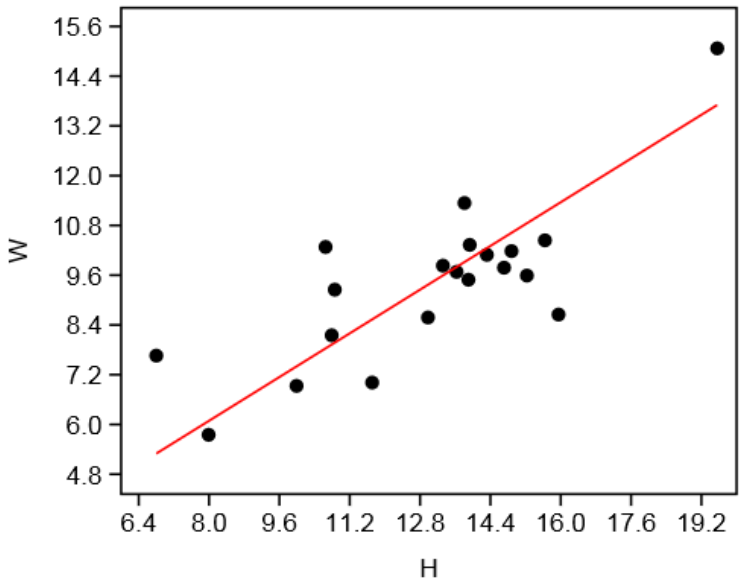

Fig. 41 RMA linear regression for W. tridentinus.

The size-distribution histogram of D (Fig. 42) shows, in opposition to the other two cases, a skewing to the left. This fits with the assumption of a population formed by more mature individuals: left skewing is in fact related to adult mortality (Hammer & Harper 2006). A maximum size of 30-35 mm is reached and then an abrupt drop in size follows. This sharp division is clearly visible also in the scatter diagrams in Fig. 32. The truncation in the histogram may be due to a limitation in size. Such a trend may then be explained as a predominance of sub-adult individuals, fitting with the comments made regarding the ornamentation. The proper adult stage of *W. tridentinus* is characterised by prominent tubercles and faint ribbing. Most of the specimens here studied present instead both of these features, indicating an intermediate stage between immaturity and maturity.

Also the other histograms (Fig. 42) present a drop in the number of specimens after reaching a certain value of W, U and H. The histogram for U is however the one which is most markedly left skewed, while the other two look slightly more symmetric. The outlier (isolated bar) in the W histogram is due to a lack of measurements for the intermediate size.

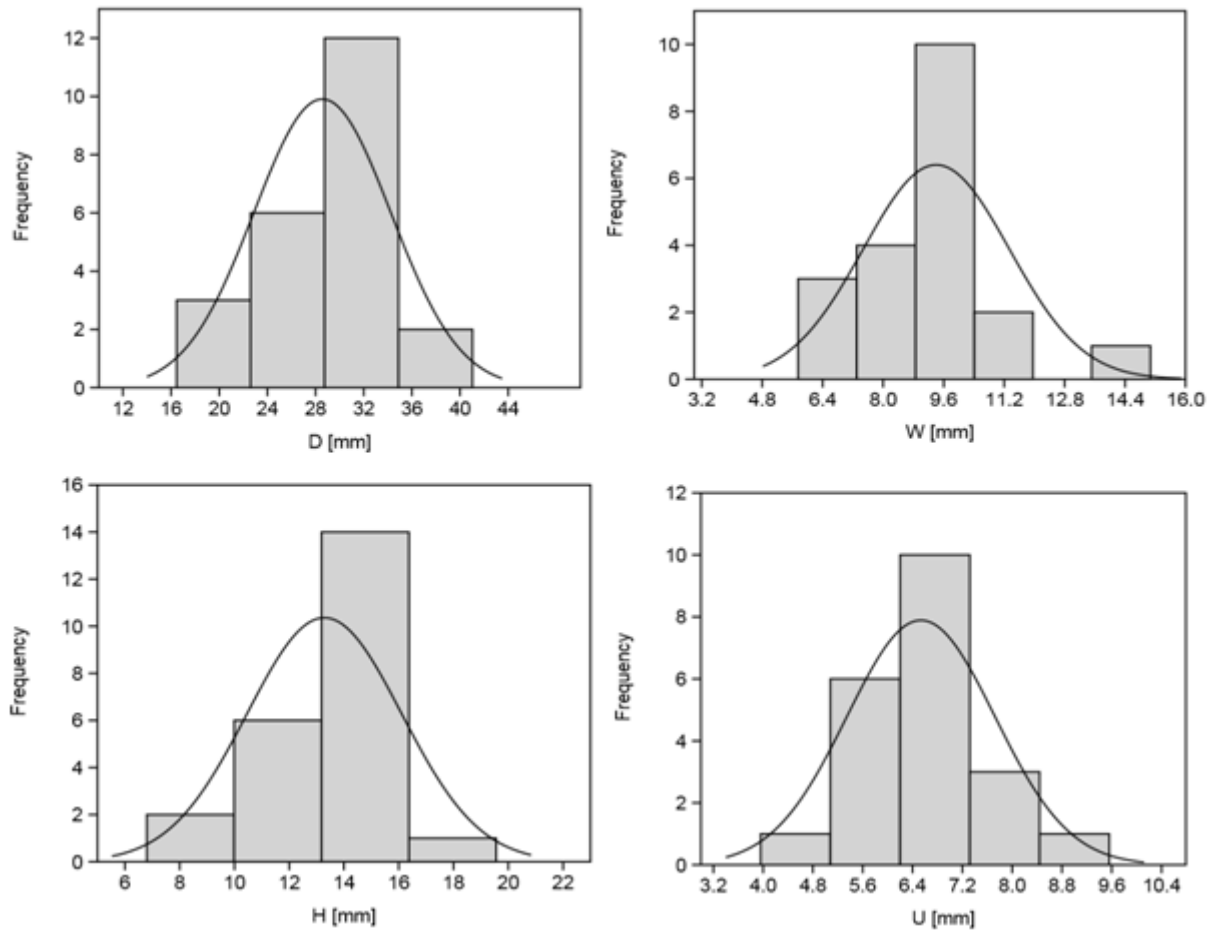

Fig. 42 Size distribution histograms for W. tridentinus.

Wasatchites spp. indet.

Changing curve trends are clearly visible both from the RMA (Fig. 43) and the scatter plots in Fig. 33. Especially in the scatter plot showing the ratios W/D, U/D, H/D and W/H it is evident that the morphology changes with increasing diameter. The trend of W/H is similar as for the other species: like among most ammonoids, the shells become more compressed. Again, in accordance with the Buckman's law of covariation, the shells also become more involute (U/D decreases). In all the plots the slope change takes place around a diameter of 15 mm.

In the RMA plot the curve presents a clear slope variation around a H value of ~8 mm (the average slope of the points before this value is highlighted by the dashed axis), as there is an increase in steepness of the curve. After that the specimens are scattered around the axis, though quite many seem to plot more closely and regularly around it. That's evidence of allometric growth. The fact that the curve between ~4-6 mm is located above the RMA axis while the one between ~7-9 mm is located below may be a simple consequence of having

fitted a straight line to the overall upward curving trend of the data set. There is therefore no particular interpretation.

This data set shows a significant improvement in r^2 with log transformation, as it increases from ~0.88 to ~0.96 (see Appendix 3 for comparisons). The slope in the transformed plot corresponds to a = 0.915 and the confidence interval for a (0.824 – 0.978) does not include 1, which fits with allometry. To be consistent in the analysis, and since the shape of the curve is the same in the simple and in the log-transformed regressions, a non-transformed RMA regression is preferred despite the improved correlation and better fit of the logarithmic curve.

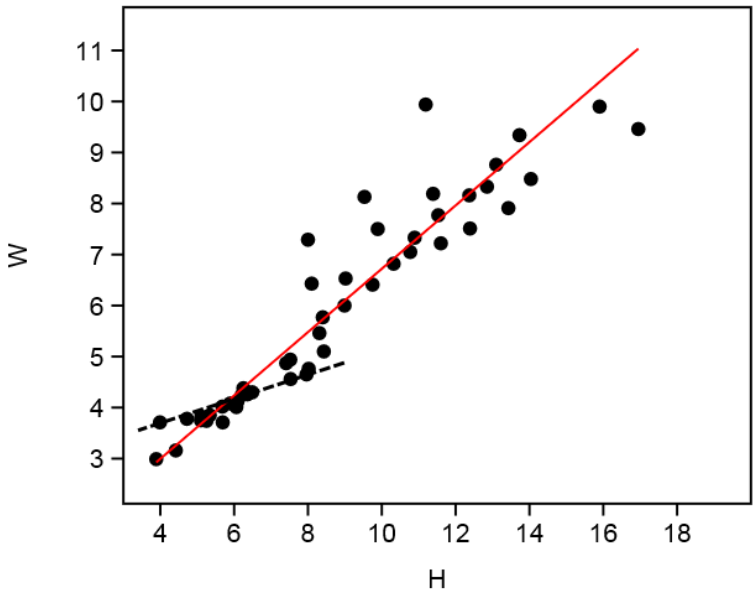

Fig. 43 RMA linear regression for Wasatchites spp. indet. *The solid line is the true RMA axis, while the dashed line was added to show the change in slope.*

The size distribution histograms are presented in Fig. 44.

There is a marked skewing to the right but no tail on the left in most cases. Most of the specimens fall in the category characterised by minimum values of D, W, U and H. This is followed by a quite gradual reduction of frequency of the larger specimens. Interestingly, this matches with the marked trend changes that were discussed above. The groups in the histograms located before the sudden drop correspond indeed to the specimens that plot before the diameter values of 15 mm, where the slope changes occur. In the RMA plot (and in the W and H histograms) it corresponds to a whorl height value around 7 mm and to a whorl width value around 5 mm.

Such trends, in a similar fashion as in the previous cases, may be explained by the lack of true juveniles and by limitation in size that an immature individual can reach.

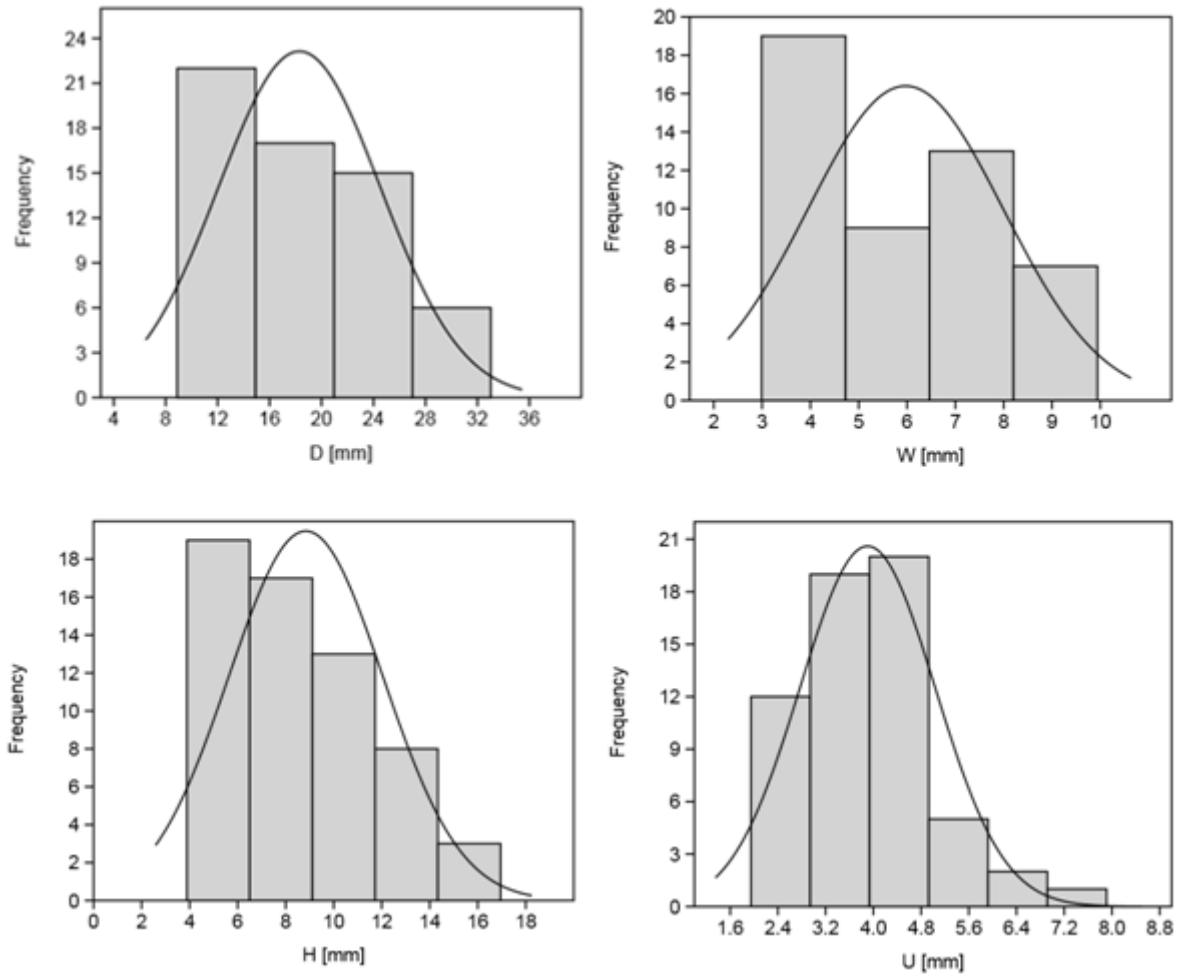

Fig. 44 Size distribution histograms for the juveniles Wasatchites spp. indet.

Wasatchites spp.

At this point it was considered interesting to analyse all the measurements obtained for the *Wasatchites* specimens in the same diagrams. This was tried already in the previous section (see the scatter diagrams in Fig. 34).

In those diagrams it is observed a quite strong overlap between the two categories of *W. tridentinus* and *Wasatchites* spp. indet. The same observations regarding the allometric growth of *Wasatchites* pointed out in the previous section are valid, and are even more visible in such scatter plots since the number of values is larger. This may suggest continuity between the two groups.

The overlap is also observed in the RMA plot (Fig. 45) as in the previously presented scatter diagrams. The overlap area likely includes the specimens that are intermediates between the more juvenile and the more adult forms, assuming that the specimens all belong to the same species.

As expected, since the logarithmic transformation improved the correlation of *Wasatchites* spp. indet., also in this case there was an increase in r^2, which went from ~0.86 to 0.89. The slope a = 0.963. However, for the same reasons explained previously, the simple RMA regression is presented and used.

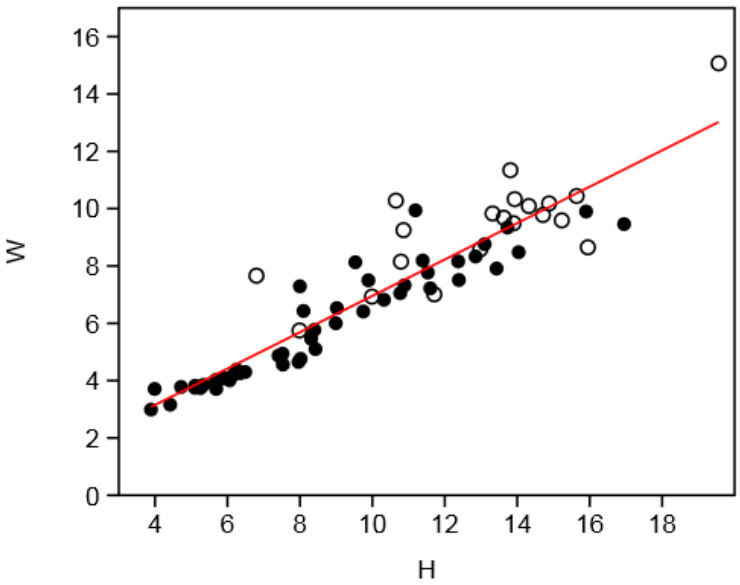

Fig. 45 RMA linear regression of Wasatchites spp. *The black points represents the measurements for Wasatchites* spp. indet., *while the white points are the ones for W. tridentinus.*

Viewing the histograms (Fig. 46) can give a more complete overview of the distributions. The distributions are actually very similar to the ones obtained for the immature *Wasatchites* specimens: a marked skewing to the right as there is a drop after a defined size category, suggesting juvenile mortality. This indeed shows that the smallest juveniles are lacking in the assemblage, though most of the population is still immature. The individuals that have reached maturity are indeed very few.

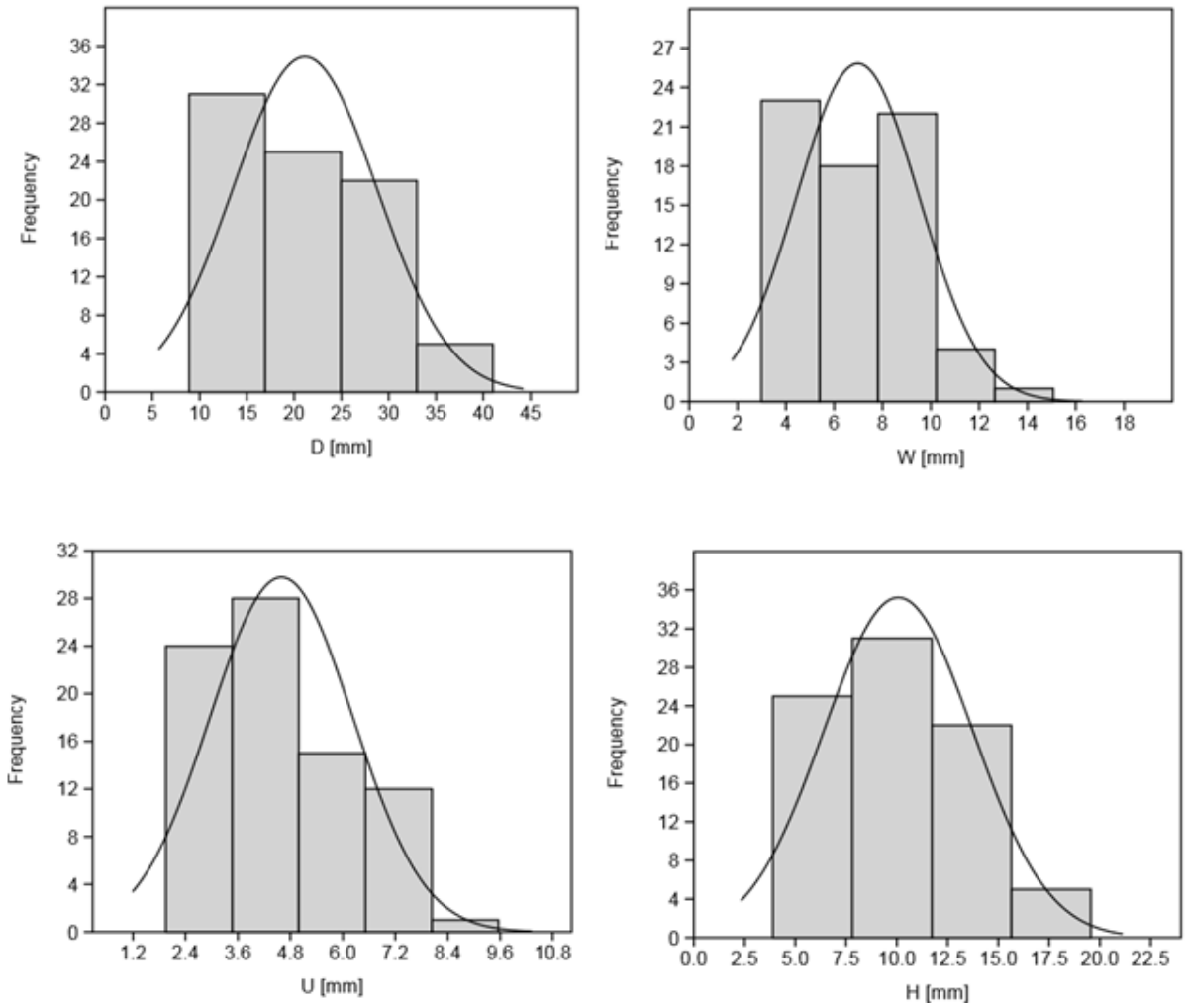

Fig. 46 Size distribution histograms for all Wasatchites specimens.

8.2.2 Multivariate analyses: PCA vs. LDA

Multivariate data are common in morphometrical studies, as many variables are considered for each specimen. The multivariate analysis permits to relate all these variables to find relationships that would be hard to see by just analysing the variables one by one. Both the discriminant and principal component analyses that were used in this project belong to the group of methods of ordination. Using both of them can be useful to get a deeper insight on the data set and help get a more complete interpretation (Smith 1999; Hammer & Harper 2006).

The background of Principal Component Analysis (PCA) and Linear Discriminant Analysis (LDA) is quite similar, as both these methods involve the projection of the data into a new set of dimensions, where the unnecessary information is ignored, to make their visualization

easier. In both methods, the data are therefore plotted in scatter, bidimensional diagrams, where the two axes represented yield most of the information. The amount of information yielded by each axis is given by the eigenvalues and eigenvectors.

The PCA is considered first in more detail.
The PCA takes its name from the set of axes, or principal components, that represent the directions where the data are mostly spread out, or in other words the combinations of variables that account for most of the variance. The axis that represents the maximum variation is the PCA axis 1. PCA axis 2 is perpendicular to the first one and accounts for the next largest variance. On such a plot it becomes easier to determine the relationships between the various groups in which the whole data set can be divided: similar points are grouped close together (Etter 1999; Hammer & Harper 2006). The total percentage of variance of the axes is equivalent to the total variation of the original variables. Therefore, if the number of axes needed to express the variation is the same as the number of variables it would often mean that the original variables were not correlated (Smith 1999).
The eigenvalues and eigenvectors give, as mentioned above, indications on the amount (or magnitude) and direction of the variation (Harper & Owen 1999). The eigenvalue represents the percentage of the total variance of a single axis. The first axis has therefore the highest eigenvalue, followed by the second highest and so on (Etter 1999).
The eigenvectors represent the loadings, the contribution of each variable, therefore the higher the loading, the greater has the variable contributed to the variance of the axis. Often one or a few variables are dominant and become characteristic for the axis (Smith 1999).

The LDA is similar to PCA and it is constructed in a similar fashion (two main axes that concentrate most of the information and related to eigenvalues and eigenvectors), but this method highlights the differences within and between the groups in a data set and finds the strongest divisions. The analysis determines then the orientation of the maximum separation between samples: this is the discriminant (Smith 1999).

In summary, while the PCA represents the maximum variance in a data set, the LDA maximizes the differences or the discriminant variables.
These two methods permit then to study the similarities and differences between the groups of samples and investigate the relationships between the various groups within the data sample, and in general analyse the total variation of the whole data set and/or a taxon. In such a way,

the validity of a species can be investigated, as well as the intra- or interspecific variation (Smith 1999).

Principal Component Analysis

The PCA shows a great overlap between the different groups (Fig. 47). The PCA axis 1, which accounts for most of the variation (~97%), is dominated by the size variable, the diameter, which bears a loading of ~0.86. The loadings for the other three variables are much lower. Bar diagrams of the loadings for PCA axis 1 are shown in Fig. 48, while the values of the loadings and eigenvalues are presented in Appendix 3. This result fits with the observations, since the whole ammonoid assemblage presents a high variation in size.

As for the PCA axis 2 (which accounts for ~2.1% of the total variance), the most influent variable is the whorl width W, having a loading of ~0.77. As observed from the bar diagram in Fig. 49 and from the values presented in the Appendix, there is a negative relationship between the variables D and H and the variables W and U. This means that, with increasing diameter and whorl height, the whorl and umbilical widths decrease relatively. In other words the bigger the specimens, the more compressed and involute they become and vice versa. This also fits with the observations.

Returning again to Fig. 47, it is observed how most of the specimens fall in the range of smaller (left half of the plot) and intermediate sizes, very few of the largest sizes (right half of the plot). The diagram moreover confirms that: the specimens of *Anasibirites kingianus* are small with quite quadrate whorl section (have positive values on the PCA axis 2). The juveniles of *Wasatchites* have on the contrary mostly negative values on the PCA axis 2, as most of the other specimens of other groups. This means that they present a more compressed whorl section. As expected, *Wasatchites* cf. *distractus* plots on the far right above corner, as it includes the largest, most evolute and thickest specimens.

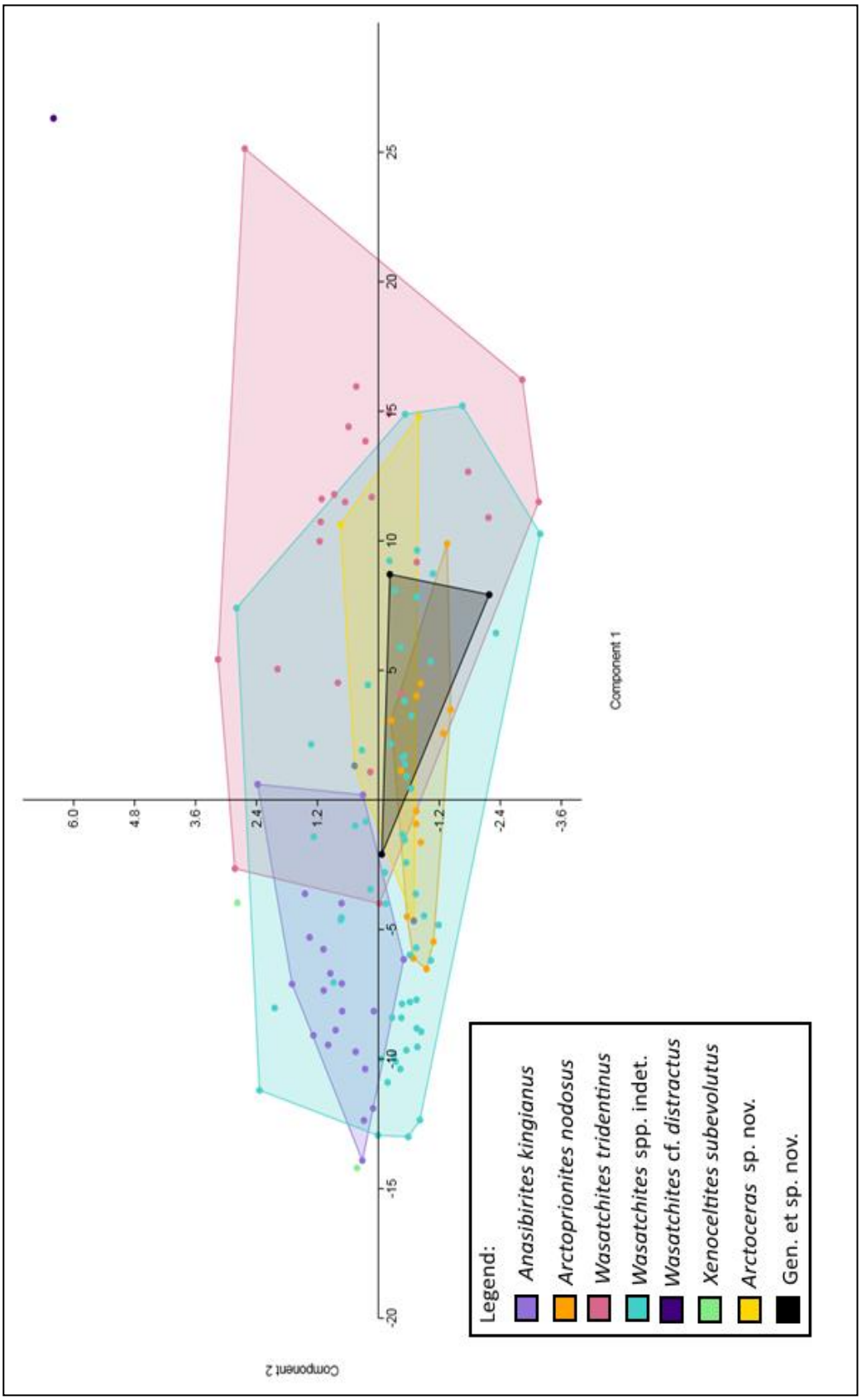

Fig. 47 Principal Component Analysis of the studied assemblage.

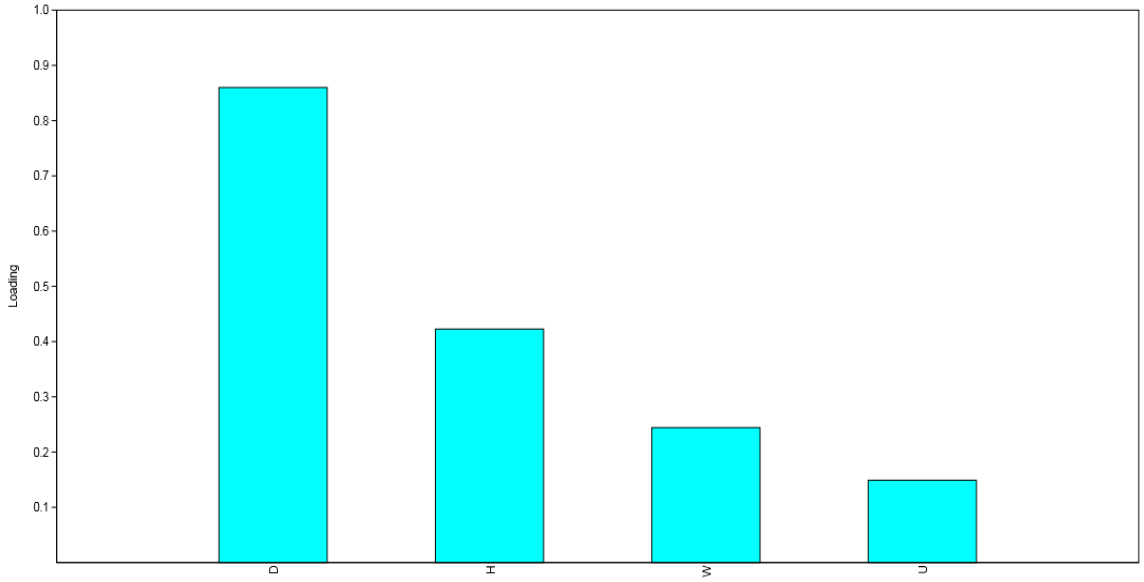

Fig. 48 Loadings for PCA axis 1.

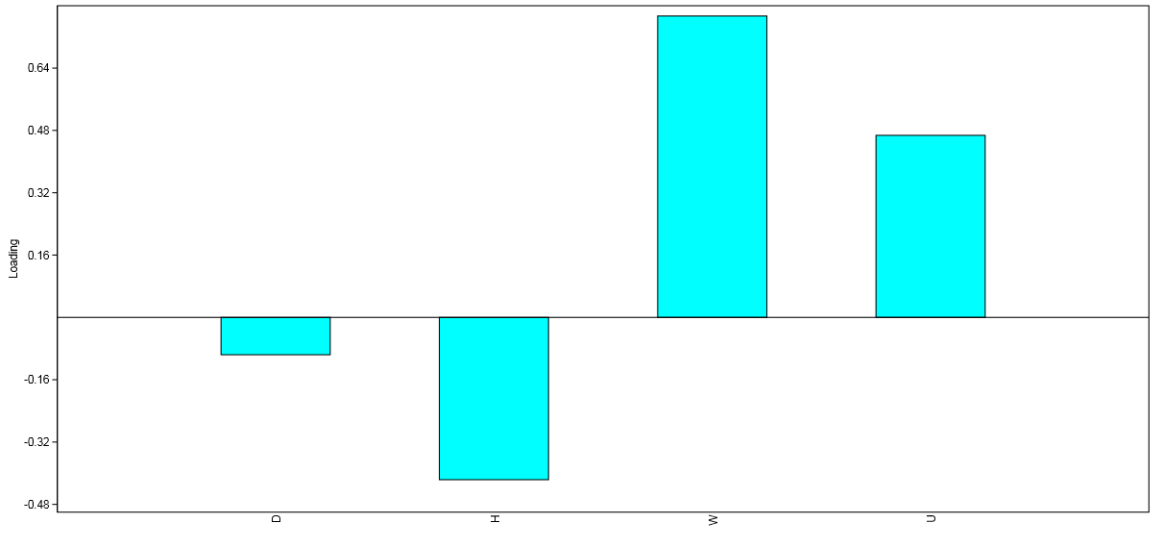

Fig. 49 Loadings for PCA axis 2.

Discriminant Analysis

As for the PCA, the discriminant analysis plot (Fig. 50) shows a great overlap between the different groups.

Axis 1 accounts for ~54% of the variation, while Axis 2 for ~23% (see Appendix 3). As in the PCA, the most influent variable on Axis 1 is the diameter, which bears a loading of ~3.2. The other variables have less significant positive loadings. That means that the most discriminant factor is the diameter size, as expected. The diameter is also the most significant variable on Axis 2, where it presents a loading of ~ (-4.4). All the other variables have also negative loadings, suggesting that no variable is actually significant to further separate the groups.

The observations above are evidence that from the discriminant analysis not enough separation is provided in order to separate most of the species, but it is to be noted that the variables analysed do not explain all the differences between the studied taxa. In fact, the species are defined also by the kind and degree of ornamentation (that is clearly different in the specimens observed) and such features are not counted in the analysis. The overlap may then be explained as a convergence of morphologies, as Fig. 25 had already suggested. Anyway, observing the plot (Fig. 50), it can be observed that *A. kingianus* is quite distinct from e.g. *Arctoceras* sp. nov., *gen. nov.* and *Arctoprionites*; it can also be partly distinguished from *W. tridentinus*. No further relevant separation is indicated by the third LDA axis as, as shown in Appendix 3, the loadings are mostly negative and very low.

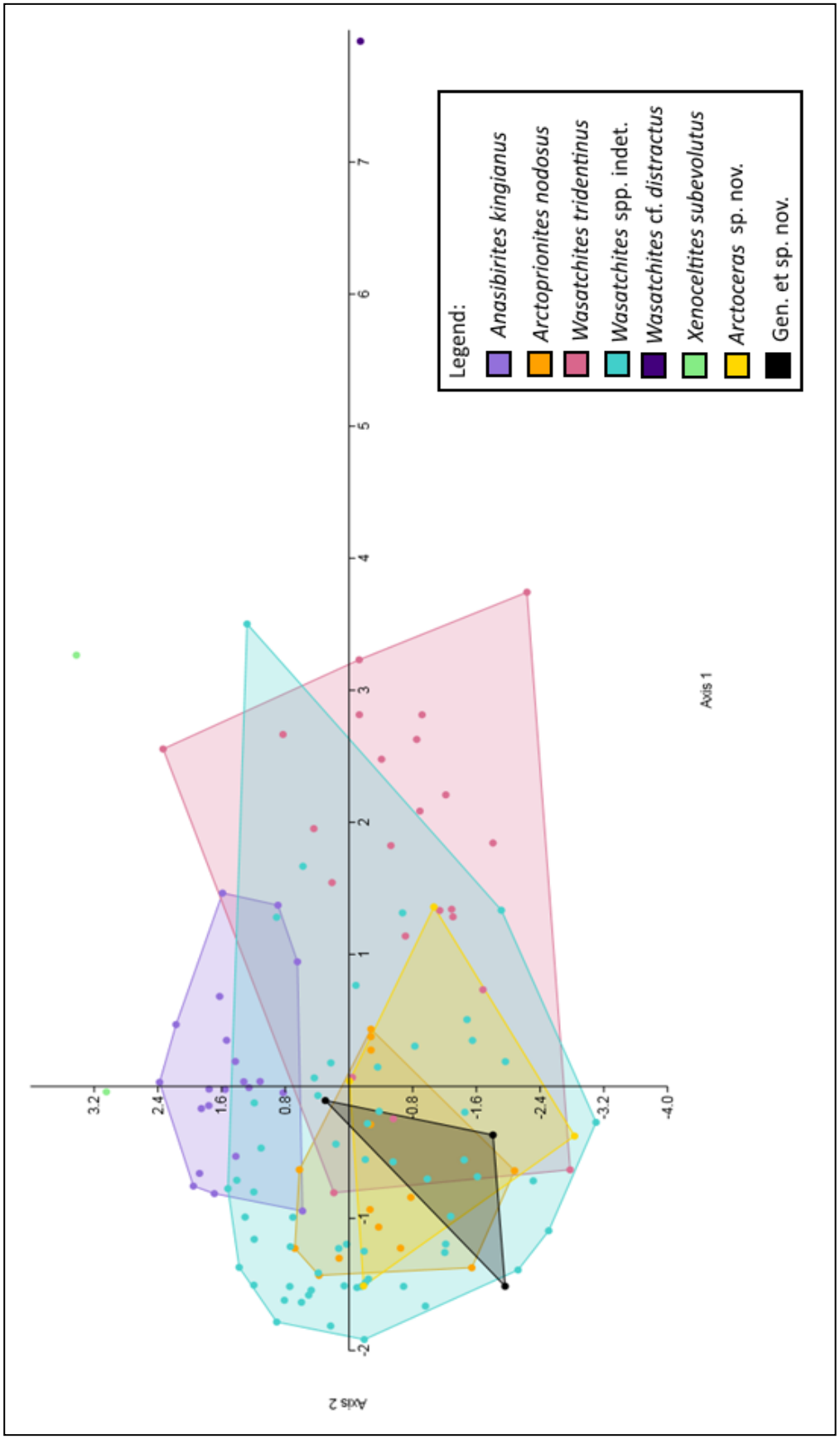

Fig. 50 Discriminant Analysis plot of the studied assemblage.

9. Interpretations

In this chapter the results are discussed to infer miscellaneous information about biostratigraphic and taxonomic implications, taphonomy, palaeoecology and palaeogeography.

9.1 Taxonomy and biostratigraphy

The studied collection provided good material to study the intraspecific variation, typical of Boreal Triassic ammonoids. The most significant variation is observed in the genus *Wasatchites*, as it is the most abundant. Species in the genera *Anasibirites* and *Arctoceras* also present usually high variability, but further observations on the matter were prevented by immaturity in the case of *Anasibirites* and by the lack of additional specimens as concerning *Arctoceras*. As most of the individuals are juveniles, it is difficult to distinguish the different groups just by considering the basic parameters, as discussed in the section about multivariate analyses. The shell morphologies seem to converge towards the discoidal and partly involute type and most of the variation is represented by the wide range of ornaments.
The species here studied present allometric growth. Explanation of this trend is the natural growth change and the need to maintain functionality as the size increases (control of buoyancy, manoeuvrability, propulsion and drag) (Foote & Miller 2007; Brayard & Escarguel 2013). This is very common in ammonoids and these results fit with the literature.

Considering in more detail the composition of the ammonoid fauna, the studied assemblage is on the whole in good agreement with other Late Smithian assemblages all over the world, which are dominated by prionitids, especially *Wasatchites* and *Anasibirites*. The presence of *Xenoceltites* is not a surprise either, since, as mentioned in Chapter 4, in Svalbard it is found associated with *Wasatchites*.

Most interesting is the finding of arctoceratids at this level. As discussed in the previous chapters, the stratigraphic range of the genus *Arctoceras* has long been uncertain. It has been considered to range up to the *tardus* Zone (e.g. Kummel 1961; Weitschat & Lehmann 1978), though arctoceratids are generally considered to be more restricted to the older *romunderi* Zone. Findings of arctoceratids (the *Arctoceras* sp. nov. at Stensiöfjellet and *Arctoceras blomstrandi* at Botneheia (Weitschat & Lehmann 1978)) can therefore most likely confirm the

long range of this genus up to the uppermost Smithian, with *Arctoceras* sp. nov. in particular possibly restricted to the *tardus* Zone. Condensation may also be an explanation to be considered, and that could be a reason why *Xenoceltites* is in Svalbard (and in Queen Elizabeth Islands) associated with *Wasatchites* while in most localities worldwide it is located in the overlying zone.

The division of the Smithian as presented by Korčinskaja in 1986 (see Section 4.2) with a single *Arctoceras blomstrandi* Zone subdivided into *romunderi* and *tardus* subzones is here not reconsidered. The typical standard division in three ammonoid zones for the Boreal Smithian is kept, since the new taxa here discussed may be peculiar of the ammonoid faunal assemblages in Svalbard, and the material available is considered to be insufficient to justify changes in the biostratigraphic zonation.

Concerning the finding of a possible new prionitid, it is pointed out in the discussion regarding this new genus that it can be compared to a described species from the Late Smithian of Siberia (wrongly) assigned to the genus *Anasibirites*. This similarity may represent a common point between Svalbard and the Siberian Province. It would be interesting for future biostratigraphic implications if this genus is present also in other areas within and/or outside the Boreal Realm (see also Section 9.4 below).

The studied fauna is also characterized by the newly recorded species from Svalbard *Arctoprionites resseri* and by the species *Wasatchites* cf. *distractus*, new in the Boreal Realm. Both are typical for the *tardus* Zone and are fitting in the assemblage as what concerns the age. *Arctoprionites resseri* has previously been recorded from Canada, strengthening the correlation and similarities with the Canadian Province. Further evidence of this is the presence of *Arctoprionites nodosus*, which is only found in Arctic Canada outside Svalbard. *Wasatchites* cf. *distractus* may in a similar fashion be used to strengthen the biostratigraphic correlations with the Tethyan Realm, in regions such as Salt Range, Spiti and Tibet where the Boreal *tardus* Zone is represented by the *W. distractus* Beds (or more precisely its lower part, as at lower palaeolatitudes the Late Smithian is divided into *Wasatchites*/*Anasibirites* and *Glyptophiceras* Beds, a division which is not extended to higher latitudes. Refer again to Fig. 10).

9.2 Taphonomy

The specimens are on the whole in good condition and in some instances the body chamber is partly preserved. When present, it occupies at most half a whorl. The presence of the body chamber is best determined when the suture lines are visible, as they get more approximated when approaching the end of the phragmocone. The body chamber itself is not chambered. When the suture lines are not visible, and it is therefore not possible to infer if the body chamber is present or not, increasing maturity is indicated by the changing proportions between whorl height H and whorl width W (the whorl section becomes more convex) and by the decreasing ornamentation degree (with associated increasing distance between ribs/megastriae). Moreover, typical features of maturity such as keels (see PMO 210.489, Pl. VIII, Figs. c-d) and constrictions (see PMO 227.988, Pl. VII, Figs. b-c) are also observed, but they are very rare.

The assemblage presents signs of diagenetic processes.

As discussed previously, the specimens are mostly internal moulds, which remained after the sediments had filled the empty space left by the soft parts and after the shell dissolved. Parts of the shell are occasionally preserved, whose original aragonitic composition, as expected, has been substituted by the more stable calcite. Calcite and mud infills are observed in several specimens (e.g. PMO 228.011, Pl. VI, Fig. h), and in some cases pyrite crystals are also present. In some particular instances it is observed that the calcite and mud infills are almost equally distributed as shown in Fig. 51. That indicates that such shells lay on the sea bottom: the part in contact with the sea-floor was filled with fine siliciclastics and the other half was later filled with calcite (Hryniewicz 2014, personal communication), forming a geopetal.

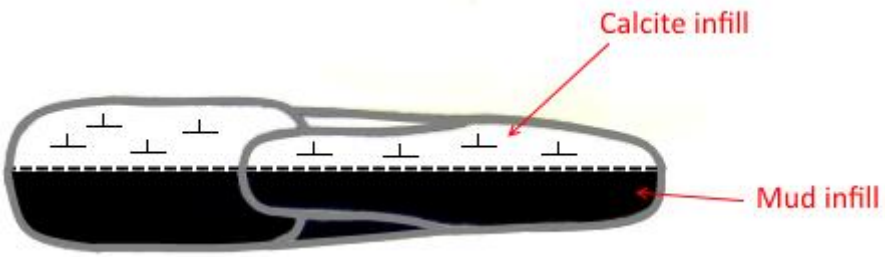

Fig. 51 Infill pattern observed in some of the specimens. This kind of infill pattern is called geopetal void fill, or geopetal infilling.

Some evidence of breakage/collapse and diagenetic compression is observed, but they are not very common. The best example is represented by the specimen of *Arctoceras* sp. nov. PMO 210.489 (Pl. VIII, Figs. c-d), which has a partly crushed body chamber and is unevenly

compressed, probably as an effect of the compression from the accumulating sediment. This may occur soon after burial. The body chamber is the most fragile part, since it is usually bigger and not sustained by the septal walls like the chambers in the phragmocone, which are therefore more resistant to crushing (Benton & Harper 2009a). No other evident sign of further physical (e.g. fragmentation, abrasion) or chemical (e.g. bioerosion, corrosion) breakage is observed.

The ammonoids were found originally with nautiloids and bivalves, the latter in some cases attached to the shells. Apart for the specimens with geopetal infilling (for which the calcite-filled part indicates the way "up"), no information about the orientation of the other fossils in the concretion is available. The formation of the carbonate concretion itself is also a diagenetic process. Such concretions usually form early in the diagenetic process, as evidenced by the generally good and uncrushed preservation of the enclosed fossils (Benton & Harper 2009a).

From these observations it is concluded that, if not completely *in situ*, the deposition occurred in a low-energy environment. These observations fit with the geological setting, as the Lusitaniadalen Member was deposited in a moderately deep shelf environment (see Section 2.3.2).

Moreover, it may be deduced from the inclusion itself of the fossils in a carbonate concretion that the depositional or diagenetic environment was supersaturated in $CaCO_3$. In $CaCO_3$ poorer locations the fossils would have been on the contrary more easily flattened and shells dissolved (Nakrem 2014, personal communication).

9.3 Ecology

The abundance of all the species (N, as referred to in Chapter 8), has been plotted in a bar chart in order of descending abundance (Fig. 52). This can give an indication about the diversity of the studied assemblage. It is observed that the histogram plot is right-skewed and that most of the species are relatively uncommon. This is a typical pattern in relative abundance diversity studies.

Just six genera are present, all of them prionitids except for *Arctoceras* and *Xenoceltites*. The composition and the low diversity of the assemblage are on the whole consistent with the other Late Smithian faunas, as mentioned in Section 9.1 above.

As in British Columbia, the studied assemblage presents common *Wasatchites* but rare *Xenoceltites*, which is the opposite of the section studied by Weitschat & Lehmann (1978) at Botneheia. This disparity may be due to various factors: it could be a result of the collection method or of the uneven distribution of *Xenoceltites* in the concretion itself and in different areas.

As discussed previously in the section about statistical analyses, the assemblage is mainly composed of immature individuals (lacking true juveniles and adults), matching the kind of assemblage composed of immature individuals of one dominant genus described by Dagys & Weitschat (1993b) (see Section 3.2). The size range is large but, as indicated by the histograms, at least the specimens of *Anasibirites kingianus* may belong to the same year class. If that is the case, the assumption can be made that a significant juvenile mortality occurred over a short period of time.

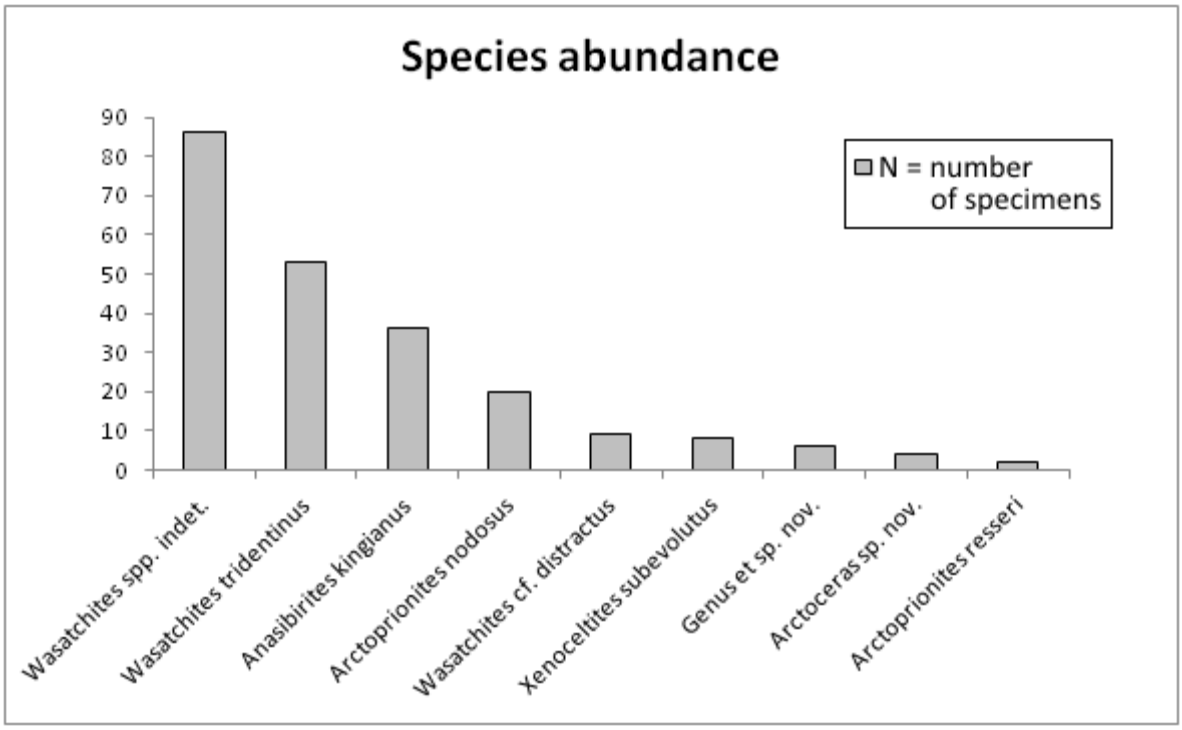

Fig. 52 Abundance bar plot, with the identified species plotted in descending order.

Comparisons can be made with modern cephalopod groups. Many species come together for breeding and spawning, so that the resulting assemblage would be composed of adults. This is clearly not the case for the current material, which may instead be evidence for gatherings of immature individuals e.g. for foraging for food or until maturity is reached (Walton et al. 2010). This may indicate that a separation occurred between adults and immature individuals. The structure of the studied assemblage moreover implies that juvenile mortality was high,

probably due to natural causes (in a similar fashion that many modern animals give birth to numerous offspring that mostly die at a young age), or may be related to the unstable conditions during the latest Smithian.

As Fig. 9 in Section 3.1 illustrates, the change in ammonoid faunal diversity from Middle to Late Smithian is very significant and decreases approaching the Spathian. This is typical for Late Smithian assemblages all over the world. A possible explanation for the diversity drop may lie in the unstable ecological conditions. Anoxia and hypercapnia (high CO_2 concentration) were common during the Early Triassic. Such conditions seem to have ended at the Smithian/Spathian boundary (Brayard et al. 2009). The renewed diversity during the Spathian is congruent with the recovery of other marine invertebrates with improved shelf environmental conditions (McGowan 2004; Galfetti et al. 2007).

9.4 Palaeobiogeography

The palaeogeographic setting of the Boreal Province of Russia and Svalbard have been extensively studied through the years in particular by Pčelina and Korčinskaja (see Pčelina & Korčinskaja 2008 for a review). They discussed the connection of these regions with the Palaeo-Pacific based on the presence of common genera in the different realms (see also e.g. Brayard et al. 2009 and Chapter 3). This would also suggest that sea-water temperatures were similar worldwide in the Olenekian (Pčelina & Korčinskaja 2008). In Section 3.1 it was discussed that in the Late Smithian the SST gradient was flat, indicating worldwide homogeneous climatic conditions.
Such statements fit with the composition of the studied assemblage, since it is composed mainly of genera which have a cosmopolitan distribution (*Wasatchites*, *Anasibirites*, *Arctoprionites*, *Arctoceras* and *Xenoceltites*).

As presented in the previous chapter and mentioned above, some species have been found in the studied assemblage, which have not been recorded from Svalbard before.
In agreement with previous literature, this fauna is most related to the Canadian assemblages among all of the Boreal areas. For instance *Arctoprionites resseri*, as discussed previously, has been recorded in Canada and in the USA. As pointed out in Section 9.1 above, this finding is evidence which may strengthen the similarities with the Canadian Province and with lower latitudes. Even more interesting is the finding of specimens similar to *Wasatchites*

distractus, which, as discussed previously, is more common in the Tethyan areas. The presence of such species in the Boreal Realm is further evidence for faunal exchange.

The presence in the studied assemblage of species from lower latitudes may then suggest various hypotheses. The Canadian Province is known for the presence of warm-water immigrants. This had however not been proved for Svalbard assemblages until now. Southern immigrants such as *Wasatchites distractus* may then have extended even more north than previously thought.

Moreover there are the implications of the presence in the studied assemblage of the prionitid Gen. et sp. nov. As mentioned, it presents similarities with a taxon recorded from Siberia, but due to the lack of additional and well preserved specimens it is hard to discuss its palaeogeographic significance.

As these two taxa (*Wasatchites* cf. *distractus* and Gen. et sp. nov.) in particular have not been recorded in the Canadian regions, the question arises whether the Svalbard fauna may be peculiar and whether the suggestion of Weitschat & Dagys (1989) of a distinct Svalbardian Province should be reconsidered. Further evidence is however needed as the new taxa discussed are uncommon in the studied assemblage.

10. Conclusions

In conclusion, the faunal assemblage here studied is characterised by a few cosmopolitan genera, most of them prionitids. This is typical for worldwide faunas from the Late Smithian. The material is generally well preserved and presents large variation in size, shell coiling and ornamentation: compressed individuals present weaker lateral ornamentation, stronger ventral ornaments and larger umbilical width. The opposite is true for more depressed individuals. This is in accordance with Buckman's law of covariation. The assemblage is therefore useful to get a deeper insight on intraspecific variation in the taxa studied.

The observations on the morphology confirmed some trends that are typical for ammonoids. Juveniles have more consistent and approximated ornamentation. With reached maturity the ornamentation diminishes and gets tighter, and sutures are more packed. Since the shell morphology is very similar in all taxa identified (so that a separation based just on the basic parameters is not possible), ornamentation is the key factor in discerning the different groups.
The immaturity of the specimens and their being mostly internal moulds have caused most of the difficulties for taxonomical identifications. The similarities between the various genera at juvenile stage are very strong, and much of the external details have been lost with the shells. The uncertainties are still many especially regarding the genus *Wasatchites*, while the access to unpublished data on the genus *Anasibirites* has considerably simplified the taxonomical identification.

Allometric growth has been proved through linear regressions, and size distributions have given information about the ecology of the assemblage. Such distributions, together with the observations on the morphology, have confirmed the composition of the assemblage of juveniles and subadult individuals, suggesting a separation from the adults. The deposition occurred in a low-energy environment. Another theoretical possibility is sorting by currents. But the lack of abrasion and fragmentation indicates that this is not a factor relevant for this material. It is unclear whether the high juvenile mortality registered in this assemblage is due to natural causes or due to disadvantageous environmental conditions like anoxia with the approach of the end Smithian extinction.

The studied fauna is in good agreement with other Boreal (especially Canadian) as well as Tethyan faunas.

The pandemic distribution of the genera characterizing the *tardus* Zone and which are present in the Spitsbergen fauna is indication of connections between different sides of Panthalassa and of homogeneous oceanic conditions that persisted during the Late Smithian prior to the extinction episode. Moreover, the presence of low-latitude taxa such as *Wasatchites* cf. *distractus*, which has not been registered from any Boreal area before, and *Arctoprionites resseri*, recorded from Canada and USA but new in Svalbard, may suggest further contacts between Svalbard and the Tethys, as known from Canada. These occurrences can be used to improve the correlation between palaeolatitudes.

The confirmed presence of arctoceratids at this level can confirm the range of the genus *Arctoceras* up to the *tardus* Zone, which had already been suggested in the previous literature.

Condensation is also a factor to be considered, which would also explain the association with *Xenoceltites subevolutus*, which in most areas worldwide is not associated with *Wasatchites* and *Anasibirites*.

The unexpected presence of the new prionitid Gen. et sp. nov. has no certain correspondent taxa in other regions (except likely for *Anasibirites ochotensis*), therefore it is hard to make an estimation of the biostratigraphic/palaeogeographic implications.

On the whole the results here presented strengthen the correlations within the Boreal Realm (especially between Svalbard and Canada) and between palaeolatitudes, since in the Tethys the *W. distractus* Beds correspond to the lower Boreal *tardus* Zone.

Since the specimens belonging to the new introduced taxa *Arctoceras* sp. nov. and Gen et sp. nov. are few, further research is considered to be needed to formally confirm the new taxa and discuss the peculiarities of the studied fauna (and whether they may support the establishment of a Svalbardian Province). Moreover, a deeper study of the genus *Wasatchites* may be necessary to untangle the complexities connected to the high intraspecific variation of this taxon.

11. Bibliography

Arkell, W.J., Furnish, W.M., Kummel, B., Miller, A.K., Moore, R.C., Schindewolf, O.H., Sylvester-Breadley, P.C. & Wright, C.W. 1957. *Treatise on Invertebrate Palaeontology. Part L. Mollusca 4: Cephalopoda, Ammonoidea.* Lawrence: University of Kansas Press and the Geological Society of America. 490 pp.

Arthaber, G. 1911. Die Trias von Albanien. *Beiträge zur Paläontologie und Geologie Österreich-Ungarns und des Orients, 24,* 169-288.

Bando, Y. 1964. The Triassic Stratigraphy and Ammonite Fauna of Japan. *Science Reports of the Tohoku University. Second Series, Geology, 36(1),* 1-137.

Benton, M.J. & Harper, D.A.T. 2009a. Taphonomy and the quality of the fossil record. *Introduction to Palaeobiology and the Fossil Record.* Chichester: Wiley-Blackwell, 57-77.

Benton, M.J. & Harper, D.A.T. 2009b. Spiralians 2: mollusks. *Introduction to Palaeobiology and the Fossil Record.* Chichester: Wiley-Blackwell, 344-351.

Brayard, A., Bucher, H., Escarguel, G., Fluteau, F., Bourquin, S. & Galfetti, T. 2006. The Early Triassic ammonoid recovery: Palaeoclimatic significance of diversity gradients. *Palaeogeography, Palaeoclimatology, Palaeoecology, 239,* 374-395.

Brayard, A. & Bucher, H. 2008. Smithian (Early Triassic) ammonoid faunas from northwestern Guangxi (South China): taxonomy and biochronology. *Fossils and Strata, 55,* 1-179.

Brayard, A., Escarguel, G., Bucher, H. & Brühwiler, T. 2009. Smithian and Spathian (Early Triassic) ammonoid assemblages from terranes: Palaeoceanographic and palaeogeographic implications. *Journal of Asian Earth Sciences, 36,* 420-423.

Brayard, A. & Escarguel, G. 2013. Untangling phylogenetic, geometric and ornamental imprints on Early Triassic ammonoid biogeography: a similarity-distance decay study. *Lethaia, 46,* 19-33.

Brayard, A., Bylund, K.G., Jenks, J.F., Stephen, D.A., Olivier, N., Escarguel, G., Fara, E. & Vennin, E. 2013. Smithian ammonoid faunas from Utah: implications for Early Triassic biostratigraphy, correlation and basinal palaeogeography. *Swiss Journal of Palaeontology, 132,* 141-219.

Brühwiler, T., Bucher, H. & Goudemand, N. 2010. Smithian (Early Triassic) ammonoids from Tulong, South Tibet. *Geobios, 43,* 403-431.

Brühwiler, T., Bucher, H., Goudeman, N. & Galfetti, T. 2012a. Smithian (Early Triassic) ammonoid faunas from exotic blocks from Oman: taxonomy and biochronology. *Palaeontographica, Abteilung A, 296*, 3-107.

Brühwiler, T., Bucher, H., Ware, D., Schneebeli-Hermann, E., Hochuli, P.A., Roohi, G., Rehman, K. & Yaseen, A. 2012b. Smithian (Early Triassic) ammonoids from the Salt Range, Pakistan. *Special Papers in Palaeontology, 88*, 1-114.

Brühwiler, T., Bucher, H. & Krystyn, L. 2012c. Middle and Late Smithian (Early Triassic) ammonoids from Spiti, India. *Special Papers in Palaeontology, 88*, 1-174.

Buchan, S.H., Challinor, A., Harland, W.B. & Parker, J. R. 1965. The Triassic stratigraphy of Svalbard. *Norsk Polarinstitutt Skrifter, 135*, 1-96.

Bucher, H., Landman, N.H., Klofak, S.M. & Guex, J. 1996. Mode and Rate of Growth in Ammonoids. *In* Landman, N.H., Tanabe, K. & Davis, R.A. (eds.). *Ammonoid Palaeobiology, Volume 13 of Topics in Geobiology*. New York: Plenum Press, 407-461.

Chaney, D.S. 1989. Hand-held mechanical preparation tools. *In* Feldmann, R.M., Chapman, R.E. & Hannibal, J.T. (eds.). *Paleotechniques. The Palaeontological Society Special Publication no. 4*. Knoxville: Dept. of Geological Sciences, University of Tennessee, 186-203.

Checa, A., Company, M., Sandoval, J. & Weitschat, W. 1997. Covariation of morphological characters in the Triassic ammonoid *Czekanowskites rieberi*. *Lethaia, 29*, 225-235.

Cuvier, G. L. 1797. *Tableau élementaire de l'Histoire Naturelle des Animaux.* Paris: Baudouin. XVI + 710 pp.

dotPDN LLC. 2014. Paint.Net drawing program. Available at: http://www.getpaint.net/

Dagys, A.S. & Ermakova, S.P. 1990. Early Olenekian ammonoids of Siberia (Ranneolenekskie ammonoidej Sibiri). *Trudy Akademiya Nauk SSSR, 737*, 1-112 [In Russian].

Dagys, A.S. & Weitschat, W. 1993a. Extensive intraspecific variation in a Triassic ammonoid from Siberia. *Lethaia, 26*, 113-121.

Dagys, A.S. & Weitschat, W. 1993b. Intraspecific variation in Boreal Triassic ammonoids. *Geobios, 15*, 107-109.

Dagys, A. & Weitschat, W. 1993c. Correlation of the Boreal Triassic. *Mitteilungen aus dem Geologisch-Paläontologischen Institut der Universität Hamburg, 75*, 249-256.

Dagys, A.S. 1994. Lower Triassic stage, substage and zonal scheme of north-eastern Asia. *In* Guex, J. & Baud, A. (eds.). *Recent developments on Triassic stratigraphy (Proceedings of the Triassic symposium, Lausanne, 20-25 Oct. 1991). Mémoires de Géologie, 22*, 15-24.

De Baets, K., Klug, C. & Monnet, C. 2012. Intraspecific variability through ontogeny in early ammonoids. *Palaeobiology, 39(1),* 75-94.

Enay, R. 1980. Paléobiogéographie et ammonites jurassiques: "Rythme faunistiques" et variations du niveau marin. Livre jubil. *Mémoires de la Société Géologique de France, 10,* 261-281.

Etter, W. 1999. Community Analysis. *In* Harper, D.A.T. (ed.). *Numerical Palaeobiology - Computer-Based Modelling and Analysis of Fossils and their distribution*. Chichester: John Wiley & Sons, 285-360.

Feldmann, R.M. 1989a. Photographic procedures. *In* Feldmann, R.M., Chapman, R.E. & Hannibal, J.T. (eds.). *Paleotechniques. The Palaeontological Society Special Publication no. 4*. Knoxville: Dept. of Geological Sciences, University of Tennessee, 336-341.

Feldmann, R.M. 1989b. Whitening fossils for photographic purposes. *In* Feldmann, R.M., Chapman, R.E. & Hannibal, J.T. (eds.). *Paleotechniques. The Palaeontological Society Special Publication no. 4*. Knoxville: Dept. of Geological Sciences, University of Tennessee, 342-346.

Flood, B., Nagy, J. & Winsnes, T.S. 1971. Geological map of Svalbard 1:500.000, sheet 1G Spitsbergen southern part. *Norsk Polarinstitutt Skrifter 154 A.*

Foote, M. & Miller, A.I. 2007. *Principles of Palaeontology.* 3rd ed. New York: W.H. Freeman, 354 pp.

Frebold, H. 1930. Die altersstellung des Fischhorizontes, des Grippianiveaus und des unteren Saurierhorizontes in Spitzbergen. *Skrifter om Svalbard og Ishavet, 28*, 1-36.

Frech, F. 1902. Die Dyas. *Lethaea Geognostica, I. Lethaea Palaeozoica, 2(4),* 579-788.

Galfetti, T., Bucher, H., Brayard, A., Hochuli, P.A., Weissert, H., Guodun, K., Atudorei, V. & Guex, J. 2007. Late Early Triassic climate change: Insights from carbonate carbon isotopes, sedimentary evolution and ammonoid palaeobiogeography. *Palaeogeography, Palaeoclimatology, Palaeoecology, 243*, 394-411.

Glørstad-Clark, E., Faleide, J.I., Lundschien, B.A. & Nystuen, J.P. 2010. Triassic seismic sequence stratigraphy and palaeogeography of the western Barents Sea area. *Marine and Petroleum Geology, 27*, 1448-1475.

Glørstad-Clark, E., Birkeland, E.P., Nystuen, J.P., Faleide, J.I. & Midtkandal, I. 2011. Triassic platform-margin deltas in the western Barents Sea. *Marine and Petroleum Geology, 28*, 1294-1314.

Guex, J. 1978. Le Trias inférieur des Salt Ranges (Pakistan): problèmes biochronologiques. *Eclogae Geologicae Helvetiae, 71(1),* 105-141.

Guex, J., Koch, A., O'Dogherty, L. & Bucher, H. 2003. A morphogenetic explanation of Buckman's law of covariation. *Bulletin de la Société Géologique de France, 174(6),* 603-606.

Hammer, Ø., Harper, D.A.T. & Ryan, P.D. 2001. PAST: Palaeontological statistics software package for education and data analysis. *Palaeontologia Electronica 4(1),* 1-9.

Hammer, Ø. & Bucher, H. 2005. Buckman's first law of covariation - a case of proportionality. *Lethaia, 38,* 67-72.

Hammer, Ø. & Harper, D.A.T. 2006. *Palaeontological data analysis.* Oxford: Blackwell Publishing. 351 pp.

Harper, D.A.T. & Owen, A.W. 1999. Quantitative and Morphometric Methods in Taxonomy. *In* Harper, D.A.T. (ed.), *Numerical Palaeobiology - Computer-based Modelling and Analysis of Fossils and their Distribution*. Chichester: John Wiley & Sons, 1-39.

Hounslow, M.W., Mørk, A., Peters, C. & Weitschat, W. 1996. Boreal Lower Triassic magnetostratigraphy from Deltadalen, Central Svalbard. *Albertiana, 17,* 3-10.

Hounslow, M.W., Peters, C., Mørk, A., Weitschat, W. & Vigran, J.O. 2008a. Biomagnetostratigraphy of the Vikinghøgda Formation, Svalbard (Arctic Norway), and the geomagnetic polarity timescale for the Lower Triassic. *Geological Society of America Bulletin*, 1305-1325.

Hounslow, M.W., Hu, M., Mørk, A., Weitschat, W., Vigran, J.O., Karloukovski, V. & Orchard, M.J. 2008b. Intercalibration of Boreal and Tethyan time scales: the magnetostratigraphy of the Middle Triassic and latest Early Triassic from Spitsbergen, Arctic Norway. *Polar Research, 27*, 469-490.

Hyatt, A. 1884. Genera of Fossil Cephalopoda. *Proceedings of the Boston Society of Natural History,* 22, 253-338.

Hyatt, A. 1900. Cephalopoda.. *In* Zittel, K.A.V. (ed.). *Textbook of palaeontology*. London: Eastman, C.R., 502-604.

Hyatt, A. & Smith, J.P. 1905. The Triassic cephalopod genera of America. *USGS Professional Paper, 40,* 1–394.

Konstantinov, A.G., Sobolev, E.S. & Yadrenkin, A.V. 2007. Detailed biostratigraphy of Triassic deposits in the Lena lower reaches (northern Yakutia). *Russian Geology and Geophysics, 48, 721-736.*

Konstantinov, A.G. 2008. Triassic Ammonoids of Northeast Asia: Diversity and Evolutionary Stages. *Stratigraphy and Geological Correlation, 16(5),* 490-502.

Konstantinov, A.G. & Klets, T.V. 2009. Stage Boundaries of the Triassic in Northeast Asia. *Stratigraphy and Geological Correlation, 17(2),* 173-191.

Korčinskaja, M.V. 1970. Olenekian ammonites of Spitsbergen (Olenekskie ammonity Špicbergena). *In Uchenye zapiski. Palaeontologiia i biostratigrafiia, 27*. Leningrad: Nauchno-issledovatelskii Institut geologii Arktiki, 80-89 [in Russian].

Korčinskaja, M.V. 1973. Biostratigraphy of Triassic deposits of Svalbard. *In* Logan, A. & Hills, L.V. (eds.). *The Permian and Triassic systems and their mutual boundary*. Calgary: Canadian Society of Petroleum Geologists, 261-268.

Korčinskaja, M.V. 1986. Biostratigraphy of the Induan stage of Spitsbergen. *In Geologija osadočnogo čehla Špicbergena (Geology of the sedimentary blanket of the Spitsbergen archipelago).* Leningrad: Production-Geological Association Sevmorgeologija, 77-93.

Korn, D. 2010. A key for the description of Palaeozoic ammonoids. *Fossil Record 13(1)*, 5-12.

Krafft, A.V & Diener, C. 1909. Lower Triassic Cephalopoda from Spiti, Malla Johar, and Byans. *Himalayan Fossils. Palaeontologia Indica, Series 15(6),* 1-186.

Kummel, B. 1961. The Spitsbergen Arctoceratids. *Bulletin of the Museum of Comparative Zoology at Harvard College, 123(9),* 499-523.

Kummel, B. & Steele, G. 1962. Ammonites from the *Meekoceras gracilitatus* Zone at Crittenden Spring, Elko County, Nevada. *Journal of Palaeontology, 36(4),* 638-703.

Lock, B.E., Pickton, C.A., Smith, D.G., Batten, D.J. & Harland, W.B. 1978. The Geology of Edgeøya and Barentsøya, Svalbard. *Norsk Polarinstitutt Skrifter 168*, 1-65.

Lucas, S.G., Goodspeed, T.H. & Estep, J.W. 2007a. Ammonoid biostratigraphy of the Lower Triassic Sinbad Formation, East-Central Utah. *New Mexico Museum of Natural History and Science Bulletin, 40,* 103–108.

Lucas, S.G. 2010. The Triassic chronostratigraphic scale: history and status. *In* Lucas, S.G. (ed.), *The Triassic Timescale. Special Publications, 334*. London: Geological Society of London, 17-39.

Lundschien, B.A., Høy, T. & Mørk, A. 2014. Triassic hydrocarbon potential in the Northern Barents Sea; integrating Svalbard and stratigraphic core data. *Norwegian Petroleum Directorate Bulletin, 11*, 3-20.

Major, H. & Nagy, J. 1972. Geology of the Adventalen map area. *Norsk Polarinstitutt Skrifter 138*, 1-58.

Mathews, A.A.L. 1929. The Lower Triassic Cephalopod fauna of the Fort Douglas area, Utah. *Walker Museum Memoirs, 1(1), 1-46.*

McGowan, A.J. 2004. Ammonoid taxonomic and morphologic recovery patterns after the Permian-Triassic. *Geology, 32(8),* 665-668.

Miller, E.L., Soloviev, A.V.,Prokopiev, A.V., Toto, J. Harris, D, Kuzmichev, A.B. & Gehrels, G.E. 2013. Triassic river systems and the palaeo-Pacific margin of northwestern Pangea. *Gondwana Research,* 1631-1645.

Mojsisovics, E. von 1886. Arktische Triasfaunen. *Mémoires de l'Académie Imperial de Sciences de St. Pétersbourg, 7, Series 33(6),* 1-159.

Mojsisovics, E. von 1896. Beiträge zur Kenntniss der obertriadischen Cephalopoden-Faunen des Himalaya. *Denkschriften der Kaiserlichen Akademie der Wissenschaften Wien, 63,* 575-701.

Mørk, A., Knarud, R., & Worsley, D. 1982. Depositional and diagenetic environments of the Triassic and Lower Jurassic succession of Svalbard. *Canadian Society of Petroleum Geologists, Memorial 8,* 371-398.

Mørk, A. 1994. Triassic transgressive-regressive cycles of Svalbard and other Arctic areas: a mirror of stage subdivision. *In* Guex, J. & Baud, A. (eds.). *Recent developments on Triassic stratigraphy (Proceedings of the Triassic symposium, Lausanne, 20-25 Oct. 1991). Mémoires de Géologie, 22,* 69-82.

Mørk, A., Dallmann, W.K., Dypvik, H., Johannessen, E.P., Larssen, G.B., Nagy, J., Nøttvedt, A. Olaussen, S., Pčelina, T.M. & Worsley, D. 1999a. Mesozoic lithostratigraphy. *In* Dallmann, W.K. (ed.), *Lithostratigraphic Lexicon of Svalbard. Upper Palaeozoic to Quaternaty bedrock. Review and recommendations for nomenclature use.* Tromsø: Norsk Polarinstitutt, 127-214.

Mørk, A., Elvebakk, G., Forsberg, A.W., Hounslow, M.W., Nakrem, H.A., Vigran, J. O. & Weitschat, W. 1999b. The type section of the Vikinghøgda Formation: a new Lower Triassic unit in central and eastern Svalbard. *Polar Research, 18(1),* 51-82.

Nakrem, H.A., Orchard, M.J., Weitschat, W., Hounslow, M.W., Beatty, T.W. & Mørk, A. 2008. Triassic conodonts from Svalbard and their Boreal correlations. *Polar Research, 27,* 523-539.

Osmundsen, P.T., Braathen, A., Rød, R.S. & Hynne, I.B. 2014. Styles of normal faulting and fault-controlled sedimentation in the Triassic deposits of Eastern Svalbard. *Norwegian Petroleum Directorate Bulletin, 11,* 61-79.

Page, K.N. 1996. Mesozoic Ammonoids in Space and Time. *In* Landman, N.H., Tanabe, K. & Davis, R.A. (eds.). *Ammonoid Palaeobiology, Volume 13 of Topics in Geobiology*. New York: Plenum Press, 755-794.

Pčelina, T.M. 1983. Novye dannye po stratigrafii mezozoja arčipelaga Špicbergen (New material on the Mesozoic stratigraphy of the Spitsbergen archipelago). *In Geologija Špicbergena (The Geology of spitsbergen)*. Leningrad: Production-Geological Association Sevmorgeologija, 121-141.

Pčelina, T.M. & Korčinskaja, M.V. 2008. Palaeogeographic reconstructions of the Russian Boreal areas and Svalbard during the Triassic. *Polar Research, 27*, 491-494.

Schenk, E.T., McMasters, J.H., Keen, A.M & Muller, S.W. 1956. *Procedure in Taxonomy.* 3rd ed. Stanford: Stanford University Press, 119 pp.

Smith, J.P. 1932. *Lower Triassic Ammonoids of North America. United States Geological Survey Professional Paper, 167, 1-199.*

Smith, J. 1999. Multivariate Techniques in Palynofacies Analysis. In Harper, D.A.T. (ed.), *Numerical Palaeobiology - Computer-Based Modelling and Analysis of Fossils and their distribution*. Chichester: John Wiley & Sons, 361-393.

Spath, L.F. 1921. On Ammonites from Spitsbergen. *Geological Magazine, 68*, 297-305.

Spath, L.F. 1930. The Eotriassic invertebrate fauna of East Greenland. *Meddelelser om Grønland, 83(1),* 1-90.

Spath, L.F. 1934. *Catalogue of the fossil Cephalopoda in the British Museum (Natural History). Part IV - The Ammonoidea of the Trias.* London: The Trustees of the British Museum, 521 pp.

Stephen, D.A., Bylund, K.G., Bybee, P.J. & Ream, W.J. 2010. Ammonoid beds in the Lower Triassic Thaynes Formation of western Utah, USA. *In* Tanabe, K., Shigeta, Y., Sasaki, T. & Hirano, H. (eds.). *Cephalopods — present and past*. Tokyo: Tokai University Press, 243-252.

Tozer, E.T. 1961. Triassic stratigraphy and faunas, Queen Elizabeth Islands, Arctic Archipelago. *Geological Survey of Canada Memoir, 316*, 116.

Tozer, E.T. & Parker, J.R. 1968. Notes on the Triassic biostratigraphy of Svalbard. *Geological Magazine, 105(6)*, 523-542.

Tozer, E.T. 1994. *Canadian Triassic Ammonoid Fauna.* Vancouver: Geological Survey of Canada. 663 pp.

Vigran, J.O., Mangerud, G., Mørk, A., Bugge, T. & Weitschat, W. 1998. Biostratigraphy and sequence stratigraphy of the lower and middle Triassic deposits from the Svalis dome, Central Barents Sea, Norway. *Palynology, 22(1)*, 89-141.

Vigran, J.O., Mangerud, G., Mørk, A., Worsley, D. & Hochuli, P.A. 2014. *Palynology and geology of the Triassic succession of Svalbard and Barents Sea*. *Special Publication, 14.* Trondheim: Geological Survey of Norway, 270 pp.

Waagen, W. 1895. Fossils from the Ceratite Formation. *Salt Range Fossils, Palaeontologia Indica, Series 13(2),* 1-323.

Walton, S.A., Korn, D. & Klug, C. 2010. Size distribution of the Late Devonian ammonoid *Prolobites*: indication for possible mass spawning events. *Swiss Journal of Geosciences, 103*, 475-494.

Weitschat, W. & Lehmann, U. 1978. Biostratigraphy of the uppermost part of the Smithian Stage (Lower Triassic) at the Botneheia, W-Spitsbergen. *Mitteilungen aus dem Geologisch-Paläontologischen Institut der Universität Hamburg, 48*, 85-100.

Weitschat, W. & Dagys, A.S. 1989. Triassic biostratigraphy of Svalbard and a comparison with NE-Siberia. *Mitteilungen aus dem Geologisch-Paläontologischen Institut der Universität Hamburg, 68*, 179-213.

Weitschat, W. 2008. Intraspecific variation of *Svalbardiceras spitsbergensis* (Frebold) from the Early Triassic (Spathian) of Spitsbergen. *Polar Research, 27*, 292-297.

Westermann, G.E.G. 1966. Covariation and taxonomy of the Jurassic ammonite *Sonninia dicra* (Waagen). *Neues Jahrbuch für Geologie und Paläontologie. Abhandlungen 124*, 289-312.

Worsley, D., Aga, O.J., Dalland, A., Elverhøi, A. & Thon, A. 1986. *Evolution of an Arctic archipelago. The geological history of Svalbard.* Stavanger: Statoil, 128 pp.

Worsley, D. 2008. The post-Caledonian development of Svalbard and the western Barents Sea. *Polar Research, 27*, 298-317.

Yacobucci, M.M. 2004. Buckman's Paradox: variability and constraints on ammonoid ornament and shell shape. *Lethaia, 37*, 57-69.

Zakharov, Y.D. 1978. *Lower Triassic ammonoids of East USSR (Rannetriasovye ammonoidei vostoka SSSR)*. Nauka, Moskva, 224 pp. [in Russian].

Zakharov, V.A., Bogomolov, Y.I., Il'ina, V.I., Konstantinov, A.G., Kurushin, N.I., Lebedeva, N.K., Meledina, S.V., Nikitenko, B.L., Sobolev, E.S. & Shurygin, B.N. 1997. Boreal zonal standard and biostratigraphy of the Siberian Mesozoic. *Russian Geology and Geophysics, 38(5)*, 965-993.

Zakharov, V.A., Shurygin, B.N., Kurushin, N.I., Meledina, S.V. & Nikitenko, B.L. 2002. A Mesozoic ocean in the Arctic: palaeontological evidence. *Russian Geology and Geophysics, 43(2)*, 143-170.

Zittel, K.A.V. 1884. *Handbuch der Paläontologie. Mollusca und Arthropoda.* Oldenbourg, R., Munich, 839 pp.

Öberg, P. 1877. *Om trias-försteningar från Spetsbergen (On Triassic fossils from Spitsbergen). Kungliga Svenska Vetenskapsakademiens Handlingar 14(4).* Uppsala: Swedish Royal Academy of Sciences, 19 pp.

Appendix 1 – Plates

All the specimens illustrated in the following plates are from the same limestone concretion of the uppermost Lusitaniadalen Member, Vikinghøgda Formation at Stensiöfjellet, Svalbard (*tardus* Zone, Late Smithian).

The scale bar used is 1 cm

Plate I

Genus ***Xenoceltites*** Spath, 1930.

Xenoceltites subevolutus Spath, 1930 (see Chapter 8, pg. 48 for descriptions).

Figs. a-b illustrate the specimens with constrictions on the venter and partly on the flanks. The last one (c) is a smooth variant.

Fig. a: PMO 227.993. Lateral view.

Fig. b: PMO 227.994. Lateral view.

Fig. c: PMO 227.979. Lateral view.

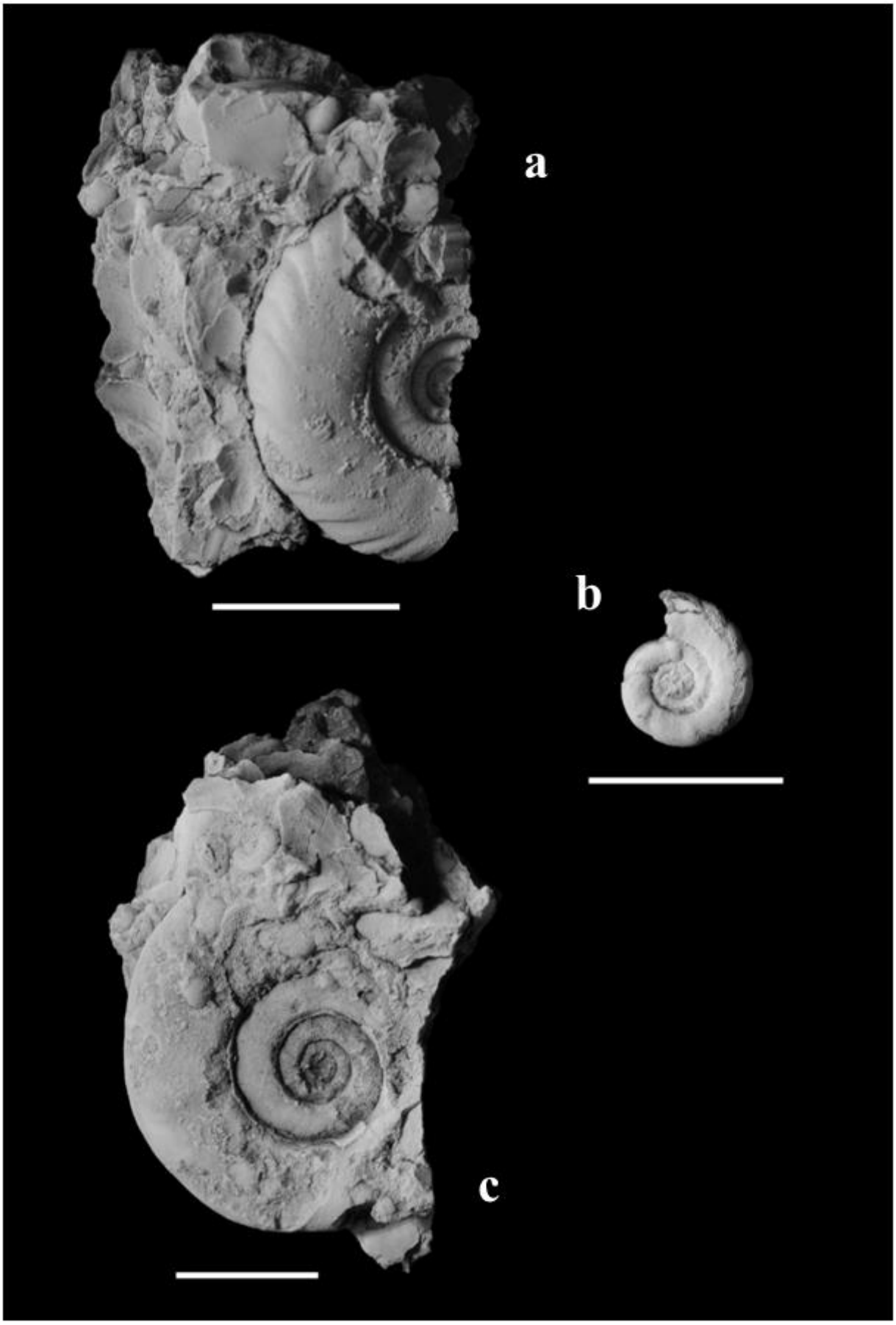
a
b
c

Plate II

Genus ***Arctoprionites*** (Frebold, 1930).

For *A. nodosus* (Frebold, 1930) refer to Chapter 8, pg. 50.

For *A. resseri* (Mathews, 1929) refer to Chapter 8, pg. 52.

While no great intraspecific variation is observed in *A. nodosus*, the two specimens of *A. resseri* are two different variants of the same species, as pointed out in the description and discussion on the above-mentioned pages.

Figs. a-b: *Arctoprionites nodosus* (Frebold, 1930). PMO 227.978. Lateral and peripheral views.

Fig. c: *Arctoprionites nodosus* (Frebold, 1930). PMO 227.990. Lateral view.

Fig. d: *Arctoprionites nodosus* (Frebold, 1930). PMO 227.991. Lateral view.

Figs. e-f: *Arctoprionites resseri* (Mathews, 1929). PMO 228.002. Lateral and peripheral views.

Fig. g: *Arctoprionites resseri* (Mathews, 1929). PMO 228.001. Lateral view.

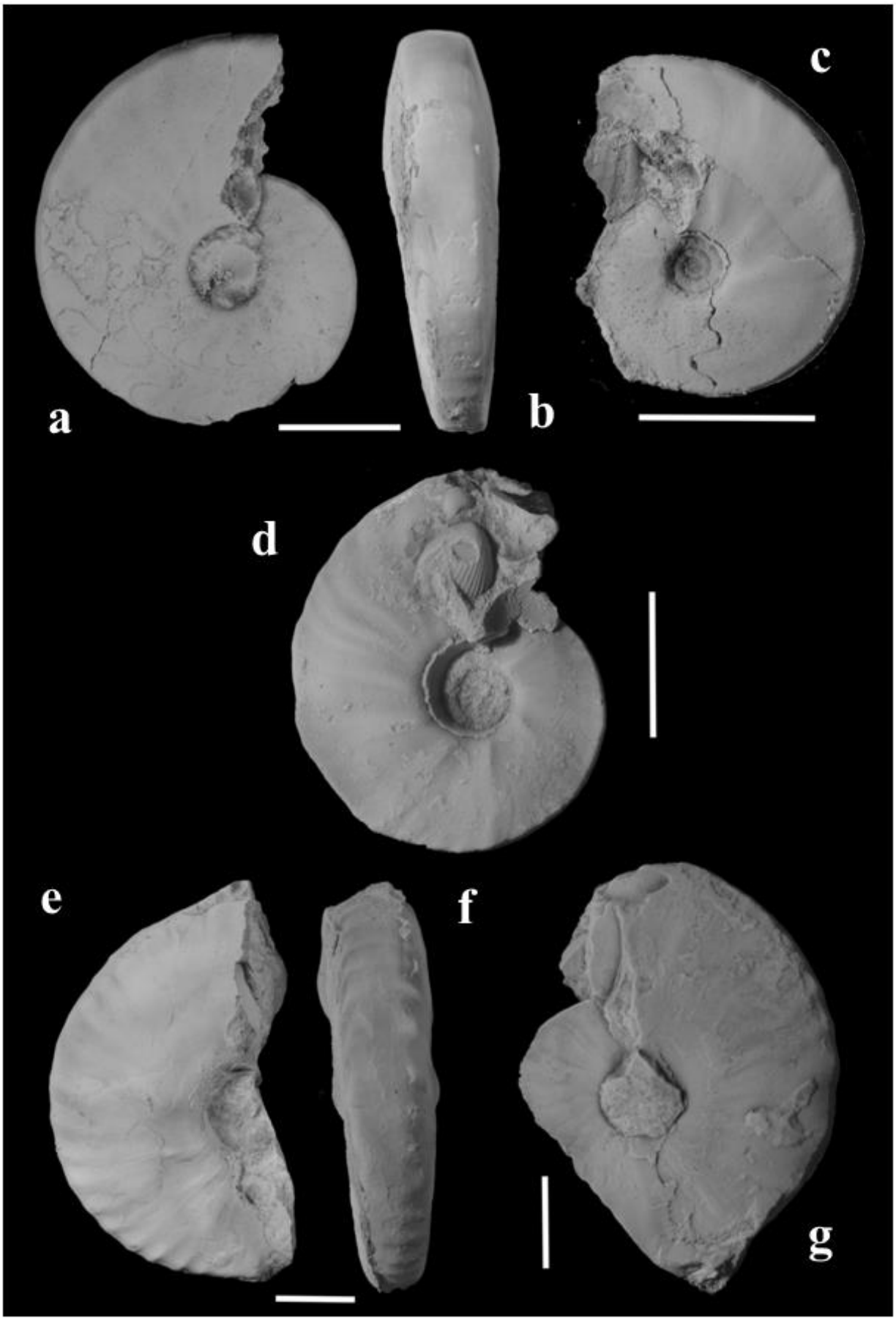
a
b
c
d
e
f
g

Plate III

Genus ***Anasibirites*** Mojsisovics, 1896

Anasibirites kingianus (Waagen, 1895) (see Chapter 8, pg. 54 for descriptions).

To be noted is the variation in ornamentation intensity and umbilical morphology in the specimens illustrated, as conforming to the Buckman‘s first law of covariation (see Chapter 5).

Fig. a: PMO 227.995. Lateral view.

Fig. b: PMO 227.996. Lateral view.

Figs. c-d: PMO 227.997. Lateral and peripheral views.

Fig. e: PMO 227.998. Lateral view.

Figs. f-g: PMO 227.980. Lateral view.

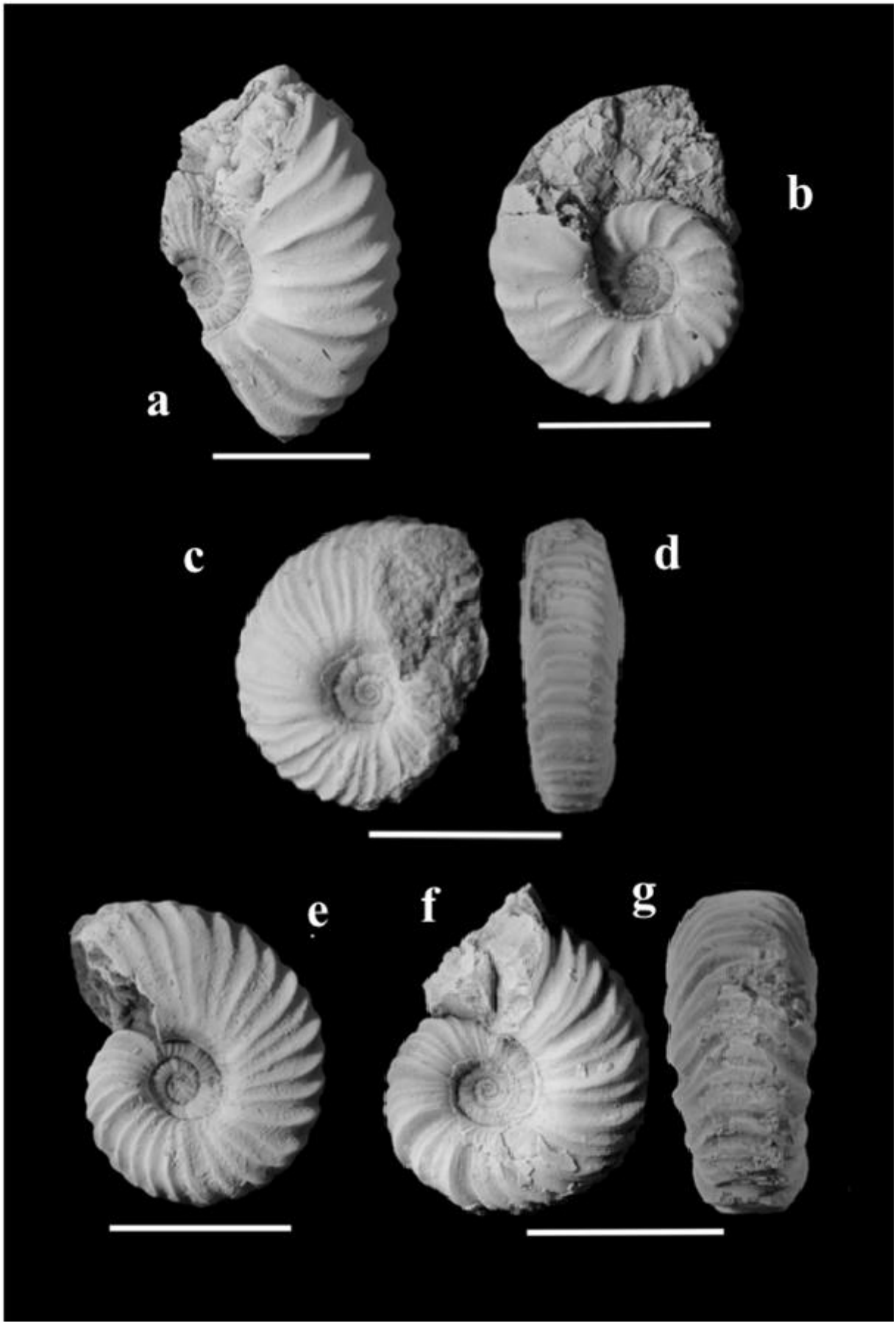
a
b
c
d
e
f
g

Plate IV

Genus ***Wasatchites*** Mathews, 1929

Wasatchites* cf. *distractus (Waagen, 1895) (see Chapter 8, pg. 59 for descriptions).

The specimens here illustrated represent both the smooth and heavily ornamented variants of the species.

Figs. a-b: PMO 228.004. Lateral and peripheral views.

Figs. c-d: PMO 228.003. Lateral and peripheral views.

Fig. e: PMO 228.005. Lateral view.

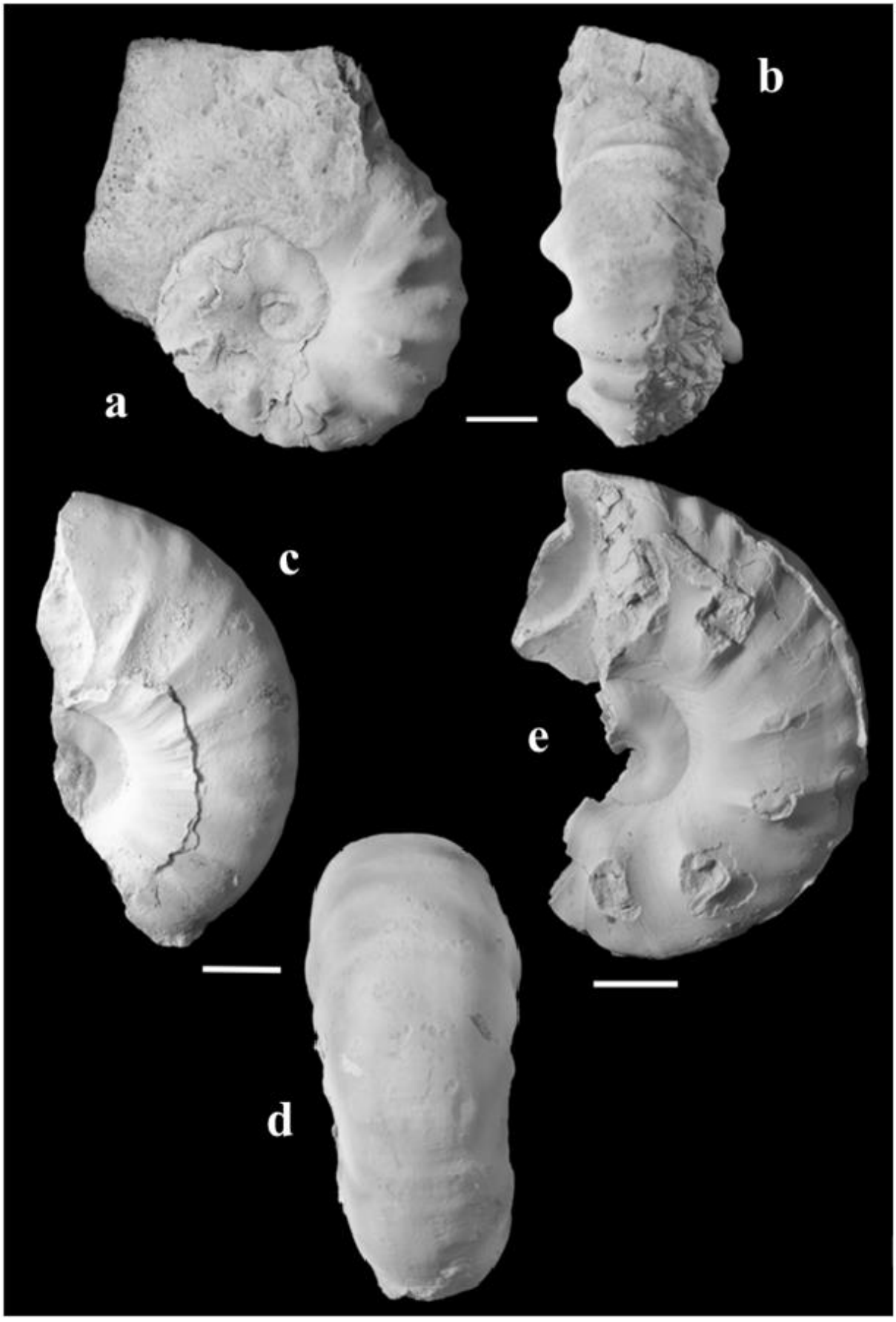
a
b
c
d
e

Plate V

Genus ***Wasatchites*** Mathews, 1929

Wasatchites tridentinus Spath, 1934 (see Chapter 8, pg. 61 for descriptions).

The illustrations were arranged such as to show the high intraspecific variation within the species. The not fully mature individuals still have defined ribbing. The adult stage, as exemplified by the specimen PMO 228.010, bears weaker ribbing.

Figs. a-b: PMO 228.006. Lateral and peripheral views.

Fig. c: PMO 228.007. Lateral view. To be noted the small nodes on the ventral shoulder.

Figs. d-e: PMO 210.495. Lateral view.

Fig. f: PMO 228.008. Lateral view.

Figs. g-h: PMO 228.009. Lateral and peripheral views.

Fig. i: PMO 228.010. Lateral view.

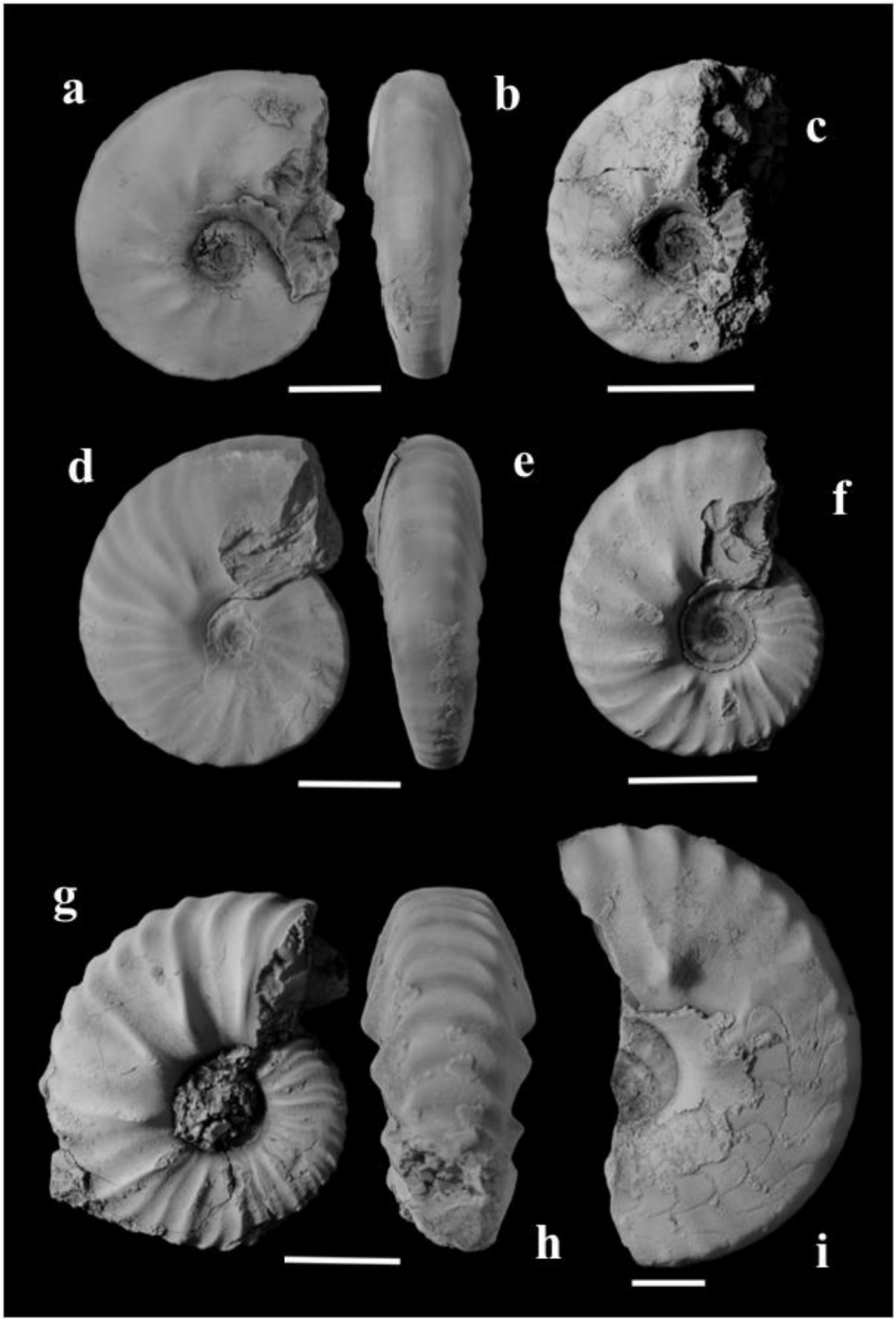
a
b
c
d
e
f
g
h
i

Plate VI

Genus ***Wasatchites*** Mathews, 1929

***Wasatchites* spp. indet.** See Chapter 8, pg. 64 for descriptions.

The specimens here illustrated clearly show intraspecific variation, with ornamentation ranging from very faint to coarse. Since the specimens bear no or very faint tubercles, they have been classified as juvenile/immature stages of *Wasatchites*.

Figs. a-b: PMO 210.487. Lateral and peripheral views.

Fig. c: PMO 228.013. Lateral view.

Figs. d-e: PMO 228.012. Lateral and peripheral views.

Figs. f-g: PMO 228.000. Lateral and peripheral views.

Fig. h: PMO 228.011. Lateral view.

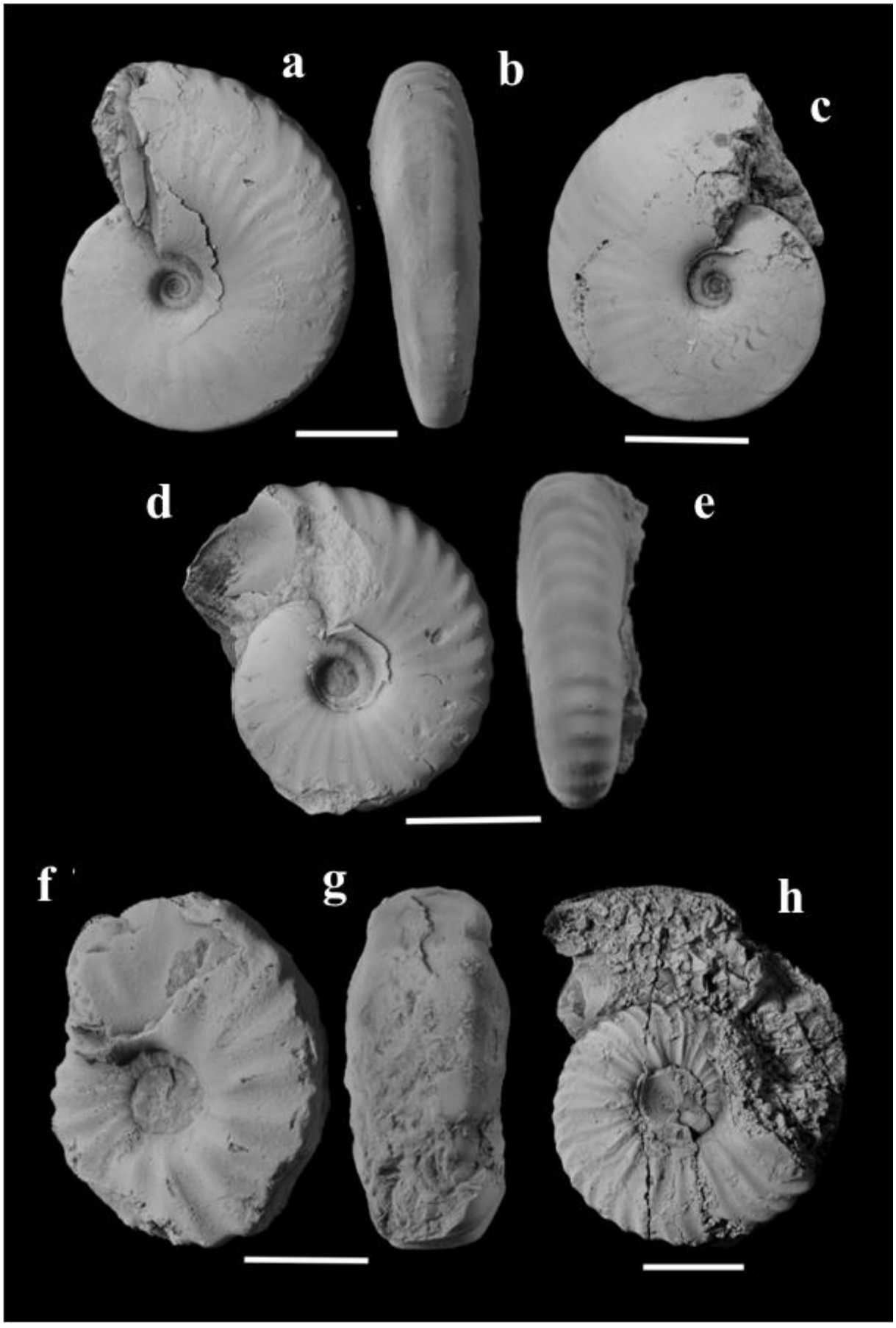
a
b
c
d
e
f
g
h

Plate VII

Gen et sp. nov. See Chapter 8, pg. 68 for descriptions.

Fig. a: PMO 227.987. Lateral view. This is the specimen preserving the most of the shell.

Figs. b-c: PMO 227.988. Lateral and peripheral views. The arrow points at the only constriction found.

Fig. d: PMO 227.989. Lateral view.

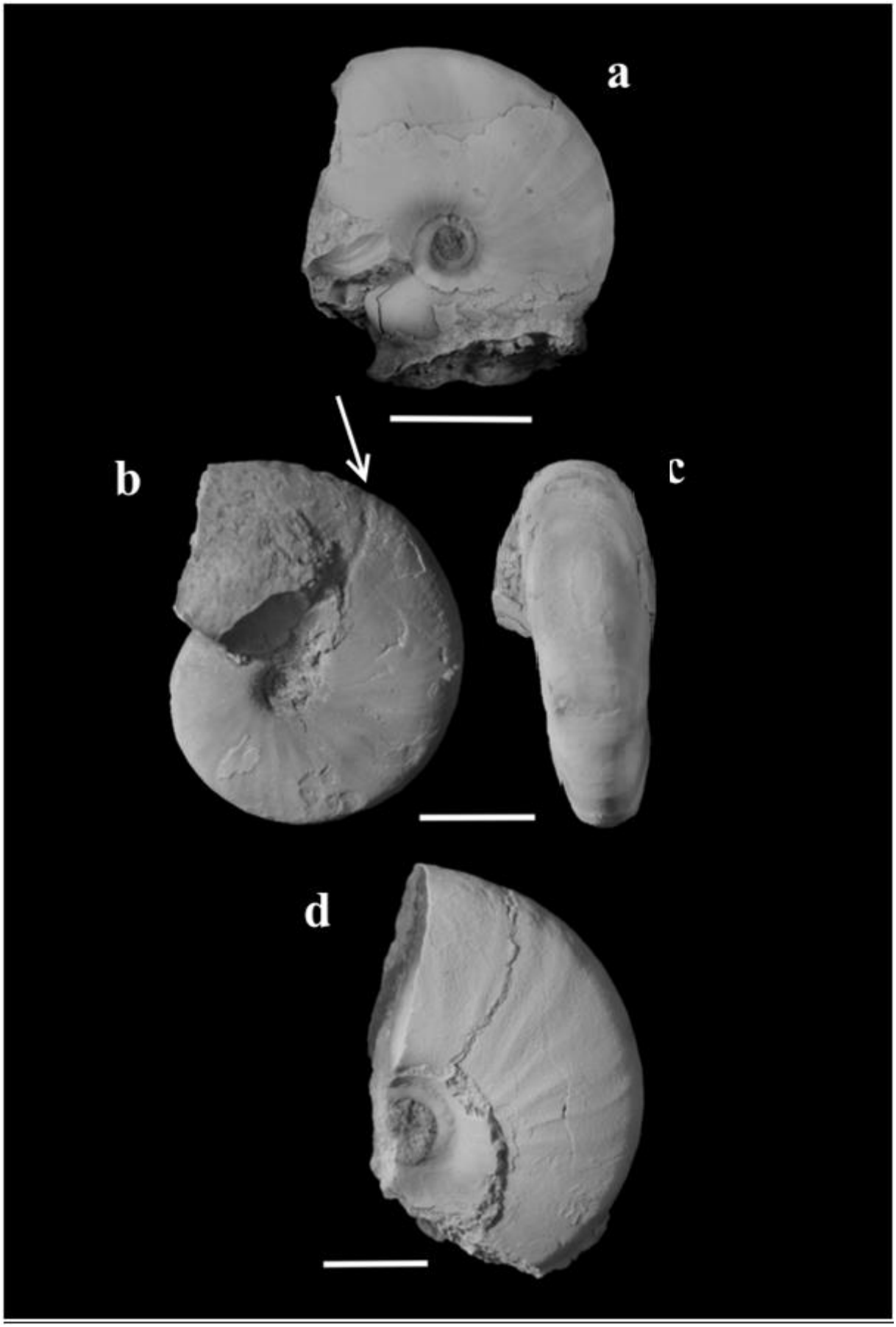
a
b
c
d

Plate VIII

***Arctoceras* sp. nov.** See Chapter 8, pg. 70 for descriptions.

Figs. a-b: PMO 227.985. Lateral and peripheral views.

Figs. c-d: PMO 210.489. Lateral and peripheral views. Note the keeled and strigated venter.


a
b
c
d

Appendix 2 – Measurements

In this appendix tables with the obtained measurements (D, H, W, U) are presented, together with the calculated ratios used for statistical analyses.

Anasibirites kingianus							
D	**H**	**W**	**U**	**H/D**	**W/D**	**U/D**	**W/H**
16.44	7.61	6.09	4.65	0.4629	0.3704	0.2828	0.8003
15.38	6.58	6.03	4.96	0.4278	0.3921	0.3225	0.9164
14.86	6.74	5.79	4.81	0.4536	0.3896	0.3237	0.8591
13.67	5.79	5.62	3.99	0.4236	0.4111	0.2919	0.9706
13.05	5.55	4.98	3.93	0.4253	0.3816	0.3011	0.8973
11.34	4.53	3.99	3.34	0.3995	0.3519	0.2945	0.8808
20.11	9.05	8.55	6.15	0.4500	0.4252	0.3058	0.9448
13.69	5.85	6.18	4.45	0.4273	0.4514	0.3251	1.0564
12.07	5.12	5.23	4.14	0.4242	0.4333	0.3430	1.0215
9.53	3.85	3.63	3.01	0.4040	0.3809	0.3158	0.9429
12.3	5.36	4.16	5.24	0.4358	0.3382	0.4260	0.7761
12.05	4.65	4.68	4.01	0.3859	0.3884	0.3328	1.0065
11.82	4.85	4.33	3.56	0.4103	0.3663	0.3012	0.8928
9.92	4.16	3.63	2.98	0.4194	0.3659	0.3004	0.8726
13.06	5.89	4.31	4.01	0.4510	0.3300	0.3070	0.7317
13.95	6.03	5.4	3.86	0.4323	0.3871	0.2767	0.8955
17.06	6.87	-	4.78	0.4027	-	0.2802	-
8.24	3.11	3.42	2.5	0.3774	0.4150	0.3034	1.0997
20.4	9.03	-	4.95	0.4426	-	0.2426	-
14.22	6.17	5.82	3.83	0.4339	0.4093	0.2693	0.9433
14.8	7.03	4.64	3.58	0.4750	0.3135	0.2419	0.6600

Arctorprionites nodosus							
D	**H**	**W**	**U**	**H/D**	**W/D**	**U/D**	**W/H**
22.9	11.93	-	4.35	0.5210	-	0.1900	-
19.12	9.67	5.79	4.39	0.5058	0.3028	0.2296	0.5988
24.1	11.5	0	5.48	0.4772	-	0.2274	-
28.37	14.67	8.07	5.67	0.5171	0.2845	0.1999	0.5501
23.64	11.32	-	5.4	0.4788	-	0.2284	-
20.98	10.21	6.45	4.8	0.4867	0.3074	0.2288	0.6317
22.25	11.25	6.08	4.82	0.5056	0.2733	0.2166	0.5404
19.48	9.98	6.06	4.29	0.5123	0.3111	0.2202	0.6072
22.79	10.7	7.1	4.95	0.4695	0.3115	0.2172	0.6636
18.64	9.21	5.59	4.02	0.4941	0.2999	0.2157	0.6069
14.75	7.3	4.23	4.08	0.4949	0.2868	0.2766	0.5795
14.48	7.14	4.2	3.38	0.4931	0.2901	0.2334	0.5882
15.47	7.53	4.48	3.17	0.4867	0.2896	0.2049	0.5950
16.27	7.69	4.79	4.08	0.4726	0.2944	0.2508	0.6229
18	9.04	-	4.07	0.5022	-	0.2261	-
17.34	8.68	5.25	3.72	0.5006	0.3028	0.2145	0.6048

Genus *Wasatchites*								
Species	**D**	**H**	**W**	**U**	**H/D**	**W/D**	**U/D**	**W/H**
tridentinus	33.94	15.64	10.44	7.58	0.4608	0.3076	0.2233	0.6675
tridentinus	29.97	13.81	11.34	5.1	0.4608	0.3784	0.1702	0.8211
tridentinus	33.27	15.23	9.59	7.1	0.4578	0.2882	0.2134	0.6297
tridentinus	23.4	11.71	7.01	5.72	0.5004	0.2996	0.2444	0.5986
tridentinus	35.11	16.1	-	7.56	0.4586	-	0.2153	-
tridentinus	32.11	14.88	10.18	6.57	0.4634	0.3170	0.2046	0.6841
tridentinus	30.36	13.63	9.68	7.24	0.4489	0.3188	0.2385	0.7102
tridentinus	30.91	14.53	-	-	0.4701	-	-	-
tridentinus	32.72	14.71	9.78	7.92	0.4496	0.2989	0.2421	0.6649
tridentinus	28.42	13.32	9.83	6.93	0.4687	0.3459	0.2438	0.7380
tridentinus	29.68	14.32	10.09	6.58	0.4825	0.3400	0.2217	0.7046
tridentinus	30.34	13.9	9.49	6.21	0.4581	0.3128	0.2047	0.6827
tridentinus	30.08	14.2	-	6.26	0.4721	-	0.2081	-
tridentinus	28.41	12.98	8.58	-	0.4569	0.3020	-	0.6610
tridentinus	16.46	7.99	5.75	3.96	0.4854	0.3493	0.2406	0.7196
tridentinus	20.85	9.99	6.93	5.08	0.4791	0.3324	0.2436	0.6937
tridentinus	30.84	15.95	8.65	5.47	0.5172	0.2805	0.1774	0.5423
tridentinus	23.99	10.79	8.15	5.78	0.4498	0.3397	0.2409	0.7553
tridentinus	24.12	10.86	9.25	6.59	0.4502	0.3835	0.2732	0.8517
tridentinus	24.25	10.65	10.28	7.23	0.4392	0.4239	0.2981	0.9653
tridentinus	28.89	13.93	10.33	6.7	0.4822	0.3576	0.2319	0.7416
tridentinus	17.7	6.8	7.66	6.08	0.3842	0.4328	0.3435	1.1265
tridentinus	41.03	19.56	15.07	9.56	0.4767	0.3673	0.2330	0.7704
cf. *distractus*	42.2	17.65	18.26	10.87	0.4182	0.4327	0.2576	1.0346

***Wasatchites* sp. indet.** *(Table continuing on the next page)*							
D	**H**	**W**	**U**	**H/D**	**W/D**	**U/D**	**W/H**
21.65	10.89	7.33	4.52	0.5030	0.3386	0.2088	0.6731
25.66	13.35	-	4.28	0.5203	-	0.1668	-
33.03	16.95	9.46	5.71	0.5132	0.2864	0.1729	0.5581
29.21	15.05	-	4.66	0.5152	-	0.1595	-
22.57	11.6	7.22	4.65	0.5140	0.3199	0.2060	0.6224
27.81	13.73	9.34	5.04	0.4937	0.3359	0.1812	0.6803
26.98	12.85	8.33	-	0.4763	0.3087	-	0.6482
23.73	11.39	8.19	4.93	0.4800	0.3451	0.2078	0.7191
18.51	9.75	6.41	3.89	0.5267	0.3463	0.2102	0.6574
27.36	14.04	8.48	4.82	0.5132	0.3099	0.1762	0.6040
28.64	13.43	7.91	6.15	0.4689	0.2762	0.2147	0.5890
21.08	9.72	-	3.87	0.4611	-	0.1836	-
18.22	8.31	5.46	3.96	0.4561	0.2997	0.2173	0.6570
18.77	8.99	6	3.85	0.4790	0.3197	0.2051	0.6674
20.22	10.32	6.82	3.7	0.5104	0.3373	0.1830	0.6609
16.64	8.59	-	3.47	0.5162	-	0.2085	-
16.22	8.02	4.76	3.7	0.4945	0.2935	0.2281	0.5935
16.86	8.43	5.1	3.98	0.5000	0.3025	0.2361	0.6050
15.96	7.96	4.65	3.16	0.4987	0.2914	0.1980	0.5842
15.09	7.52	4.94	3.05	0.4983	0.3274	0.2021	0.6569
17.78	8.1	6.43	2.97	0.4556	0.3616	0.1670	0.7938
13.51	6.21	4.25	2.97	0.4597	0.3146	0.2198	0.6844
11,08	5.34	3.85	2.76	0.4819	0.3475	0.2491	0.7210
14,64	7.53	4.56	2.98	0.5143	0.3115	0.2036	0.6056
11,94	5.69	3.71	2.76	0.4765	0.3107	0.2312	0.6520
13,28	6.36	4.26	3.37	0.4789	0.3208	0.2538	0.6698
12,38	6.09	4.12	2.37	0.4919	0.3328	0.1914	0.6765
13,48	6.49	4.3	2.85	0.4815	0.3190	0.2114	0.6626
12,51	6.06	4.01	2.74	0.4844	0.3205	0.2190	0.6617
13,58	6.6	-	2.62	0.4860	-	0.1929	-
9,1	3.89	2.99	2.15	0.4275	0.3286	0.2363	0.7686
9,58	4.42	3.16	1.95	0.4614	0.3299	0.2035	0.7149
24,57	12.39	7.51	4.47	0.5043	0.3057	0.1819	0.6061
23,21	11.53	7.77	4.11	0.4968	0.3348	0.1771	0.6739
32,92	15.9	9.9	6.44	0.4830	0.3007	0.1956	0.6226
24,99	12.37	8.16	4.74	0.4950	0.3265	0.1897	0.6597
26,95	13.1	8.76	5.02	0.4861	0.3250	0.1863	0.6687
19,32	8.95	-	4.53	0.4633	-	0.2345	-
21,47	10.38	-	4.7	0.4835	-	0.2189	-
15,86	7.37	-	3.47	0.4647	-	0.2188	-
21,8	9.89	7.5	4.59	0.4537	0.3440	0.2106	0.7583
14,8	7.41	4.87	3.28	0.5007	0.3291	0.2216	0.6572
11,73	5.68	4.02	2.66	0.4842	0.3427	0.2268	0.7077

D	H	W	U	H/D	W/D	U/D	W/H
12.74	6.25	4.38	2.99	0.4906	0.3438	0.2347	0.7008
8.89	3.99	3.71	2.28	0.4488	0.4173	0.2565	0.9298
11.53	5.11	3.82	3.5	0.4432	0.3313	0.3036	0.7476
12.91	5.89	4.08	3.59	0.4562	0.3160	0.2781	0.6927
20.93	10.77	7.05	4.14	0.5146	0.3368	0.1978	0.6546
11.43	5.25	3.74	3.13	0.4593	0.3272	0.2738	0.7124
11.79	5.1	3.75	3.14	0.4326	0.3181	0.2663	0.7353
16.24	8.4	5.77	3.98	0.5172	0.3553	0.2451	0.6869
10.8	4.72	3.78	2.8	0.4370	0.3500	0.2593	0.8008
21.36	10.65	-	4.85	0.4986	-	0.2271	-
9.91	4.16	-	2.81	0.4198	-	0.2836	-
19.02	9.02	6.53	5.13	0.4742	0.3433	0.2697	0.7239
12.67	5.63	-	4.05	0.4444	-	0.3197	-
15.51	8.1	-	4.02	0.5222	-	0.2592	-
21.92	9.53	8.13	5.39	0.4348	0.3709	0.2459	0.8531
26.27	11.19	9.94	7.91	0.4260	0.3784	0.3011	0.8883
18.89	8	7.29	4.69	0.4235	0.3859	0.2483	0.9113

Xenoceltites subevolutus							
D	**H**	**W**	**U**	**H/D**	**W/D**	**U/D**	**W/H**
8,12	2.72	2.6	3.71	0.3350	0.3202	0.4569	0.9559
16,83	5.85	-	6.67	0.3476	-	0.3963	-

***Arctoceras* sp. nov.**							
D	**H**	**W**	**U**	**H/D**	**W/D**	**U/D**	**W/H**
32.29	16.92	9.91	6.63	0.5240	0.3069	0.2053	0.5857
28.95	13.86	9.88	6.56	0.4788	0.3413	0.2266	0.7128
20.9	10.16	7.19	5.47	0.4861	0.3440	0.2617	0.7077
15.91	8.05	5.16	3.43	0.5060	0.3243	0.2156	0.6410

Gen. nov. sp. nov.							
D	**H**	**W**	**U**	**H/D**	**W/D**	**U/D**	**W/H**
27.1	13.93	8.88	5.82	0.5140	0.3277	0.2148	0.6375
18.29	8.5	6.03	4.23	0.4647	0.3297	0.2313	0.7094
26.68	14.3	-	5.62	0.5360	-	0.2106	-

Appendix 3 – Statistical values

In this appendix the statistical values obtained from Past 3.05 (RMA, PCA and LDA analyses) are presented in tables. Explanations of the values obtained with such analyses and their interpretations are presented in Section 8.2.

Linear regressions (RMA)

Arctoprionites nodosus

RMA Regression: H-W			
Slope a:	0.55242	Std. error a:	0.051838
Intercept b:	0.42478	Std. error b:	0.25312
95% bootstrapped confidence intervals (N=1999)			
Slope a:	(0.32869; 0.62604)		
Intercept b:	(-0.24283; 2.281)		
Correlation			
r:	0.95496		
r^2:	0.91195		
t:	10.177		
p (uncorr.):	1.3534E-06		
Permutation p:	0.0001		

Anasibirites kingianus

RMA Regression: H-W			
Slope a:	0.88015	Std. error a:	0.10515
Intercept b:	0.078655	Std. error b:	0.37728
95% bootstrapped confidence intervals (N=1999)			
Slope a:	(0.72307; 1.079)		
Intercept b:	(-0.89853; 1.0069)		
Correlation			
r:	0.87028		
r^2:	0.75738		
t:	7.2849		
p (uncorr.):	1.2747E-06		
Permutation p:	0.0001		

Wasatchites tridentinus

RMA Regression: H-W			
Slope a:	0.6588	Std. error a:	0.096469
Intercept b:	0.8182	Std. error b:	1.6617
95% bootstrapped confidence intervals (N=1999)			
Slope a:	(0.47498; 0.88911)		
Intercept b:	(-2.1783; 3.5313)		
Correlation			
r:	0.7836		
r^2:	0.61404		
t:	5.3513		
p (uncorr.):	4.3681E-05		
Permutation p:	0.0002		

***Wasatchites* spp. indet.**

RMA Regression: H-W			
Slope a:	0.62082	Std. error a:	0.03085
Intercept b:	0.51265	Std. error b:	0.083542
95% bootstrapped confidence intervals (N=1999)			
Slope a:	(0.53705; 0.67863)		
Intercept b:	(0.082337; 1.1236)		
Correlation			
r:	0.94149		
r^2:	0.88641		
t:	18.946		
p (uncorr.):	2.3224E-23		
Permutation p:	0.0001		

***Wasatchites* spp. indet. (log-transformed)**

RMA Regression: H-W			
Slope a:	0.91034	Std. error a:	0.039551
Intercept b:	-0.081209	Std. error b:	0.0013485
95% bootstrapped confidence intervals (N=1999)			
Slope a:	(0.82375; 0.97763)		
Intercept b:	(-0.14318; -0.002944)		
Correlation			
r:	0.9556		
r^2:	0.91317		
t:	21.995		
p (uncorr.):	4.7496E-26		
Permutation p:	0.0001		

***Wasatchites* spp. (*W. tridentinus* + *W.* spp. indet.)**

RMA Regression: H-W			
Slope a:	0.68457	Std. error a:	0.031633
Intercept b:	0.10827	Std. error b:	0.11464

95% bootstrapped confidence intervals (N=1999)	
Slope a:	(0.62246; 0.75209)
Intercept b:	(-0.45034; 0.63167)

Correlation	
r:	0.92686
r^2:	0.85908
t:	20.058
p (uncorr.):	8.6859E-30
Permutation p:	0.0001

Principal component analysis (PCA)

PC	Eigenvalue	% Variance
1	75.4915	97.076
2	1.64149	2.1108
3	0.481135	0.6187
4	0.151427	0.19472

Loadings

	PC 1	PC 2	PC 3	PC 4
D	0.85995	-0.095945	-0.21015	-0.4551
H	0.42265	-0.41669	0.33949	0.72972
W	0.24423	0.77378	0.58377	0.028797
U	0.149	0.46737	-0.70696	0.50948

Discriminant analysis (LDA)

Axis	Eigenvalue	Percent
1	1.3849	54.06
2	0.73712	28.78
3	0.33908	13.24
4	0.10053	3.924

Loadings

	Axis 1	Axis 2	Axis 3	Axis 4
D	3.1681	-4.3982	-1.0776	-0.23811
H	1.2169	-2.4771	-0.62675	0.022129
W	1.2187	-1.0441	0.30212	0.61886
U	0.87265	-0.40504	-0.41348	0.32937

Appendix 4 – List of figures